Aus dem Forschungszentrum Borstel
Leibniz-Zentrum für Medizin und Biowissenschaften
Programmbereich Asthma & Allergie
Forschungsgruppe Immunbiologie

THE ROLE OF THE ACTIN-REGULATORY PROTEINS CORONIN 1A AND CORONIN 1B IN THE REGULATION OF NATURAL KILLER CELL DEVELOPMENT AND FUNCTION

DISSERTATION
zur Erlangung des Doktorgrades
der Mathematisch-Naturwissenschaftliche Fakultät
der Christian-Albrechts-Universität zu Kiel

vorgelegt von
André Jenckel

Bad Segeberg, 2013

Erste/r Gutachter/in:	Prof. Dr. Dr. Silvia Bulfone-Paus
Zweite/r Gutachter/in:	Prof. Dr. Thomas Roeder
Tag der mündlichen Prüfung:	09.01.2014
Zum Druck genehmigt:	09.01.2014

gez. Prof. Dr. Wolfgang J. Duschl, Dekan

Table of contents

Abbreviations

α	alpha
ADF	actin-depolymerizing factor
ADP	adenosine 5'-diphosphate
APS	ammonium persulfate
ATP	adenosine 5'-triphosphate
β	beta
BC	B cell
BMDC	bone marrow-derived dendritic cell
BMMC	bone marrow-derived mast cell
BMMΦ	bone marrow-derived macrophage
BSA	bovine serum albumin
CCL	chemokine (C-C motif) ligand
CXCL	chemokine (CXC motif) ligand
CCL5 (RANTES)	chemokine (C-C motif) ligand 3
cDNA	complementary deoxyribonucleic acid
CFDA-SE	carboxyfluorescein diacetate succinimidyl ester
CLP	common lymphoid progenitor
Coro1a	coronin 1a
C1a KO	*coronin 1a* knockout
Coro1b	coronin 1b
C1b KO	*coronin 1b* knockout
cSMAC	central supramolecular activation complex
CXCL10	chemokine (C-X-C motif) ligand 10
CXCL12 (SDF-1)	chemokine (C-X-C motif) ligand 12
DAPI	4',6-Diamidino-2-Phenylindole, Dihydrochloride
DKO	*coronin 1a*/*coronin 1b* double-knockout
DMSO	dimethyl sulfoxide
dNTPs	deoxyribonucleotide triphosphates
DP	double-positive
DTT	dithiothreitol
EDTA	ethylenediaminetetraacetic acid
EGTA	ethylene glycol tetraacetic acid
ELISA	enzyme-linked immunosorbent assay
EtOH	ethanol
F-actin	filamentous actin

FACS	fluorescence-activated cell sorting
FCS	fetal calf serum
FSC	forward scatter
γ	gamma
G-actin	globular actin
GAPDH	glyceraldehyde-3-phosphate dehydrogenase
GM-CSF	granulocyte macrophage colony-stimulating factor
GrzA	granzyme A
GrzB	granzyme B
hDia1	human diaphanous homolog 1
HGNC	Human Genome Nomenclature Committee
Hoechst 33342	bisbenzimide H 33342 trihydrochloride
Hprt	hypoxanthine phosphoribosyltransferase
IFN-γ	interferon gamma
iNK	immature NK cells
IMDM	Iscove's Modified Dulbecco's media
IL	interleukin
JNK	c-Jun N-terminal kinase
KIR	killer cell immunoglobulin-like receptor
KLRG1	killer cell lectin-like receptor 1
LAMP-1	lysosome-associated membrane protein 1
LDH	lactate dehydrogenase
LFA-1	lymphocyte function-associated antigen 1
µ	micro
m	mili
mAb	monoclonal antibody
MHC	major histocompatibility complex
MAPK	mitogen-activated protein kinase
MFI	mean fluorescence intensity
mNK	mature NK cells
mRNA	messenger ribonucleic acid
NCR	natural cytotoxicity triggering receptor
NK/NK cell	natural killer cell
NKP	NK cell precursor
NKR	natural killer receptor
No.	number

NPF	nucleation promoting factor
n.s.	not significant
PAMPs	pathogen-associated molecular patterns
PBS	phosphate buffered saline
PFA	paraformaldehyde
Pi	inorganic phosphate
PI3K	phosphatidylinositide 3-kinase
PMA	phorbol-12- myristate-13-acetate
Prf	perforin
PRRs	pattern recognition receptors
pSMAC	peritheral supramolecular activation complex
rhIL-15	recombinant human interleukin-15
RNA	ribonucleic acid
RPMI	Roswell Park Memorial Institute medium
RT	room temperature
SCID	severe combined immunodeficiency
SD	standard deviation
SDS	sodium dodecyl sulfate
sec. Ab	secondary antibody
SDS-PAGE	SDS polyacrylamide gel elektrophoresis
SEM	standard error of the mean
SSC	side scatter
SSH1L	slingshot homolog 1L
TC	T cell
TNF-α	tumor necrosis factor-alpha
TRAIL	TNF-related apoptosis-inducing ligand
TX-100	tritonX-100
vs.	versus
WASp	Wiskott-Aldrich Syndrome protein
WIP	WASp-interacting protein
WT	*wild type*

List of figures

List of tables

1 Introduction

1.1 The immune system

Changing environmental conditions and the continuous competition between different species, including host-pathogen interactions, require an ongoing evolutionary advancement of a species to ensure survival. Humans as well as other species are ubiquitously exposed to a variety of pathogens like bacteria, viruses, protozoa and other parasites, however, long lasting infections or life-threatening diseases tend to be the exception rather than the rule. This is the result of protective mechanisms that evolved as a response against the omnipresent threat by pathogens in the course of evolution. These mechanisms include simple concepts like barriers at interfaces to prevent pathogen entry but also complex strategies, as pathogen clearance by the cooperative activity of highly specialized cells. Altogether, these defense mechanisms are known as the immune system.

In relation to evolutionary and functional aspects, the immune system can be divided into two systems, the innate- and the acquired immunity. The evolutionary older innate immune system acts immediately or shortly delayed upon primary contact with the pathogen at the site of entry as first line of defense. Innate defense mechanisms include physical barriers like the skin or the mucosa, humoral factors, such as the complement system, antimicrobial peptides (AMPs) or enzymes but also cellular components, which together act against a broad spectrum of pathogens [1,2]. Mammalian cellular innate immune responses are mainly carried out by phagocytes [3–5], granulocytes [6–8], mast cells (MCs) [7] and natural killer cells (NK cells) [9–12]. The initiation of the cellular innate immune response is primarily based on the recognition of evolutionary highly conserved structures on pathogens, which are known under the collective term of pathogen-associated molecular patterns (PAMPs), by a limited repertoire of germ line-encoded invariable receptors on immune cells, the pattern recognition receptors (PRRs) [13]. The activation of innate immune cells upon engagement of PAMPs by PRRs results in a timely elimination of infected cells or pathogens and leads to the activation of the acquired immunity as a result of antigen-presentation or stimulation by secreted humoral factors.

In contrast to the innate immunity, the full establishment of the acquired immunity requires a number of days and the initiation is carried out distantly from the pathogen entry site in adjacent lymphoid organs. Acquired immune responses are carried out by lymphocytes, which can be subdivided into two major populations namely T- (T cells, TCs) and B lymphocytes (B cells, BCs). In contrast to innate immune cells, T- as well as B cells are characterized by the expression of individual isoforms of either T- or B cell receptors as a consequence of somatic recombination and hypermutation of a small number of T- or B cell receptor-gene segments. These processes generate a vast number of receptor specificities

and in turn lead to a variety of unique T- and B cells which are separately highly specific for one individual epitope of an antigen. Upon engagement of their cognate ligands and typically co-stimulatory signals, naïve T- or B cells proliferate and differentiate into effector- as well as memory cells, enabling the establishment of a humoral- (B cells) or cell-mediated (T cells) acquired immune response and the development of immunological memory [14–16].

Innate- and acquired immunity are closely linked and jointly contribute to the achievement of the major tasks of the immune system, namely: (i) Inhibition of infections by pathogens (immunological protection) and (ii) development of memory for better protection to a subsequent encounter with the pathogen (immunological memory) [17]. In addition to its prominent role in the protection of an organism against pathogens, the immune system is also indispensable for the elimination of transformed cells to prevent cancer [18,19].

The fulfillment of these tasks requires the use of powerful tools, which need an adequate regulation to avoid the injury of the host organism. The undue reaction against otherwise harmless agents in the case of allergens or the reactivity against self-antigens in the context of autoimmune diseases are only two examples for dysfunctions of the immune system which have serious impacts and result in pathology [20,21].

As reported above, cell-mediated immune responses are an inherent part of the innate- as well as the acquired immunity and are carried out by various cell types. The focus of this thesis is on NK cells and their cytotoxic function.

1.2 Natural killer cells

In the beginning of the 1970s, a new subset of lymphocytes which was characterized by spontaneous cytotoxic activity against transformed cells was described independently by two groups. Due to their cytolytic activity these cells were named natural killer- or briefly NK cells [9–12]. NK cells are large granular lymphocytes which are closely related to cytotoxic T cells. Both, NK- as well as cytotoxic T cells share common characteristics including similarities in the morphology, the expression of lymphoid markers and in broader sense lytic mechanisms [22]. In contrast to T- or B cells, NK cells lack antigen-specific cell surface receptors that underlie somatic recombination [23–26]. However, NK cells express a variety of germ line encoded receptors that can either stimulate NK cell reactivity (activating receptors) or extenuate their activities (inhibitory receptors) [27–30]. Therefore, NK cells are primarily dedicated to the innate immunity [23].

NK cells constitute approximately 5% - 15% of human circulating lymphocytes [31]. In humans and mice, mature NK cells (mNKs) are further present in the spleen, lung, liver, gastrointestinal tract, the uterus in the case of pregnancy and to a minor extent in lymph nodes and lymphoid tissues as well as in the bone marrow [32–36]. In addition to their role in tumor immune surveillance, NK cells have been attributed to the control of viral and

intracellular bacterial infections [23,37–41]. Main targets of NK cells are stressed (malignant or infected) cells that are characterized by down-regulated major histocompatibility complex (MHC) class 1 molecule expression ("missing self" hypothesis), which are normally expressed on almost every cell of the body (Figure 1-1) [42,43].

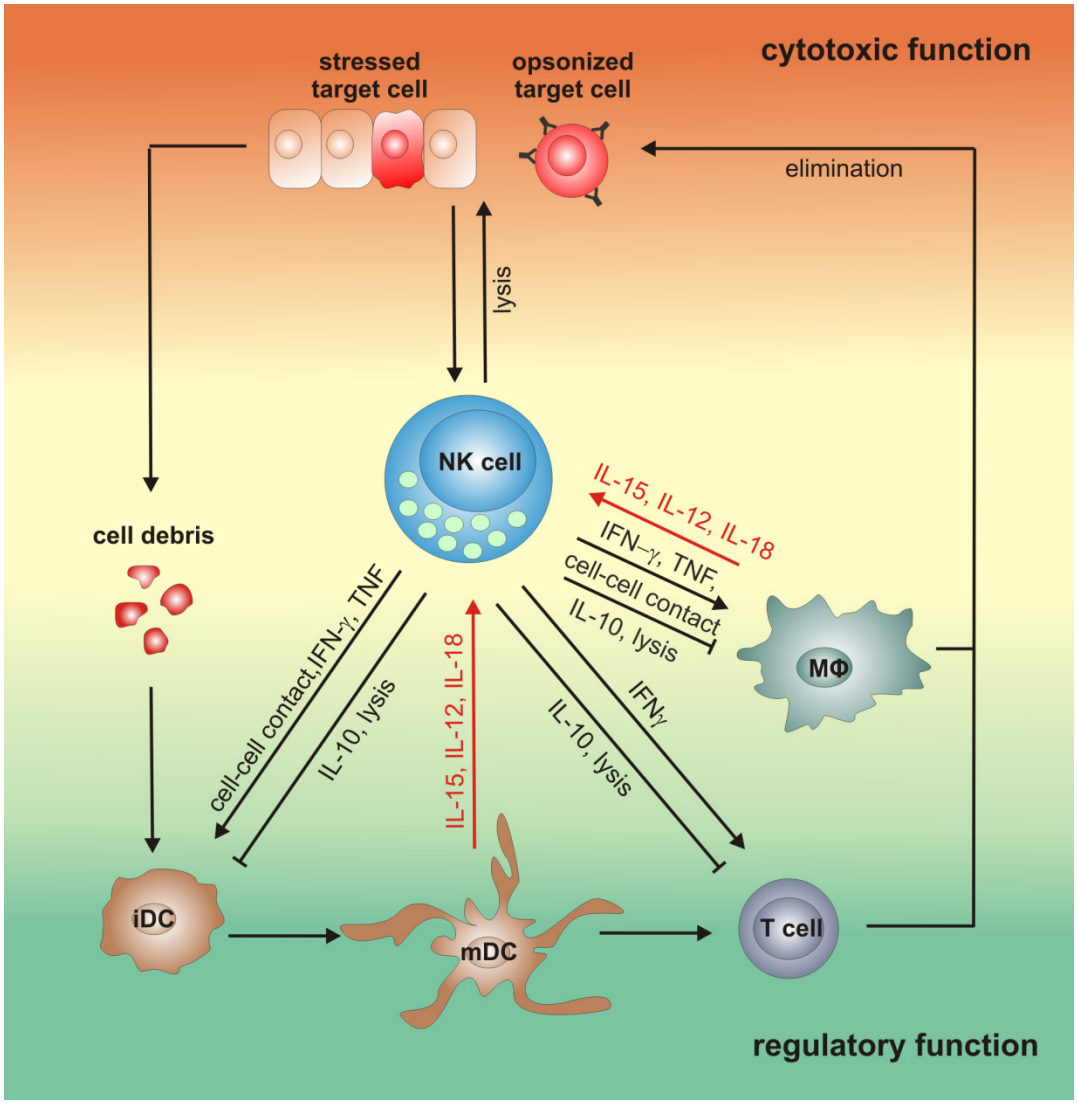

Figure 1-1. Schematic overview of biological NK cell functions.
As potent effector cells of the innate immunity, NK cells are capable to kill stressed (malignant or infected) cells in the presence or absence of antibodies. In addition, NK cells contribute to the regulation of other immune cells, such as immature DCs (iDCs), T cells and MΦ indirect via secretion of proinflammatory or immunosuppressive cytokines or through a direct physical contact. This regulatory crosstalk influences not only NK cell counterparts but also affects the effector potential of the NK cells that require priming by IL-15, IL-12 and/or IL-18 produced by mDCs and MΦ to achieve their full effector potential. Furthermore, NK cell-mediated killing of infected cells also promote the antigen cross-presentation to cytotoxic T cells, for instance by DCs. [Adapted from E. Vivier *et al.*, Poster on NK cells: receptors and functions., Nature Reviews Immunology, Dec 2010, Vol 10 No 12]

Down-regulation of MHC class 1 molecules often goes along with tumor growth and is a common protective mechanism of pathogens to escape from the elimination by cytotoxic T cells [44,45]. For this reason, the cytolytic activity of NK cells is an important defense

mechanism of the immune system to overcome viral evasion of the adaptive immunity. Importantly, NK cells are potent effector cells which are capable to kill aberrant cells in the absence of prior sensitization [9,11]. However, priming of NK cells by various factors including interleukin (IL)-15, IL-12 or IL-18 increases their effector potential and is required to achieve an fully activated state (Figure 1-1) [46–49].

Besides their cytolytic function, NK cells contribute to the initiation and regulation of innate and acquired immune responses, not only by the secretion of humoral factors but also through physical contact with other immune cells (Figure 1-1) [23,50–56]. In this context, NK cells are important producers of interferon gamma (IFN-γ) but also of other proinflammatory or immunosuppressive cytokines such as tumor necrosis factor-alpha (TNF-α) or IL-10, respectively [57–60]. These soluble factors are crucial for the activation as well as regulation of other immune cells like dendritic cells (DCs) [52,61,62], T cells [51,63] and macrophages (MΦ) [55,64] as shown in Figure 1-1. In addition, activated NK cells secrete growth factors such as the granulocyte macrophage colony-stimulating factor (GM-CSF) [65] and a variety of chemokines including chemokine (C-C motif) ligand 3, (CCL3 or MIP1-α), CCL4 (MIP1-β), CCL5 (RANTES) or chemokine (CXC motif) ligand 8 (CXCL8 or IL-8) [23,66–68] that are important for the recruitment of other immune cells, for instance DCs, to the site of inflammation [69]. Furthermore, target cell debris as consequence of cytolytic NK cell activities likely promote antigen cross-presentation to cytotoxic T cells (Figure 1-1) [70]. Besides these indirect regulatory activities, NK cells also physically interact with DCs [50,62], MΦ [64,71], T cells [53] and neutrophils [56] in a regulatory manner to promote or extenuate immune responses (Figure 1-1). Thus, NK cells are not only potent effector cells of the innate immune system but also important modulators of acquired immune responses.

Due to the fact that NK cell activities are mainly controlled in the context of MHC class I molecules, expressed by potential target cells [42,43], a proper regulation of NK cells is important to guarantee NK cell tolerance toward “normal” cells and in turn avoid pathology. In this context, recent work revealed that engagement of “self” MHC class 1 molecules by inhibitory NK cell receptors during NK cell development promotes the maturation of fully functional NK cells in humans and mice through a process called “NK cell education” [72,73]. The importance of this process becomes evident in MHC class 1-deficient mice and transporter associated with antigen processing 1 (TAP1)-deficient humans. NK cells from these mice or from the TAP-1-deficient patients are hyporesponsive in both cytokine production and cytotoxicity [74,75]. Up to now, the underlying mechanisms which are responsible for the induction of NK cell “self” tolerance are poorly understood and controversially discussed. Various models such as the “licensing”- [73], the “disarming”- [76], the “rheostat”- [77,78] or the “cis interaction”-model [79] have been proposed, trying to

explain the processes which are necessary to induce NK cell tolerance, however, further work is required to dissolve various discrepancies.

Furthermore, recent work revealed that NK cells are able to generate a form of antigen-specific immunological memory, which enables an improved NK cell-mediated immune response upon secondary challenge, at least for a few months [80–84]. Thus, NK cells are equipped with features that are attributed to both, innate- as well as acquired immunity, and which are crucial for their essential effector functions within the immune system.

1.2.1 Stages of NK cell development

The origin of NK cells is the bone marrow where they derive from a common lymphoid progenitor (CLP) as T- and B cells do [85–88]. While initial steps of NK cell development, including commitment to the NK cell lineage, early maturation processes as well as NK cell education mainly occur in the bone marrow, final steps of NK cell maturation takes place in the periphery [88–91]. However, NK cell development has also been reported in the thymus and lymph nodes, indicating other potential sites of differentiation or an access of early developmental NK cell stages to the circulation [92–95]. Interestingly, thymic NK cells differ from NK cells that derived in the bone marrow in several aspects. Thymic NK cell development depends on the presence of IL-7 and not on IL-15, as reported for the bone marrow NK cells and both subsets differ in their functionality [95]. In humans and mice, another NK cell subset develops and resides in the liver starting prior to birth [96–98]. These NK1.1^{+}/CD49b^{-}/TRAIL^{+}/Mac-1^{-}/Ly49^{-} NK cells are maintained in the liver up to adulthood, however, the subset decreases over time [94,97].

NK cell development and maturation is a multi-stage process governed by cell-intrinsic signals like transcription factors and the impact of environmental cues like cytokines, such as IL-15 and other factors produced by stroma cells [95,99,100]. Besides its crucial role during initial developmental steps in the bone marrow, IL-15 trans-presentation is also indispensable for the survival of mNKs in the periphery [101,102]. NK cell development is characterized by a progressive upregulation/downregulation of various activating- and inhibitory receptors, adhesion molecules as well as chemotactic- and cytokine receptors and is further accompanied by changes in NK cell functionality (Figure 1-2) [31,89,95,103,104]. Because this work was performed on mouse NK cells, the following overview focusses on NK cell development in the murine system.

Almost ten years ago, Rosmaraki *et al.* described the so far earliest mouse NK cell committed precursor (NKP) within the bone marrow and linked NK cell commitment to the expression of CD122 [88]. Recently, the phenotypical definition of this NKP was further refined (rNKP, Figure 1-2, step I) and an NK cell committed precursor upstream of the rNKP was described, which lacks CD122-expression (pre-NKP) [105,106].

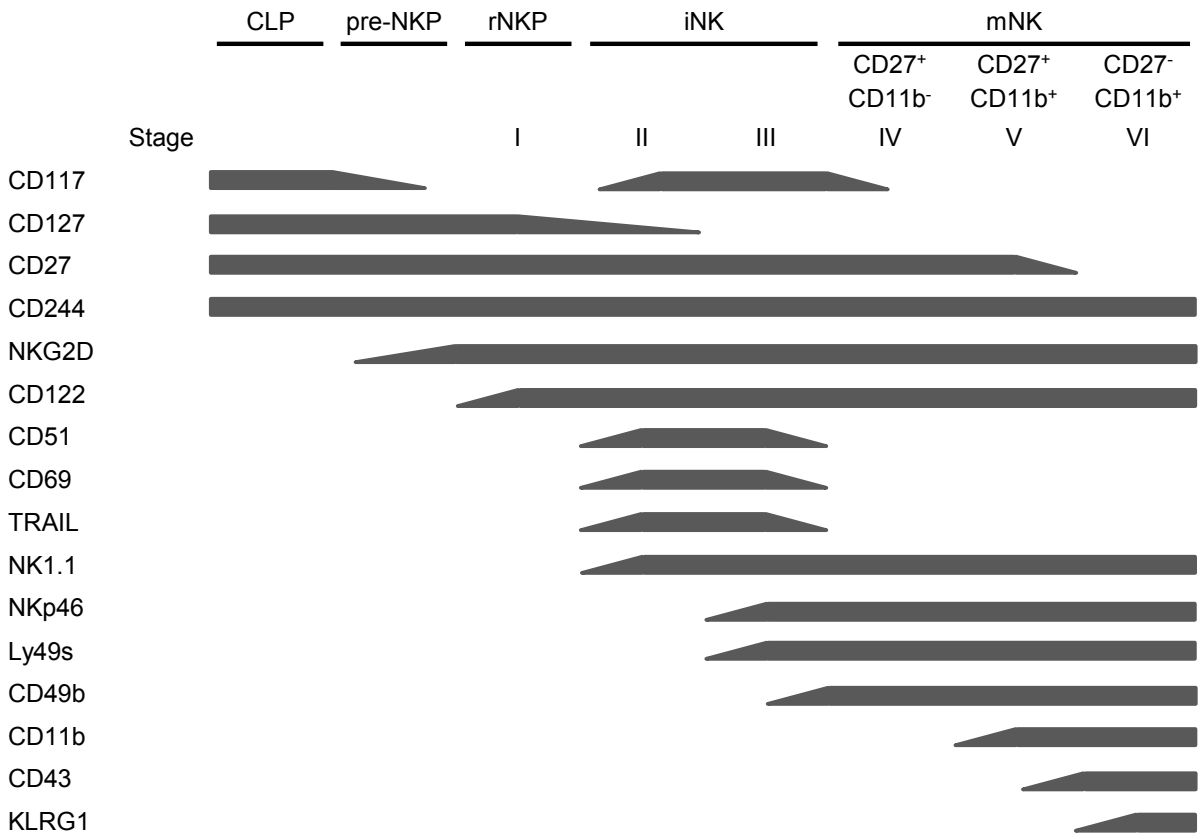

Figure 1-2. Stages of NK cell development in the mouse.
NK cells derive from a common lymphoid progenitor (CLP) in the bone marrow. NK cell commitment is associated with the upregulation of CD122 on NK cell precursors (NKPs) which can be subdivided into early NKPs (pre-NKP, $CD122^-$) and the "refined" NK cell committed precursor (rNKP, $CD122^+$, stage I). Immature NK cells (iNKs, stage II and III) are characterized by the expression of NK1.1 and TRAIL and can be further subdivided according to the expression of the surface molecules listed on the left. In contrast to iNKs, mature NK cells (mNKs, stage IV – VI) express CD49b and are further characterized by the absence of TRAIL and the stepwise downregulation of CD27 as well as the progressive upregulation of CD11b, CD43 and KLRG1. [Adapted from Huntington *et al.*, Vosshenrich *et al.* [107,108].]

In C57BL6-mice, the acquisition of the activating NK cell receptor NK1.1 defines a further step of NK cell development: the immature NK cell stage [88,89,95]. Immature NK cells (iNKs) are $CD122^+/NK1.1^+/CD27^+$, express the TNF-related apoptosis-inducing ligand (TRAIL) and stepwise upregulate further surface molecules including adhesion molecules and activating- as well as inhibitory NK cell receptors in the course of their further maturation (Figure 1-2, step II and III) [91,95]. The progressive expression of CD49b represents the next developmental stage of NK cells and is used to define early mNKs [59,89,95]. Early mNKs, which are $CD122^+/NK1.1^+/CD27^+/CD49b^+/Ly49^+$ emigrate from the bone marrow into the periphery and continue to adapt to their environment (Figure 1-2, stage IV - VI) [89,91,95,103]. Peripheral NK cell maturation includes the downregulation of TRAIL- and CD27-expression as well as the gradually upregulation of CD11b, CD43 and the killer cell lectin-like receptor 1 (KLRG1 or MAFA) [34,89,91,94,97,104,109,110] as shown in Figure 1-2, stage IV – VI. Fully mature NK cells are

$CD122^+/NK1.1^+/CD27^-/CD49b^+/Ly49^+/CD11b^+/CD43^+/KLRG1^+$ (Figure 1-2, stage VI). The progressive upregulation/downregulation of CD11b- and CD27-expression, respectively, on $CD49b^+$ NK cells in the course of their maturation affords the further division of this population into distinct subsets [89,91,97,110,111]. In between these subsets, there is a linear progression from $CD11b^{low}/CD27^{high}$ (immature/early mature) over $CD11b^{high}/CD27^{high}$ (double-positive; DP) to $CD11b^{high}/CD27^{low}$ (mature) NK cells, as schematically shown in Figure 5-7 A [91,104,110]. As mentioned above, NK cell development and maturation is not only associated with phenotypic changes, this processes are also accompanied by changes of NK cell functionality. Kim *et al.* and Chiossone *et al.* revealed that the capacity of NK cells to proliferate decreases in the course of maturation [89,91]. Furthermore, $CD27^{high}$ NK cells stimulated with either IL-12 or IL-18 secrete higher amounts of IFN-γ compared to $CD27^{low}$-subsets, not only upon stimulation with cytokines but also in response to DCs [104,110]. Interestingly, fully mature NK cells seem to be restricted in their capacity to proliferate or elicit effector function compared to more immature subsets [89,91,110]. One possible explanation for this discrepancy may be their tight regulation [104,110].

1.2.2 NK cell cytotoxicity and its regulation

Human as well as mouse NK cells express multiple activating and inhibitory receptors on their surface [27,29,30,112]. The inhibitory NK cell receptors comprise several members out of the human inhibitory killer cell immunoglobulin-like family (KIR) as well as out of the mouse C-type lectin-like family (inhibitory Ly49-receptors), while Ly49-receptors are the functional mouse orthologs of the human KIRs. Further inhibitory receptors are the heterodimer CD94-natural killer group 2A (NKG2A)-receptor and KLRG1 which are present in human and mice. Activating receptors of both species include members out of the activating natural cytotoxicity triggering receptor-family (e.g. NKp46) or the natural killer-receptor (NKR)-family (e.g. NKR-P1C or NK1.1), the activating KIR- and NKG2-receptors as well as the low-affinity Fc receptor for IgG (FcγRIII or CD16) [29,112–114]. Beside these receptors, various cytokine-, chemotactic- or other receptors like 2B4 (CD244) as well as adhesion molecules (e.g. the lymphocyte function-associated antigen 1 (LFA-1) or the macrophage-1 antigen (Mac-1)) are involved in the activation of NK cells [23,68,115–117]. Selected NK cell receptors and their reported ligands, which are particularly relevant for this thesis, are listed in Table 1-1.

Table 1-1. Selected NK cell receptors with reported ligands in mice and human

Receptor	Species mouse	Species human	Reported ligand(s)
Inhibitory receptors			
NKG2A (CD159A)/CD94	x	x	Qa-1^b (mouse); HLA-E (human)
KLRG1	x	x	E-, N-, and R-cadherin
Activating receptors			
NKR-P1C (NK1.1, Ly-55, CD161c)*	x		?
NKp46 (NCR1; CD335)	x	x	Influenza-infected cells, *Fusobacterium nucleatum* (mouse); HSPG, heparin, vimentin, HA (IV, VV, ECTV), HN (SeV, NDV), PfEMP-1 (*Plasmodium falciparum), Fusobacterium nucleatum* (human)
NKG2D (CD314)	x	x	RAE-1a, RAE-1b, RAE-1d, RAE-1e, RAE-1g, H60a, H60b, H60c, MUTL1 (mouse); MICA/B, ULBP1-6 (human)
NKG2C (CD159C)/CD94, NKG2E (CD159E)/CD94	x	x	Qa-1^b (mouse); HLA-E (human)
Ly49H (Klra8)	x		m157 (MCMV)

*) expressed in C57BL, FVB/N, NZB mice (Koo 1984), ECTV, Ectromelia virus; H60, histocompatibility antigen 60; HA, haemagglutinin; HLA, human leukocyte antigen; HN, hemagglutinin-neuraminidase; HSPG, heparin sulfate proteoglycan; IV, Influenza virus; MCMV, Mouse Cytomegalovirus**,** MIC, MHC class I chain-related protein; NDV, Newcastle disease virus; RAE, retinoic acid early-inducible protein; SeV, Sendai virus; ULBP, UL16 binding protein; VV, Vaccinia virus [Adapted from Campbell *et al.*[114]]

While signals from inhibitory NK cell receptors are mainly triggered upon engagement of particular MHC class I-isoforms, activating NK cell receptors can be stimulated in an MHC class I-dependent as well as independent manner [29,114]. Inhibitory NK cell receptors are characterized by the presence of one or more cytoplasmic immunoreceptor tyrosin-based inhibition motives (ITIMs). These motives initiate the activation of downstream signaling molecules by recruitment and activation of the SH2-containing protein tyrosine phosphatase (SHP)-1 or SHP-2 or by the SH2-containing inositol polyphosphate-5-phosphatase (SHIP) [118–121]. These tyrosine phosphatases suppress NK cell responses by dephosphorylating the protein substrates of the tyrosine kinases linked to activating NK receptors [120,122]. Signal transduction of activating NK cell receptors occurs through immunoreceptor tyrosin-based activation motives (ITAM)-containing adaptor molecules like the high-affinity Fc receptor for IgE (FcεRIγ), CD3ζ and DAP12 as well as non-ITAM-bearing proteins like DAP10 or the signaling lymphocytic activation molecule–associated protein (SAP) [27,29,30,112]. The engagement of cognate ligands by activating NK cell receptors initiates the recruitment and activation of various molecules involved in signal transduction like the spleen tyrosine kinase (Syk), phosphatidylinositide 3-kinase (PI3K), phospholipase

C, gamma (PLCγ), protein kinase C (PKC), Vav-1 as well as others [118,119,123–128]. This in turn, leads to the activation of the mitogen-activated protein kinase (MAPK)- and c-Jun N-terminal kinase (JNK)-pathway which are involved in the initiation of the NK cell cytolytic responses [126–129].

NK cell cytotoxicity is regulated by a balance of signals derived from the activating- or inhibitory surface receptors mentioned above [29,30,130]. The interplay of these signals determines the further outcome of NK cell responses and thereby decides on the fate of the target cell. Under “normal” conditions (no cellular stress), NK cell counterparts are protected from killing since there is a balance between activating as well as inhibitory signals. However, in the context of missing inhibitory signals due to the downregulation of MHC class I molecules (“missing self” recognition) [42,43], the detection of microbial molecules (“infectious non-self recognition”) [131,132] or upon upregulation of stimulatory “self” ligands, which are rarely expressed on “normal” but increased on “stressed” cells (“stress-induced self recognition”) [133–135], the stimulatory signals received from activating receptors are unopposed, resulting in NK cell activation and target cell lysis [113,114,136].

NK cells are capable to eliminate abnormal cells by various means. Killing of infected or transformed cells can be mediated by the release of preformed granules containing the pore-forming protein perforin and cytotoxic serine proteases, named granzymes, in the presence or absence of antibodies [137–144]. While the elimination of abnormal cells lacking antibody opsonization can be induced by the majority of activating NK cell receptors, antibody-dependent cell cytotoxicity (ADCC) strictly depends on FcγRIII [29,112–114,143,144]. In addition, the cytolytic NK cell activity can be triggered by the interaction of TRAIL and Fas ligand (FasL or CD95L) with their corresponding antagonists [50,56,145–147].

The directed exocytosis of cytotoxic granules is the result of a tightly regulated complex process that involves multiple stages [115–117,148,149]. The initial contact between an NK cell and a target cell induces the formation of an immunological/cytolytic synapse that is tightened in the presence of sufficient stimulatory signals [115]. In the following effector stage, adhesion molecules like LFA-1 or Mac-1 segregate into the outer region of the cytolytic synapse, known as peripheral supramolecular activation complex (pSMAC), and thereby contribute to the further stabilization of the conjugate [115,118,150]. In addition, LFA-1 initiates various signaling cascades which, among others, stimulate the reorganization of filamentous (F)-actin at the site of the forming cytolytic synapse [115,124,127,130,150,151]. In contrast to adhesion and co-stimulatory molecules which are found in the pSMAC-region, activating- and inhibitory NK cell receptors accumulate in the central supramolecular activation complex (cSMAC)-region of the cytolytic synapse [118,119,152–154]. Synergistic events from activating NK cell receptors stimulate the

reorientation of the microtubule-organizing center (MTOC), the Golgi apparatus and the cytotoxic granules toward the target cell [115,116,128,149,155,156]. Subsequently, the cytolytic granules pass through locally hypodense areas of a pervasive F-actin network within the cSMAC-region mediated by myosin IIA-activity [156–162]. The final docking- and fusion process of the granules and the plasma membrane is initiated and regulated by docking and priming proteins [117,163,164]. The consequent release of cytotoxic granule contents leads to the immediate death of the target cell by the induction of apoptosis [138,142].
The directed exocytosis of cytolytic granules is highly regulated (reviewed in Orange *et al.* and Krzewski *et al.*) [116,117]. In this context, a number of studies indicate a crucial role of the actin cytoskeleton in the regulation of NK cell activities, including exocytic pathways [165–171].

1.3 The actin cytoskeleton and its function

In animals, actin filaments (microfilaments), intermediate filaments and microtubules constitute an intracellular protein scaffold which is termed cytoskeleton. The cytoskeleton determines the shape of cells and is involved in cellular processes like cell division, cellular motility or the intracellular transport of vesicles and organelles [172–174].
Actin is a highly conserved protein that is abundant in eukaryotic cells [175]. The actin cytoskeleton as the major component of the eukaryotic cytoskeleton is a highly dynamic structure which underlies a constant remodeling including branching as well as de-branching as reviewed by Pollard *et al.*, 2009 [172]. It consists of bundles or networks of two helically arranged actin filaments (F-actin), which are polymerized from actin monomers (globular actin or G-actin). The assembled F-actin filaments are polar in the sense that they bear a fast-growing barbed end and a slower-growing pointed end [176]. F-actin polymerization requires the hydrolysis of G-actin bound adenosine 5'-triphosphate (ATP) to adenosine 5'-diphosphate (ADP) that remains bound to F-actin and inorganic phosphate (P_i) mediated by the intrinsic ATPase-activity of actin subunits [176]. In this context, the release of the P_i is much slower than the hydrolysis of ATP resulting in areas of newly polymerized F-actin retaining the hydrolyzed P_i [177]. Release of P_i induces a conformational change of the assembled actin monomers which facilitates F-actin de-branching at the pointed end [172].
To maintain the steady-state level of the actin cytoskeleton or for quick remodeling under certain conditions, eukaryotic cells dispose more than 100 actin associated proteins. This network of actin nucleators, nucleation-promoting factors (NPFs), regulatory proteins, monomer-sequestering proteins and others is required to maintain a pool of actin monomers, initiate polymerization, restrict the length of actin filaments, regulate the assembly and turnover of actin filaments and cross-link filaments into networks or bundles as reviewed by Pollard *et al.*, 2009 [172]. The significance of proteins associated with actin regulation and

the crucial role of the actin cytoskeleton for basal cellular activities of NK cells becomes evident upon loss of their function. In eukaryotic cells, *de novo* F-actin polymerization is mainly initiated by two classes of actin nucleators, the Arp2/3-complex and the formins. While Arp2/3 mediates the assembly of a branched actin network by initiating the formation of new “daughter” filaments at the side of existing “mother” filaments, formins interact with the barbed end of actin filaments and promote incorporation of new actin monomers [178–180]. It has been shown that the activation of NK cells via signals from integrins or activating NK cell receptors initiates signaling cascades which in turn activates actin nucleators like the Arp2/3-complex [124,181,182]. NK cells lacking the Wiskott-Aldrich Syndrome protein (WASp), an NPF required for the activation of the Arp2/3-complex and linked to the Wiskott-Aldrich Syndrome, show defective polarization, F-actin assembly, migration and cytotoxicity [165–169]. In this context, the disruption of expression of the WASp-interacting protein (WIP), which is involved in the regulation of WASp but also of other actin-regulatory proteins, impairs granule polarization and NK cell cytotoxicity, whereas overexpression of the protein enhanced NK cell cytolytic capability [183]. Loss of function of the hematopoietic cell-specific homolog of cortactin, HS1, another NPF linked to the activation of the Arp2/3-complex in immune cells, results in defective lysis of target cells, and defects in cell adhesion, chemotaxis and F-actin assembly at the lytic synapse in NK cells [170]. As predicted by the data described above, loss of Arp2/3-function in NK cells leads to defects in cell adhesion and F-actin assembly at the lytic synapse resulting in an ineffective target cell lysis [171]. In contrast to Arp2/3, the loss of the formin diaphanous homolog 1 (hDia1) does not disrupt F-actin assembly at the lytic synapse however, leads to perturbations in the microtubule cytoskeleton, including the targeting of microtubules to the lytic synapse and therefore impairs NK cell cytotoxicity [171].

Another family of actin-regulatory proteins, the coronins, also interacts with the Arp2/3-complex [184,185]. In this context, it has been shown that coronins inhibit the Arp2/3-complex activity and therefore were suggested to be the first described inhibitors of the protein complex [185–187]. However, up to now, the role of coronins in the regulation of the actin cytoskeleton is poorly understood.

1.4 Coronins

Coronins constitute an evolutionary highly conserved family of actin-binding proteins that have been implicated in the regulation of actin cytoskeletal dynamics (reviewed in de Hostos, 1999, Uetrecht *et al.,* 2006 and Chan *et al.,* 2011) [188–192]. Although coronins are known since more than 20 years and notable progress in their understanding has been made in the last decade, these proteins and their contribution in the regulation of actin-dependent processes are still poorly understood.

Coronin was originally extracted and purified from precipitated actin-myosin complexes isolated from the slime mold *Dictyostelium discoideum*. In *Dictyostelium*, coronin was found to localize to crown-like actin-rich projections of the cell cortex, leading to the name of the protein (*corona* is Latin for crown) [193]. *Dictyostelium coronin*-null cells showed a reduction in cell-migration speed and were impaired in growth, cytokinesis and fluid-phase endocytic uptake [194–197]. Subsequently, coronins were described in a variety of different protozoan and metazoan [185,188,194,198–207]. Due to the fact that coronins were discovered independently by several groups, which adopted their own names and classifications, nomenclature of coronins is confusing (see Table 1.2). In this work, the nomenclature system developed by the Human Genome Nomenclature Committee (HGNC) is used.
(http://www.genenames.org/genefamilies/CORO)

1.4.1 Coronins: Structure, classification and expression in mammalian tissues/cells

Coronins can be divided according to their domain arrangement into two subtypes, namely in short and long coronins [208]. While up to now, several subclasses of short coronins were defined, only one type of long coronins was described [207]. Both, short as well as long coronins are characterized by the presence of a common structural core motif, which is highly conserved among species [207]. This coronin core motif consists of a β-propeller unit, the associated N- and C-terminal extensions and a unique region, as shown in Figure 1-3. The main structural characteristic of the coronin core motif is the presence of a tryptophan (W) and aspartic acid (D)-repeats (WD40-repeats) containing β-propeller, which can be found in a variety of signaling- and adaptor proteins and has been proposed to mediate protein-protein interactions [209–211]. The core WD40-repeat region of the β-propeller is flanked by short, highly conserved N- and C-terminal extensions, which contribute to the formation of the β-propeller and possibly are involved in the regulation of protein interactions and/or stabilization of the β-propeller [209,212]. Subsequent to the C-terminal extension, coronins contain a highly variable unique region that varies in length and sequence among these proteins [207]. Additionally to the coronin core motif, short coronins contain a classical coiled-coil domain located at the C-terminal end of the protein (Figure 1-3, type I/II coronins). This structure enables the homo-oligomerization of short coronins, which is crucial for their functionality [200,212–216]. Representatives of long coronins, like coronin 7 (Coro7 or POD), are distinct in structure compared to the other coronins, given that the proteins consists of two complete β-propeller units including the associated N- and C-terminal extensions and the unique region (coronin core motif), arranged in a tandem (Figure 1-3, type III coronins) [189,201,217]. Additionally, Coro7 is characterized by the absence of a coiled-coil domain. In contrast to short coronins, Coro7 contains a highly acidic region, situated at the C-terminal end of the protein [189]. Recently, another coronin subtype was defined by Eckert *et al*.

based on phylogenetic analyses [207]. For these coronins, a protein expressed in *Dictyostelium*, namely villidin, would be a representative [207,218]. According to the HGNC nomenclature Eckert *et al*. suggested to term these proteins coronin 4 (Coro4) [207]. Most type IV coronins consists of the classical coronin core motif followed by variable numbers of C-terminal pleckstrin-homology- and gelsolin domains and contain a villin headspace domain at the C-terminal end of the protein. Furthermore, several proteins with short sequences following the coronin core motif are included within this subtype [207].

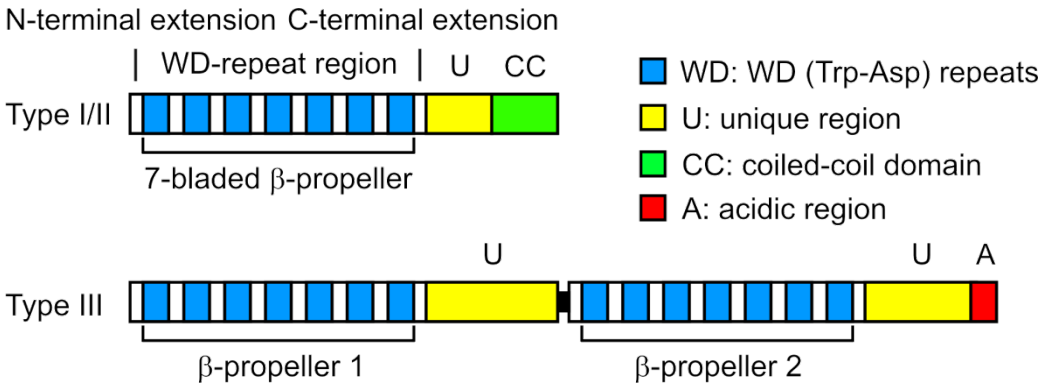

Figure 1-3. Scheme of short and long coronin structural domain arrangements.
Coronins share a conserved domain arrangement consistent of a tryptophan (W) and aspartic acid (D)-repeat region (β-propeller), which is flanked by an N-terminal- and a C-terminal extension followed by a unique region (U). Short coronins (Type I/II) contain additionally a C-terminal coiled-coil domain (CC). Long coronins (Type III) lack a coiled-coil domain and consist of two linked β-propeller units (including N- and C-terminal extensions and the unique region) and a C-terminal acidic region (A).

With respect to the HGNC nomenclature, coronins can be divided into up to four subclasses namely I and II (short coronins), III (long coronins) and the new class IV suggested by Eckert *et al.* [189,207]. While orthologous coronins conforming to type I and III structure are present in the majority of species, type II coronins are unique to metazoan [207]. In contrast, class IV coronins are exclusively encoded in the genome of individual protozoa, amoeba and fungi [207]. Hence, they will here not be further referred to.

Up to now, the best studied members of the coronin family are the mammalian ones. The mammalian genome encodes seven coronins, covering coronin subclasses I to III. In mammals, type I coronins consists of coronin 1a (Coro1a), -1b (Coro1b) and -1c (Coro1c) as shown in Table 1-2 for mouse coronins. Another type I coronin, coronin 6 is encoded in the genome. However, further data about this protein are missing. Further, coronin 2a (Coro2a) and -2b (Coro2b) of the type II coronin subclass and Coro7, as representative of the type III coronins, are expressed in mammalian tissues (Table 1-2) [189].

Noteworthy, coronins display distinct tissue expression patterns with at least one type I coronin and Coro7 expressed in all tissues and cell types [190]. In contrast, type II coronins show a more restricted expression and are mainly associated with epithelial and neuronal

cells [212,219]. The current available data on their differential tissue expression (see Table 1-2) suggests also a different cellular function.

Table 1-2. The mammalian coronin family, nomenclature and tissue expression.

Subclass	Name	HGNC gene symbol	Synonyms	Protein length (amino acids) mouse/human	Main tissue expression (mouse and human)
I	Coronin 1a	Coro1a	Coronin 1 or -4*, (CRN4), clabp, clipinA,TACO, p57	461/461	Haematopoietic lineage, liver, brain, thymus, spleen, bone marrow and lymph nodes [187,203,220–222]
	Coronin 1b	Coro1b	Coronin 2 or -1*, (CRN1), $coronin_{se}$, p66	484/489	Ubiquitous, liver, spleen, kidney, lung, smooth muscle cells [187,212,222–225]
	Coronin 1c	Coro1c	Coronin 3 or -2*, (CRN2), HCRNN4	474/474	Ubiquitous, lung, kidney spleen [187,212,213,221,226,227]
	Coronin 6	Coro6	Coronin 6 or -3*, (CRN3), ClipinE, Coro1d	471/472	Up to now, only gene expression
II	Coronin 2a	Coro2a	Coronin 5*, (CRN5), clipinB, IR10, WDR2	524/525	Prostate, testis, ovary, uterus and brain [212,219,221]
	Coronin 2b	Coro2b	Coronin 6*, (CRN6), clipinC,	480/480	Brain [219,221]
III	Coronin 7	Coro7	Coronin 7*, (CRN7), POD	922/925	Ubiquitous, thymus, spleen, brain [187,212,217]

*) Nomenclature Morgan & Fernandez [228]

1.4.2 Coronins and the actin cytoskeleton

Since their discovery in *Dictyostelium*, coronins have been implicated in the regulation of actin dynamics in various organisms and cell types [189–191,208]. In this context, diverse functions of coronins on actin filaments have been reported including F-actin binding/bundling, F-actin disassembly and inhibition of the Arp2/3-complex [185,186,200,214,229–233].

One common functional characteristic of short coronins is their capability to bind F-actin [193,207,229,234,235]. Over time, various putative F-actin-binding sites have been mapped to nearly every part of coronin proteins [189,199,213,215,236,237]. Genetic approaches based on the analysis of the crystal structure of murine Coro1a revealed that a charged patch located on the top surface of the β-propeller seems to be crucial for high affinity F-actin

binding of class I coronins [209,229,234]. The mutation of a single conserved residue (Arg30 to Asp (R30D)) located within this patch, in Coro1b or the equivalent residue in Coro1a as well as Coro1c resulted in the loss of high affinity F-actin binding [222,229,238,239]. Additionally, in a recent study, a second potential actin binding site of Coro1c was described [240]. In contrast to class I coronins, the R30 residue is not conserved in class II coronins. However, it could be recently confirmed that the class II coronin Coro2a also interacts with F-actin using conserved sequence features required for the interaction of murine Coro1a with F-actin [235]. As mentioned before, F-actin filaments are characterized by the presence of either ATP, ADP+P_i or ADP bound to the actin subunits of the filament [176,177]. Recently, it could be shown that Coro1b preferentially binds ATP/ADP+P_i F-actin over ADP-bound F-actin [229]. Similar observations have been made for budding-yeast coronin, thus, linking class I coronin F-actin binding mainly to areas of F-actin synthesis [233].

The majority of short coronins is characterized by the expression of a C-terminal coiled-coil domain which is necessary for the homo-oligomerization of the proteins [200,212–216]. The capability to form di- and/or trimeres in connection with their F-actin-binding properties enables short coronins to bundle and crosslink actin filaments [186,200,214,215,229,231].

Additionally, class I coronins interact in an inhibitory manner with the Arp2/3-complex [184,186,187,241]. Similar findings were obtained for budding-yeast coronin [185]. Recently, for yeast coronin a concentration-dependent activation or inhibition of Arp2/3 nucleating-activity was reported. In this context, low concentrations of coronin activated the Arp2/3-complex while higher concentrations resulted in the inhibition of the nucleating-activity [233]. For yeast coronin, the activation of the Arp2/3-complex was linked to the presence of a CA-like sequence, located in the unique region of the protein, which is conserved in WASp proteins, the principal activators of the Arp2/3-complex [242]. However, this CA-like sequence is not conserved in metazoan class I and II coronins, hence supporting the idea of a cell type and/or context-dependent actin-regulation by coronins [233].

Up to now, the mechanisms responsible for the inhibition of the Arp2/3-complex by coronins are poorly understood. Cai *et al.* revealed that binding of Coro1b to F-actin networks promote debranching and recycling of the Arp2/3-complex in lamellipodia by inducing Arp2/3-complex dissociation and counteracting the effect of cortactin, a factor known to facilitate and stabilize actin nucleation by interacting with the Arp2/3-complex [230,243]. However, individual coronins have been implicated in various cellular functions and show diverse tissue expression patterns. Hence, further studies are necessary to clarify whether this is also true under other conditions.

In addition to regulating the Arp2/3-complex, class I coronins were also linked with the regulation of the actin depolymerizing factor (ADF)/cofilin, here referred to as cofilin, in yeast as well as in mammals [186,200,229,232,233,244]. Cofilin and the related ADF are involved

in the depolymerisation of ADP-bound F-actin by severing actin filaments [245]. Up to now, the underlying mechanisms of coronin and cofilin interaction are poorly understood and are controversially discussed. So far, coronins were linked to both, the promoting as well as the inhibition of cofilin-mediated actin disassembly [229,246]. Interestingly, the regulation of Coro1b in the lamellipodia of fibroblasts was attributed, among others, to the recruitment of slingshot homolog 1L (SSH1L), a protein phosphatase which is known to activate cofilin [186,247]. A recent model for coronin-cofilin interaction, based on studies on yeast coronin, postulates that the binding of coronin to the ADP-actin subunits of older actin filaments facilitates severing of cofilin and thereby disassembly. However, the binding of coronin to ATP/ADP+Pi subunits in newly synthesized actin filaments protects the filaments from the severing action of cofilin [233]. Indeed, Gandhi *et al.* suggested that the binding of yeast coronin to ATP/ADP+Pi subunits is mediated by an actin-binding site located in the coiled-coil domain of the protein [233]. Importantly, the existence of this low-affinity actin-binding site in yeast coronin could not be confirmed by another group and there is no evidence for a similar site in mammalian coronins [242]. Thus, further experiments will be required to resolve these discrepancies.

1.4.3 Regulation of coronins

Although coronins were first recognized almost 20 years ago, it took about 10 years until a first mechanism for the regulation of coronins was described. Itoh *et al.* revealed that PKC-mediated phosphorylation of Coro1a triggers its dissociation from phagosomes [248]. Further evidence supporting a regulatory role of PKC-dependent phosphorylation of coronins *in vivo* as well as *in vitro* came from studies on Coro1b. It could be shown that a serine located at position two in Coro1b was a major target for phosphorylation by PKC-isoforms [212]. Furthermore, a critical role of Ser2 phosphorylation for the interaction of Coro1b with the Arp2/3-complex was revealed by the analysis of mutants which either prevent phosphorylation at Ser2 (serine to alanine mutation (S2A)) or mimic phosphorylation (serine to aspartic acid mutation (S2D)). In this context, the S2A mutant showed a stronger interaction with the Arp2/3-complex relative to *wild type*, whereas the S2D mutant exhibited weaker interaction, indicating that the interaction between Coro1b and the Arp2/3-complex is regulated by phosphorylation of Ser2 via PKC [212]. This effect seems to be conserved in Coro1a, since the interaction of the protein with the Arp2/3-complex is also controlled by phosphorylation of Ser2 [204]. As mentioned in the previous section, the regulation of Coro1b at the leading edge was attributed to the recruitment of SSH1L. It has been shown that Coro1b is a target for SSH1L activity since the protein was efficiently dephosphorylated by SSH1L *in vitro* as well as *in vivo* [186]. Recent work revealed another regulatory

phosphorylation event of Coro1a in T cells, involving the phosphorylation of threonine 418 by the cyclin-dependent kinase 5 [249].

Regulatory phosphorylation events of coronins control not only the interaction of the proteins with the Arp2/3-complex, they were also linked to the regulation of F-actin binding of coronins [204,212,222,250]. Observations by Oku *et al.* as well as Föger *et al.* suggest that phosphorylation of Ser2 of Coro1a but also Coro1b decreases the capability of the coronins to bind F-actin leading to a transient subcellular relocation of the proteins upon phosphorylation [222,250]. Recently, it was demonstrated that the interaction of Coro1a with the cytoskeleton additionally requires the phosphorylation/dephosphorylation of a second amino acid residue located in the coiled-coil domain of the protein, namely threonine 412 [251]. Taken together, these data indicate that phosphorylation is crucial for the regulation of coronin function.

1.4.4 Functions of coronins in the mammalian system

Type I, II and III coronins show not only differences in the tissue expression, as mentioned previously, they are also characterized by a quite distinct subcellular localization. Type I coronins mainly localize to lamellipodia, vesicular structures and the immunological synapse and have been linked to the regulation of cellular motility and membrane trafficking [186,187,203,204,212,222,241,248,252,253]. In contrast, type II coronins are localized to stress fibers and focal adhesions and therefore are associated with the regulation of focal adhesion-turnover events but they play also a role in cellular motility and have been implicated in the regulation of TLR-signaling as component of the nuclear corepressor complex [219,235,254]. Coro7, the sole representative of type III coronins in mammalians, localizes to the Golgi apparatus, where it is involved in the maintenance of the Golgi morphology and membrane trafficking. It is important to know that mammalian Coro7, in contrast to other orthologous type III coronins, apparently has no F-actin binding capability [217]. However, the majority of mammalian coronins is poorly investigated and our current knowledge about these proteins is mainly based on studies examining the function of Coro1a and Coro1b.

As mentioned above, coronins are highly conserved proteins. Murine Coro1a (mCoro1a) and its human ortholog hCoro1a as well as Coro1b, respectively are characterized by a high similarity (at least 94% identities for both pairs) suggesting comparable functions and regulatory mechanisms in human and mice (Table 10-1, Figures 10-2 and 3). Additionally, mCoro1a and -1b show a high amino acid sequence homology indicated by 63% identities and a similarity of 79% (Table 10-1, Figure 10-1). Coro1a is preferentially expressed in cells of the hematopoietic lineage [187,204,222,248,253,255–258]. Interestingly, in humans and mice, mutation or deletion of *Coro1a* results in a severe combined immunodeficiency (SCID)

that has mainly been attributed to defective actin regulation in T lymphocytes [204,259–262]. In this context, it has been shown that *Coro1a*$^{-/-}$ T cells are defective in chemokine-mediated migration and exhibit impaired thymic egress and homing to lymph nodes. Furthermore, Coro1a was linked to the regulation of T cell survival [204,263]. For macrophages, it has been shown that Coro1a as coat on phagosomes is crucial for intracellular survival of mycobacteria in infected cells, however, the relevant mechanisms are not fully understood and are a subject of controversial discussion [252,253,264,265]. Recently, it has been suggested that Coro1a-function is required for chemotaxis and phagocytosis in human neutrophils, however, seems to be dispensable for these F-actin-dependent processes in murine equivalents [187,257]. In this context, it is important to know that this discrepancy may be the result of different approaches used to block Coro1a-function, thus further studies are required to solve this issue. Recent work on MCs provides evidences for a role of Coro1a in exocytic pathways. The loss of Coro1a-function in bone marrow-derived MCs resulted in increased FcεRI-mediated degranulation of secretory lysosomes as well as significantly reduced secretion of cytokines *in vitro* and enhanced passive cutaneous anaphylaxis *in vivo* [222]. However, another study failed to confirm these observations utilizing another *Coro1a*-deficient mouse strain [266]. Coro1a is also expressed in B cells as well as in dendritic cells, however, recent work revealed no effects on fundamental mechanisms required for their immune cell function upon loss of *Coro1a* [256,258].

In contrast to the immune specific expression pattern of Coro1a, Coro1b is ubiquitously expressed, indicating a more general role in the regulation of actin dynamics [187,212,222–225]. So far, Coro1b was mainly linked to the modulation of F-actin in lamellipodia via Arp2/3- as well as ADF/cofilin-mediated pathways and therefore was associated with the regulation of the cellular motility of rat fibroblasts and human lung endothelial cell chemotaxis [186,212,229,267]. Additionally, Coro1b seems to be involved in the regulation of neuronal plasticity since *Coro1b* messenger ribonucleic acid (mRNA) was upregulated upon spinal cord injury and loss of Coro1b-function in PC-12 cells reduced neurite outgrowth [224]. A first evidence for a role of Coro1b in immune cell function was provided by the study on MCs by Föger *et al.* [222]. Although the single-loss of *Coro1b* had no impact on MC-function, the observed hyperdegranulation of *Coro1a*$^{-/-}$ MCs was further augmented by the additional loss of *Coro1b*, implicating an overlapping role of Coro1a and Coro1b in MCs [222].

Up to know, no data are available about the impact of *coronin*-deficiency on NK cell function. However, loss of *Coro1a* and *Coro1b* impairs various cellular functions of other immune cells which are also crucial for NK cell biology. In the context of the observed SCID phenotype in patients with mutated coronin 1a, a detailed analysis of the impact of *coronin*-deficiency on NK cells will reveal important new information on the physiological/pathophysiological function of these proteins for the immune system.

2 Aim of the study

The actin cytoskeleton is a highly dynamic structure involved in various cellular processes like cell division, cellular motility or the intracellular transport of vesicles and organelles [172,174]. More than 100 accessory proteins orchestrate the maintenance as well as the quick remodeling of the actin cytoskeleton under certain conditions [172]. One particular family of proteins implicated in the regulation of actin cytoskeletal dynamics is the coronin family [188–192]. Coronins are evolutionary highly conserved proteins which have been described in a variety of species [185,188,194,198–207]. The mammalian genome encodes seven coronins with distinct tissue expression and function [188–190,268]. Most of our current knowledge about these proteins is based on studies examining the function of Coro1a and Coro1b. Interestingly, the loss of Coro1a-function in humans and mice results in a SCID which has been mainly attributed to defective actin-regulation in T lymphocytes [204,259–262]. A number of studies indicate a crucial role of the actin cytoskeleton in NK cell functions [165–171]. However, the impact of *coronin*-deficiency on NK cells is still unclear. Therefore, the aim of the present study was to investigate the role of coronin proteins and in turn of the actin cytoskeleton in the biology and function of NK cells by utilizing a unique system of *Coro1a*- and/or C*oro1b*-deficient mice. In this context, one major task of my work was to clarify the impact of *coronin*-deficiency on the development and maturation of naïve NK cells *in vivo*. Additionally, the impact of Coro1a and Coro1b on fundamental NK cell functions like cytotoxicity, cellular motility or exocytosis should be evaluated by *in vitro* studies on IL-15-expanded and primed *coronin*-deficient NK cells. Together these investigations may clarify the role of NK cells under pathologic conditions like the inborn loss of *Coro1a* in humans and mice and reveal the requirements on coronin proteins and the actin cytoskeleton for NK cell development and function.

3 Materials

3.1 Mice and cell lines

Coro1a$^{-/-}$-, *Coro1b*$^{-/-}$- and *Coro1a*$^{-/-}$*Coro1b*$^{-/-}$ mice were described previously [204,222]. All mice were backcrossed for >10 generations onto C57BL/6N background. Mice were provided by Dr. Niko Föger, Research Center Borstel, and housed at the Animal Care Facility of the Research Center Borstel under pathogen-free conditions.

The mouse T cell lymphoma cell line YAC-1 (ACC-96) was purchased from the DSMZ, A20 mouse B cell lymphoma cells (ATCC, TIB-208) were kindly provided by Dr. Kyeong-Hee Lee from the Research Center Borstel.

3.2 Chemicals and reagents

Accutase™	PAA Laboratories, Pasching, Austria
Acrylamide/bis-acrylamide solution, 30%	Bio-Rad, Munich, germany
Ammonium chloride (NH_4Cl)	Roth, Karlsruhe, Germany
Ammonium persulfate ($(NH_4)_2S_2O_8$)	Bio-Rad, Munich, germany
Aqua B. Braun H_2O	Braun, Melsungen, Germany
Bovine serum albumin (BSA)	Biochrom AG, Berlin, Germany
Brefeldine A	Sigma-Aldrich, Steinheim, Germany
Bromophenol blue	Sigma-Aldrich, Steinheim, Germany
CFDA-SE	Life Technologies, Darmstadt, Germany
Clean-Blot™ IP Detection Reagent (HRP)	Thermo Scientific, Rockford, USA
Complete protease inhibitor cocktail	Roche, Mannheim, Germany
Collagenase	StemCell Technologies, Grenoble, France
DAPI	Life Technologies, Darmstadt, Germany
Dispase	StemCell Technologies, Grenoble, France
Dimethyl sulfoxide (DMSO)	Sigma-Aldrich, Steinheim, Germany
DNase I	StemCell Technologies, Grenoble, France
deoxyribonucleotide triphosphates (dNTPs)	Roche, Mannheim, Germany
Dithiothreitol (DTT)	Life Technologies, Darmstadt, Germany
eFluor® 670	eBioscience, Frankfurt, Germany
ethylenediaminetetraacetic acid (EDTA)	Roth, Karlsruhe, Germany
ethylene glycol tetraacetic acid (EGTA)	Sigma-Aldrich, Steinheim, Germany
Ethanol	Roth, Karlsruhe, Germany
Fetal calf serum (FCS)	Biochrom AG, Berlin, Germany
Fixable blue fluorescent reactive dye	Life Technologies, Darmstadt, Germany

Glycerol	Sigma-Aldrich, Steinheim, Germany
Glycine	Roth, Karlsruhe, Germany
HEPES buffer	PAA Laboratories, Pasching, Austria
Hoechst 33342	Sigma-Aldrich, Steinheim, Germany
Ibidi Mounting Medium	Ibidi, Martinsried, Germany
IC Fixation buffer	eBioscience, Frankfurt, Germany
Iscove's Modified Dulbecco's media (IMDM)	PAA Laboratories, Pasching, Austria
Immobilon™ Western Chemiluminescent HRP Substrate	Merck Millipore, Billerica, USA
Jasplakinolide	Life Technologies, Darmstadt, Germany
Ionomycin	Sigma-Aldrich, Steinheim, Germany
Latrunculin B	Enzo life sciences, Lörrach, Germany
L-Glutamine	PAA Laboratories, Pasching, Austria
Lympholyte®-M	Cedarlane, Ontario, Canada
LysoTracker® Red DND-99 and LysoTracker® Green DND-26	Life Technologies, Darmstadt, Germany
Magnesium chloride ($MgCl_2$)	Roth, Karlsruhe, Germany
Methanol	Roth, Karlsruhe, Germany
Non-essential amino acids	Life Technologies, Darmstadt, Germany
NP-40	Roth, Karlsruhe, Germany
Paraformaldehyde (PFA)	Roth, Karlsruhe, Germany
Penicillin/Streptomycin	PAA Laboratories, Pasching, Austria
Permeabilization Buffer (10X)	eBioscience, Frankfurt, Germany
Phalloidin	Life Technologies, Darmstadt, Germany
Phosphate buffered saline (PBS) 10x	PAA Laboratories, Pasching, Austria
PIPES buffer	Sigma-Aldrich, Steinheim, Germany
Phorbol-12- myristate-13-acetate (PMA)	Sigma-Aldrich, Steinheim, Germany
Potassium chloride (KCl)	Roth, Karlsruhe, Germany
Precise Plus Protein Dual Color Standard	Bio-Rad, Munich, Germany
Recombinant murine IL-3, IL-15, CXCL10, CXCL12 and GM-CSF	R&D Systems, Wiesbaden-Nordenstadt, Germany
Recombinant human M-CSF	Tebu-bio, Offenbach, Germany
Restore™ Plus Western Blot Stripping Buffer	Thermo Scientific, Rockford, USA
Roswell Park Memorial Institute medium (RPMI)	Life Technologies, Darmstadt, Germany
Sodium dodecyl sulfate (SDS)	Roth, Karlsruhe, Germany
Sodium carbonate (Na_2CO_3)	Roth, Karlsruhe, Germany

Sodium chloride (NaCl)	Roth, Karlsruhe, Germany
Sodiume fluoride (NaF)	Roth, Karlsruhe, Germany
Sodium pyruvate	Life Technologies, Darmstadt, Germany
Sodium orthovanadate (Na_3VO_4)	Roth, Karlsruhe, Germany
Streptavidin microspheres	Polyscience, Inc., Eppelheim, Germany
SuperBlock® T20 (TBS) Blocking Buffer	Thermo Scientific, Rockford, USA
Tetramethylethylenediamine (TEMED)	Roth, Karlsruhe, Germany
Tris(hydroxymethyl)aminomethane (Tris)	Roth, Karlsruhe, Germany
Tris hydrochlorid (Tris-HCl)	Roth, Karlsruhe, Germany
Triton X-100 Alternative	Roth, Karlsruhe, Germany
Trypanblue solution	Biochrom AG, Berlin, Germany
Tween20	Sigma-Aldrich, Steinheim, Germany
Vitamins	Life Technologies, Darmstadt, Germany
β-Mercaptoethanol	Life Technologies, Darmstadt, Germany

All chemicals used, were of purity grade pro analysis (p.a.).

3.3 Molecular and cell biology kits and reagents

Kits listed below were purchased from the indicated companies and used according to manufacturer's instructions.

CD49b (DX5) MicroBeads	Miltenyi, Bergisch Gladbach, Germany
CytoTox 96® Non-Radioactive Cytotoxicity Assay	Promega, Mannheim, Germany
DuoSet Elisa Kit (IFN-γ, CCL5)	R&D Systems, Wiesbaden-Nordenstadt, Germany
LightCycler® 480 probes master Kit	Roche, Mannheim, Germany
RNase-Free DNase Set	QIAGEN, Hilden, Germany
RNeasy Plant Mini Kit	QIAGEN, Hilden, Germany
SuperScript™ II Reverse Transcriptase Kit	Life Technologies, Darmstadt, Germany

3.4 Primer and UPL probes

All primers listed in Table 3-1 were synthesized by Metabion (Martinsried, Germany), TaqMan probes from the Universal Probe Library (UPL) for mouse were purchased from Roche (Mannheim, Germany).

Table 3-1. Primer sequences and corresponding UPL probe IDs for real-time PCR

Gene	Primer	Sequence (5'-3' direction)	UPL probe ID
Hprt	HPRT #95 left	TCCTCCTCAGACCGCTTTT	#95
	HPRT #95 right	CCTGGTTCATCATCGCTAATC	
Coro1a	Coro1a #18 left	CTACTTGGGAGGGGTCACG	#18
	Coro1a #18 right	TTTGCTGGAGCGAACCAC	
Coro1b	Coro1a #17 left	TTCAGCCGCATGAGTGAAC	#17
	Coro1a #17 right	GTAGAGCCCCATTGCTTGAA	
Coro7	Coro7 #29 left	ATCACCTGACCCTCACAAGG	#29
	Coro7 #29 right	TCCACATCCTGAATGTCACAC	
IFN-γ	Ifng #21 left	ATCTGGAGGAACTGGCAAAA	#21
	Ifng #21 right	TTCAAGACTTCAAAGAGTCTGAGGTA	

3.5 Antibodies

3.5.1 Antibodies for flow cytometry and immunofluorescence microscopy

Antibodies used for flow cytometry (Table 3-2) were fluorochrome-conjugated and were diluted 1:100 or as stated. For immunofluorescence microscopy, antibodies were used as indicated in methods (see chapter 4.3.2 and Table 3-2).

For detection of unconjugated primary antibodies used for flow cytometry or immunofluorescence microscopy, 1:2000 diluted fluorochrome-conjugated source specific secondary antibodies were used (see Table 3-3).

Table 3-2. Antibodies for flow cytometry and immunofluorescence microscopy

Antibody (clone)	Company
CD3ε (145-2C11) PE/APC	eBioscience, Frankfurt, Germany
CD11b (M1/70) FITC	BioLegend, Fell, germany
CD25 (IL-2Rα) (PC61.5) PE-Cy7	eBioscience, Frankfurt, Germany
CD27 (LG.3A10) APC	BioLegend, Fell, germany
CD43 (S7) FITC	BD Biosciences, Franklin Lakes, USA
CD45R (B220) (RA3-6B2) PE-Cy7	eBioscience, Frankfurt, Germany
CD49b (DX5) FITC	BioLegend, Fell, germany
CD51(Integrin alpha V) (RMV-7) PE	eBioscience, Frankfurt, Germany
CD69 (H1.2F3) PE-Cy7	BioLegend, Fell, germany
CD107a (LAMP-1) (eBio1D4B (1D4B) Alexa Fluor® 488/Alexa Fluor® 647	eBioscience, Frankfurt, Germany
CD117 (c-Kit) (2B8) PE-Cy7	eBioscience, Frankfurt, Germany
CD122 (IL-2Rβ) (TM-β1) PE	BioLegend, Fell, germany
CD127 (IL-7Rα) (A7R34) FITC	eBioscience, Frankfurt, Germany
CD132 (common γ chain) (TUGm2) PE	BD Biosciences, Franklin Lakes, USA
CD314 (NKG2D) (CX5) PE-Cy7	eBioscience, Frankfurt, Germany
CD335 (NKp46) (29A1.4) PE	eBioscience, Frankfurt, Germany
Coro1a (5E10.3.7) DyLight 649	Provided by Niko Föger
Coro1b (2E6.4.4) unconjugated	Provided by Niko Föger
Granzyme A (3G8.5) unconjugated	Santa Cruz, Heidelberg, Germany
Granzyme B (GB12) PE	Life Technologies, Darmstadt, Germany
IFN-γ (XMG1.2) Alexa Fluor® 647	eBioscience, Frankfurt, Germany
KLRG1 (MAFA) (2F1) APC	eBioscience, Frankfurt, Germany
Ly49G2 (eBio 4D11) FITC	eBioscience, Frankfurt, Germany
Ly49H (3D10) FITC	eBioscience, Frankfurt, Germany
NK1.1(PK136) FITC, PE, PerCP-Cy5.5, APC	eBioscience, Frankfurt, Germany
NKG2A/C/E (20d5) FITC	BD Biosciences, Franklin Lakes, USA
Armenian Hamster IgG isotype control (eBio299Arm) PE, PE-Cy7, APC	eBioscience, Frankfurt, Germany
Mouse IgG_1, κ isotype control (P3.6.2.8.1) FITC	eBioscience, Frankfurt, Germany
Mouse IgG_{2a}, κ isotype control (eBM2a) PerCP-Cy5.5	eBioscience, Frankfurt, Germany
Mouse IgG_{2b} negative control	Dako, Hamburg, Germany
Rat anti-mouse IgG_{2b} (R12-3) Biotin	BD Biosciences, Franklin Lakes, USA
Rat IgG_1, κ isotype control PE, PE-Cy7	eBioscience, Frankfurt, Germany
Rat IgM, κ isotype control FITC	eBioscience, Frankfurt, Germany
Rat IgG_{2a}, κ isotype control FITC, PE, PE-Cy7	eBioscience, Frankfurt, Germany
Rat IgG_{2b}, κ isotype control FITC, PE, PE-Cy7	eBioscience, Frankfurt, Germany

Table 3-3. Secondary antibodies and reagents

Antibody	Company
Goat anti-armenian hamster IgG (H+L) DyLight 649-conjugated	Jackson ImmunoResearch, Suffolk, UK
Streptavidin-APC	BioLegend, Fell, Germany

3.5.2 Antibodies used for stimulation

Listed functional grade purified or biotinylated anti-mouse antibodies were used as indicated in methods (4.1.10) to stimulate NK cells.

Table 3-4. Antibodies used for stimulation

Antibody (clone)	Company
NK1.1 Biotin (PK136)	eBioscience, Frankfurt, Germany
NK1.1 Functional Grade Purified (PK136)	eBioscience, Frankfurt, Germany
CD314 (NKG2D) Biotin (A10)	eBioscience, Frankfurt, Germany
CD314 (NKG2D) Functional Grade Purified (A10)	eBioscience, Frankfurt, Germany

3.5.3 Antibodies for Western blotting

Listed antibodies for immunoblot analysis (Table 3-5) were purchased from the indicated companies and used according to manufacturer's instructions or as stated.

Table 3-5. Primary antibodies for Western blotting

Antibody (clone)	Source	Company
ACTIN (I-19)	Goat	Santa Cruz, Heidelberg, Germany
Akt (55/PKBa/Akt)	Mouse	BD Biosciences, Franklin Lakes, USA
Coro1a (5E10.3.7)	Hamster	Provided by Niko Föger
Coro1b (2E6.4.4)	Hamster	Provided by Niko Föger
Coro1b (C-terminus)	Rabbit	ECM Biosciences, Versailles, USA
Erk-2 (C-14),	Rabbit	Santa Cruz, Heidelberg, Germany
GAPDH (6C5)	Mouse	Santa Cruz, Heidelberg, Germany
p-Akt (Ser473) (D9E)	Rabbit	Cell Signaling, Danvers, USA
p-p44/42 MAPK (Erk1/2) (Thr202/Tyr204) (D13.14.4E)	Rabbit	Cell Signaling, Danvers, USA
p-Ser2-Coro1b	Rabbit	ECM Biosciences, Versailles, USA
Perforin (eBioOMAK-D)	Rat	eBioscience, Frankfurt, Germany
Vimentin (RV202)	Mouse	BD Biosciences, Franklin Lakes, USA

For detection of primary antibodies, following horseradish peroxidase-conjugated source specific secondary antibodies were used:

Table 3-6. Secondary antibodies

Antibody	Company
Rabbit anti-goat IgG, HRP-conjugated	Thermo Scientific, Rockford, USA
Goat anti-armenian hamster IgG (H+L)	Jackson ImmunoResearch, Suffolk, UK
Sheep anti-mouse IgG, HRP-conjugated	GE Healthcare, Munich, Germany
Goat anti-rabbit IgG (H&L), HRP-conjugated	Cell Signaling, Danvers, USA
Goat anti-rat IgG, HRP-conjugated	Thermo Scientific, Rockford, USA

Secondary antibodies were diluted 1:30000. Alternatively, Clean-Blot^{TM} IP Detection Reagent (HRP) (1:2000) was used for detection of primary antibodies.

3.6 Laboratory equipment

Analytical Balance SBC 31	Denver Instrument, Göttingen, Germany
AutoMACS®	Miltenyi, Bergisch Gladbach, Germany
Bench MSC Advantage	Thermo Scientific, Rockford, USA
BioPhotometer	Eppendorf, Hamburg, Germany
Centrifuge 5810 R	Eppendorf, Hamburg, Germany
Centrifuge 5415 R	Eppendorf, Hamburg, Germany
Centrifuge 4K15	Sigma, Osterode am Harz, Germany
Confocal laser scan microscope SP5	Leica, Wetzlar, Germany
ELISA reader Infinite M200	Tecan, Männedorf, Switzerland
ELISA washer Anthos fluido	Anthos Microsystems, Krefeld, Germany
FACS Calibur	BD Biosciences, Franklin Lakes, USA
FACS LSRII	BD Biosciences, Franklin Lakes, USA
Incubator Hera Cell 150	Thermo Scientific, Rockford, USA
Intelli-Mixer RM-2M	ELMI Ltd., Riga, Latvia
Kodak M35 X-OMAT processor	Kodak, Rochester, USA
LightCycler 480 System	Roche, Mannheim, Germany
Microscope CK40	Olympus, Hamburg, Germany
Mini Protean® Tetra Cell System	Bio-Rad, Munich, Germany
Mini Trans-Blot® Electrophoretic Transfer Cell System	Bio-Rad, Munich, Germany
ph meter sevenEasy	Mettler-Toledo, Greifensee, Switzerland
Pipettes	Eppendorf, Hamburg, Germany
Precision Balance 440-45 N	Kern, Balingen-Frommern, Germany
Power supply (Power PAC Universal)	Bio-Rad, Munich, Germany
Thermoblock	Grant Instruments, Hillsborough, USA

Thermomixer comfort	Eppendorf, Hamburg, Germany
Shaker Duomax 1030	Heidolph Instruments, Schwabach, Germany
Shaker MS3 basic	IKA, Staufen, Germany
Shaker PMR-30	Grant Instruments, Hillsborough, USA
Water bath	Memmert, Schwabach, Germany

3.7 Laboratory supplies

Amersham Hyperfilm® ECL®	GE Healthcare, Munich, Germany
Cell strainer (40 µm, 70 µm); BD Falcon	BD Biosciences, Franklin Lakes, USA
Centrifugation tubes (15 ml, 50 ml)	Sarstedt, Nümbrecht, Germany
FACS tubes	Sarstedt, Nümbrecht, Germany
HTS Transwell®-96 permeable supports plate with 5 µm pore size	Corning, Corning, USA
ibiTreat µ-Slide VI^{0,4}	Ibidi, Martinsried, Germany
Immobilon™-P PVDF membrane	Merck Millipore, Billerica, USA
LightCycler® 480 Multiwell Plate 96, white	Roche, Mannheim, Germany
LS Columns	Miltenyi, Bergisch Gladbach, Germany
Microcentrifuge tubes (0.5 ml, 1.5 ml, 2 ml)	Sarstedt, Nümbrecht, Germany
Needles	BD Biosciences, Franklin Lakes, USA
6-/24-/96-well cell culture plates	Nunc, Rochester, USA
Petri dish (92 x 16 mm, sterile)	Sarstedt, Nümbrecht, Germany
Petri dish (100 x 15 mm, bacterial grade, non-adherent, sterile); BD Falcon®	BD Biosciences, Franklin Lakes, USA
Pipette tips	Sarstedt, Nümbrecht, Germany
Plastic pipettes (5 ml, 10 ml, 25 ml)	Sarstedt, Nümbrecht, Germany
Tissue culture flasks	Sarstedt, Nümbrecht, Germany
Syringe (1 ml, 5 ml, 10 ml)	BD Biosciences, Franklin Lakes, USA
Whatmann paper	GE Healthcare, Munich, Germany

3.8 Software

FlowJo (version 7.6.5)	Tree Star, Inc., Ashland, USA
ImageJ (version 1.43u)	National Institutes of Health, Bethesda, USA
Leica LAS AF (version 2.4.1)	Leica, Wetzlar, Germany
LightCycler® 480 software (version 1.5 SP4)	Roche, Mannheim, Germany
Magellan (version 6.6)	Tecan, Männedorf, Switzerland
Prism (version 5.03)	GraphPad, La Jolla, USA

4 Methods

4.1 Cell isolation, cultivation and stimulation

4.1.1 Isolation of cells from spleen, lymph nodes, bone marrow and liver

Mice were sacrificed by euthanasia and spleen, lymph nodes, liver as well as the femurs and tibiae were excised. To generate a single-cell suspension, spleen and lymph nodes were mashed through a 40 µm pore size nylon mesh cell strainer using a 5 ml syringe pestle. Cells were centrifuged at 400 x g for 5 minutes (min) at 4°C and erythrocytes were lysed with 2 ml ice cold erythrocyte lysis buffer (0.83% (w/v) NH_4Cl, 0.168% (w/v) Na_2CO_3, 1 mM ethylenediaminetetraacetic acid (EDTA), pH 7.3) for 10 min at room temperature (RT). Cells were washed with YAC-1 medium (RPMI 1640, 10% inactivated fetal calf serum (FCS), 2 mM L-glutamine, 100 µg/ml streptomycin and 100 U/ml penicillin) and counted. All cell washing steps were performed at 400 x g for 5 min at 4°C. For counting, cells were diluted 1:10 in trypan blue solution (0.05% trypan blue in 0.9% NaCl-solution) to enable dead cell exclusion and living cells were counted using a Neubauer counting chamber and an optical microscope. Total spleen cells were used for further analysis or for NK- and B cell purification. Cells obtained from lymph nodes were used together with spleen cells to enrich T cells.

Bone marrow (BM) was flushed out of the femurs and tibiae of mice with phosphate buffered saline (PBS). Cells were centrifuged at 400 x g for 5 min at 4°C and erythrocytes were lysed with 2 ml ice cold erythrocyte lysis buffer for 15 min at RT. Cells were washed with YAC-1 medium and counted. BM cells were used for further analysis or for the generation of bone marrow-derived mast cells (BMMCs), bone marrow-derived dendritic cells (BMDCs) and bone marrow-derived macrophages (BMMΦs).

To isolate liver lymphocytes, the gall bladder was removed from the liver and the organ was cut into small pieces within a petri dish on ice. The liver pieces were portioned into three 15 ml centrifuge tubes and 5 ml collagenase-dispase-medium (IMDM, 5% inactivated FCS, 0.2 mg/ml collagenase, 0.2 mg/ml dispase and 10 µg/ml DNase I; enzymes all from Stemcell Technologies) was added to each tube. The tubes were incubated at 37°C in a water bath for 45 min. Every 3 to 5 min the solution was mixed by pipetting using a Pasteur pipette. The solution was subsequently passed through a 70 µm pore size nylon mesh cell strainer and PBS was added up to 50 ml. Cells were centrifuged at 400 x g for 5 min at 4°C and resuspended in 15 ml YAC-1 medium. Lymphocytes were isolated using Lympholyte®-M according to manufacturer's instructions. In brief, 5 ml cell suspension was layered over 5 ml Lympholyte®-M in a 15 ml centrifuge tube. Tubes were centrifuged at 1250 x g for 20 min at

RT. After centrifugation the interface was removed from the gradient and transferred into a new tube. Lymphocytes were washed three times with YAC-1 medium and counted. Isolated liver lymphocytes were used for further analysis.

4.1.2 Cell cultivation

All primary cells and cell lines were maintained at 37°C, 5% CO_2 and a humidity of 95% in the incubator unless otherwise stated.

4.1.3 Purification and expansion of NK cells

Total spleen cells were isolated as described in 4.1.1. NK cells were enriched by MACS®-separation using CD49b MicroBeads and LS columns according to the manufacturer's instructions. In brief, spleen cells were centrifuged at 300 x g for 10 min at 4°C. The supernatant was discarded and cells were resuspended in 90 µl of MACS®-buffer (PBS, pH 7.2, 0.5% bovine serum albumin (BSA) and 2 mM EDTA) per 10^7 cells. In addition, 10 µl CD49b MicroBeads were added per 10^7 cells, the cell suspension was mixed and incubated for 20 min at 4°C, every 5 min the suspension was mixed by hand. Cells were washed by adding 12 ml MACS®-buffer and centrifuged at 300 x g for 10 min at 4°C. Pellet was resuspended in 500 µl MACS®-buffer and transferred into the equilibrated LS column. Columns were washed three times with MACS®-buffer and then NK cells were eluted. MACS®-buffer was removed by centrifugation and enriched NK cells were cultured in a 12-well cell culture plate in 3 ml NK medium (RPMI 1640, 10% inactivated FCS, 2 mM L-glutamine, 100 µg/ml streptomycin, 100 U/ml penicillin, 1 mM sodium pyruvate, 50 µM β-mercaptoethanol and 10 mM HEPES) supplemented with 50 ng/ml IL-15 (R&D Systems, Wiesbaden-Nordenstadt) for 2 days. At day 2, NK cells were split 1:2. To that end, 1 ml NK medium was removed, adherent cells were detached by pipetting and 1 ml of the cell suspension was transferred to another 12-well. Two ml NK medium supplemented with 50 ng/ml IL-15 was added to each well. On day 3 NK cells were transferred to a 6-well cell culture plate and 3 ml NK medium supplemented with IL-15 (50 ng/ml) were added to each well. The cells were maintained for additional 3 days in the incubator. Phenotypical analysis and functional assays were performed using 6-9 days old NK cells. Within this period, NK cells were cultured at a concentration of about 0.75 x 10^6 cells/ml in a 6-well cell culture plate in the presence of IL-15. Purity was routinely >90% as determined by flow cytometric analysis of CD3 and NK1.1 expression.

4.1.4 Purification of $CD4^+$ and $CD8^+$ T cells

Total spleen cells and cells from the lymph nodes were isolated as described in 4.1.1 and $CD4^+$ or $CD8^+$ T cells were enriched by depletion of unwanted cells. In brief, mixed total

spleen cells and cells from the lymph nodes were centrifuged at 300 x g for 10 min at 4°C. The supernatant was discarded and the pellet was resuspended in MACS®-buffer (1 x 10^8 cells/ml). Cells were incubated with FITC-conjugated monoclonal antibodies (mAbs, 0.5 µl per 10^7 cells) directed against CD11b, CD11c, B220, DX5, F4/80 and CD4 or CD8 to label all cells with the exception of $CD4^+$ or $CD8^+$ cells, for 15 min on ice, every 5 min the suspension was mixed. Cells were washed with MACS®-buffer and incubated with anti-FITC MicroBeads (8 µl MicroBeads per 1 x 10^7 cells) as described before. Cells were washed with MACS®-buffer, the supernatant was discarded and the pellet was resuspended in 1-2 ml MACS®-buffer. Non-T cells and $CD4^+$ or $CD8^+$ cells were depleted using the program "depletes" of the autoMACS®. Purity was routinely >90% as determined by flow cytometric analysis of CD4 and CD8 expression.

4.1.5 Purification of B cells

Total spleen cells were isolated as described in 4.1.1. B cells were enriched by depletion of non-B cells. In brief, total spleen cells were centrifuged at 300 x g for 10 min at 4°C. The supernatant was discarded and the pellet was resuspended in MACS®-buffer (1 x 10^8 cells/ml). Spleen cells were incubated with FITC-conjugated mAbs (0.5 µl per 10^7 cells) directed against Thy1.2, CD11b, CD11c and NK1.1 to label non-B cells, for 15 min on ice, every 5 min the suspension was mixed. Cells were washed with MACS®-buffer and incubated with anti-FITC MicroBeads (8 µl MicroBeads per 1 x 10^7 cells) as described before. Cells were washed with MACS®-buffer, the supernatant was discarded and the pellet was resuspended in 1-2 ml MACS®-buffer. Non-B cells were depleted using the program "depletes" of the autoMACS®. Purity was routinely between 85% and 90% as determined by flow cytometric analysis of CD4, CD8, CD11b, CD11c, NKp46 and CD45R expression.

4.1.6 Generation of bone marrow-derived mast cells

BMMCs were prepared as described previously [269]. In brief, BM cells were isolated as described in 4.1.1 and the BMMCs were selectively grown in BMMC medium (IMDM, 10% inactivated FCS, 2 mM L-glutamine, 100 µg/ml streptomycin, 100 U/ml penicillin, 1 mM sodium pyruvate, 50 µM β-mercaptoethanol, non-essential amino acids and vitamins) in the presence of 10 ng/ml rmIL-3 for 5-10 weeks. Cell purity was routinely determined by flow cytometric analysis of c-Kit, FcεRI-α and T1/ST2 cell surface expression.

4.1.7 Generation of bone marrow-derived macrophages

BMMΦs were generated as described previously [270]. Briefly, bone marrow cells were isolated as described in 4.1.1. Cells were seeded (1 x 10^6 cells/ml) in bacterial grade, non adherent petri dishes in 10 ml BMMΦ medium (RPMI 1640, 10% inactivated FCS, 4 mM

L-glutamine, 50 µg/ml streptomycin, 50 U/ml penicillin, 1 mM sodium pyruvate and non-essential amino acids) supplemented with 20 ng/ml rhM-CSF to induce differentiation. At day 3, 10 ml fresh medium containing 20 ng/ml rhM-CSF was added to the plate. At day 6, 10 ml cell-free culture medium was exchanged by fresh medium containing 10 ng/ml rhM-CSF. After 8 days of culture, cells were harvested using Accutase™ and washed twice with medium. Purity was routinely >95% as determined by flow cytometric analysis of F4/80, CD11c, CD45R, CD3 and NK1.1 expression.

4.1.8 Generation of bone marrow-derived dendritic cells

BMDCs were generated as described previously [271]. In brief, bone marrow cells were isolated as described in 4.1.1. Cells were seeded (0.3 x 10^6 cells/ml) in bacterial grade, non-adherent petri dishes in 10 ml BMDC medium (RPMI 1640, 10% inactivated FCS, 2 mM L-glutamine, 100 µg/ml streptomycin, 100 U/ml penicillin and 50 µM β-mercaptoethanol) supplemented with 20 ng/ml rmGM-CSF to induce differentiation. At day 3, 10 ml medium containing 20 ng/ml rmGM-CSF was added to the plate. At day 6, 10 ml cell-free culture medium was exchanged by fresh medium containing 10 ng/ml rmGM-CSF. After 8 days of culture, cells were harvested using Accutase™ and washed twice with medium. Purity was routinely >95% as determined by flow cytometric analysis of CD11c expression.

4.1.9 Culture of YAC-1 and A20 cells

YAC-1 cells were thawed and propagated in YAC-1 medium. Cells were cultured in YAC-1 medium within a T25 or T75 cell culture flask in the incubator. After 2-3 days of culture, medium was completely exchanged and cells were split in a 1:15 to 1:20 ratio. Aliquots of 2 x 10^6 cells were frozen in 10% dimethyl sulfoxide (DMSO) in FCS. For the use in functional assays, cells were thawed at least one week before the assay and maintained as described above for no longer than 4 weeks.

A20 cells were maintained in BMDC medium within a T75 cell culture flask in the incubator. Cells were seeded at a density of 4 x 10^4 cells/ml and passaged every 2-3 days.

4.1.10 NK cell stimulation

IL-15-expanded NK cells were stimulated either with plate-bound (mRNA-production, intracellular FACS staining, enzyme-linked immunosorbent assay (ELISA) or bead-bound mAbs against NK1.1 or NKG2D (Western blot (WB) analysis, fractionation), 500 ng/ml phorbol-12-myristate-13-acetate (PMA) plus 5 µM ionomycin or left untreated. In brief, for stimulation with plate-bound mAbs, a 24-well cell culture plate was coated with 2.5 µg/ml NK1.1 or NKG2D mAbs in PBS over night at 4°C. The wells were washed three times with PBS and 500 µl NK medium was added. In addition, non-coated wells containing 500 µl NK

medium (medium control) or NK medium supplemented with 2x concentrated PMA/ionomycin were prepared. 1 x 10^6 NK cells were added within 500 µl NK medium containing 10 ng/ml IL-15. The plate was centrifuged at 250 x g for 3 min and incubated at 37°C and 5% CO_2 for the time indicated in each experiment. Cells and cell free supernatants were collected and used for further analysis.

For stimulation with bead-bound NK1.1 mAbs, streptavidin microspheres (6 µm) were coated with mAbs according to manufacturer's instructions. In brief, streptavidin conjugated microspheres (beads) were incubated with biotinylated NK1.1 mAb (10 µg/ml) in binding buffer (PBS, 1% (w/v) BSA) for 30 min at 4°C in a rotating shaker. The beads were washed three times with binding buffer (6000 x g for 5 min at 4°C), counted and adjusted to a concentration of 10 x 10^6/ml. 1 x 10^6 NK cells in 200 µl NK medium supplemented with 10 ng/ml IL-15 were pre-incubated for at least 15 min in a thermo shaker at 37°C. 200 µl NK1.1-coupled beads, NK medium supplemented with 2x concentrated PMA/ionomycin or NK medium (medium control) were added and cells were incubated at 37°C for the time indicated in each experiment. Stimulated cells were lysed and used for SDS-PAGE or subcellular fractionation.

4.2 Quantitative real-time PCR analysis

4.2.1 Total RNA isolation

Total ribonucleic acid (RNA) from resting IL-15-expanded NK cells and other immune cells (B cells, BMDCs, BMMCs, BMMΦs and T cells) or IL-15-expanded NK cells, stimulated with plate-bound mAbs against NK1.1, PMA/ionomycin or left untreated for 1 hour (see 4.1.10) was extracted using the RNeasy Plant Mini Kit according to the manufacturer's instructions.

4.2.2 cDNA synthesis

Total RNA was reverse transcribed to complementary deoxyribonucleic acid (cDNA) using oligo(dt)-primers and SuperScript™ II Reverse Transcriptase according to the manufacturer's instructions. In brief, 1 µg RNA was mixed with 1.25 µl cDNA-synthesis-primer (10 pmol/µl) and H_2O was added to obtain a total volume of 12.5 µl. The mixture was incubated at 70°C for 10 min. To each sample, 12.5 µl of a mixture of 5x first strand reaction buffer, dithiothreitol (DTT), deoxyribonucleotide triphosphates (dNTPs), RNase inhibitor, SuperScript™ II and H_2O (see Table 4-1) were added and reverse transcription was performed at 42°C for 3 hours, following 15 min at 70°C. cDNA was diluted 1:3 with H_2O.

Table 4-1. Mastermix for cDNA synthesis

Components	Volume [µl]
5x first strand reaction buffer	5.0
DTT (0,1 M)	2.5
dNTPs (10 mM)	1.25
RNase inhibitor	0.5
H_2O	2.75
SuperScript™ II (200 U/µl)	0.5
Σ	12.5

4.2.3 Quantitative real-time PCR

To assess *Coro1a* and *Coro1b* gene expression in IL-15-expanded NK cells and other immune cells or *Interferon gamma* (*IFN-γ*) gene expression upon stimulation of IL-15-expanded NK cells, quantitative real-time polymerase chain reaction (quantitative real-time PCR) using TaqMan probes from the Universal Probe Library (UPL, Roche) was performed. For this, cDNAs from resting or stimulated cells were mixed with fluorescent labeled TaqMan probes and target gene-specific primers (for both see section 3.4) as indicated in Table 4-2.

Table 4-2. Mastermix for TaqMan real-time PCR

Components	Volume [µl]
LC 480 probes master	5
Primermix (10 µM)	1
UPL probe	0.1
H_2O	1.9
Σ	8

To this mix, 2 µl diluted cDNA was added and the quantitative real-time PCR was performed in a Roche LightCycler® 480 using the following conditions:

Table 4-3. Conditions for quantitative real-time PCR

	Step	Temperature [°C]	Time	
Pre-incubation	Initial denaturation	95	10 min	
Amplification	Denaturation	95	10 sec	55 cycles
	Annealing	56	30 sec	
	Elongation	72	1 sec	
Cooling		40	∞	

Coro1a, *Coro1b* and *IFN-γ* gene expression was measured relative to *hypoxanthine phosphoribosyltransferase* (*Hprt*) in duplicates. Data were analyzed using the LightCycler® 480 software.

4.3 Flow cytometry and intracellular staining

4.3.1 Analysis of surface molecules

For surface staining, 2 x 10^6 total spleen cells or BM cells, 0.5 x 10^6 liver lymphocytes or 0.25 x 10^6 IL-15-expanded NK cells were incubated with Mouse BD Fc Block™ (anti-mouse CD16/CD32, diluted 1:200) for 15 min at 4°C in a total volume of 50 µl FACS buffer (PBS, 2% (v/v) FCS) within a 96-well round bottom plate. 50 µl FACS buffer supplemented with fluorochrome-conjugated mAbs or corresponding isotype controls (see section 3.5.1) were added and cells were incubated for additional 20 min at 4°C in the dark. After incubation, cells were washed three times with PBS and fixed in 2% (w/v) paraformaldehyde (PFA) in PBS. To exclude dead cells, cells were stained in addition with fixable blue fluorescent reactive dye (diluted 1:500) according to manufacturer's instructions. Flow cytometric analysis of living NK1.1$^+$/CD3$^-$ cells was performed on a FACSCalibur™ or a LSRII. To separate living NK1.1$^+$/CD3$^-$ single cells, gates were set as shown exemplarily in section 10.2. Data were analyzed using the FlowJo software. Cells stained with isotype controls were used as controls.

4.3.2 Intracellular FACS staining

To analyze intracellular contents of Coro1a, Coro1b, F-actin or granzymes, untreated IL-15-expanded NK cells were fixed, permeabilized and incubated with fluorochrome-conjugated mAbs or phalloidin. Briefly, 0.5 x 10^6 cells were stained for NK1.1 and CD3 as described in 4.3.1, fixed in 4% (w/v) PFA in PBS for 45 min at RT and permeabilized with 0.2% (v/v) Triton X-100 in PBS for 5 min at RT. After blocking with blocking buffer (PBS, 1% (w/v) BSA) for 45 min at 4°C, cells were incubated with the following mAbs: Directly fluorescence-labeled mAbs against Coro1a (1:4000) and against granzyme B (GrzB, 1:100), unconjugated mAb against Coro1b (1:10000) + anti-hamster IgG-DyLight 649 secondary Ab (sec. Ab, 1:2000) and mAb against granzyme A (GrzA, 1:100) + anti-mouse IgG_{2b}-Biotin (1:100) + streptavidin-APC (1:200) or phalloidin (1:100). Staining was performed in a total volume of 100 µl blocking buffer within a 96-well round bottom plate and cells were washed with blocking buffer in between incubation with primary and sec. Abs. In addition to the described method, intracellular FACS staining was also performed using fixation- and permeabilization buffers from eBioscience, according to the standard protocol provided by the company. To assess intracellular IFN-γ content upon

activation, IL-15-expanded NK cells were stimulated with plate-bound NK1.1 mAbs, PMA/ionomycin or left untreated for 6 hours, as described in 4.1.10. To block cytokine secretion, 3.0 μg/ml brefeldin A was added after 1 hour of stimulation. Cells were harvested, stained for NK1.1 and CD3, fixed, permeabilized and incubated with fluorescence-labeled mAbs against IFN-γ (1:100) according to standard procedures. Flow cytometric analysis of living $NK1.1^+/CD3^-$ cells and data analysis were performed as described before (4.3.1). Either cells stained with isotype controls or sec. Abs or corresponding knockout cells were used as control.

4.4 SDS polyacrylamide gel elektrophoresis (SDS-PAGE) and Western blot (WB)

4.4.1 Sample preparation

To investigate cellular proteins, 1 x 10^6 resting IL-15-expanded NK cells or cells stimulated with bead-bound mAbs against NK1.1 (5 + 20 min), PMA/ionomycin (20 min) or left untreated (see 4.1.10) were lysed in 100 µl lysis buffer (1% (v/v) NP-40, 50 mM Tris-HCl, pH 8.0, 150 mM NaCl, 1 mM Na_3VO_4, 10 mM NaF and protease inhibitors (complete protease inhibitor cocktail) for 20 min on ice. After centrifugation at 15000 x g at 4°C for 15 min, lysates were collected and used for SDS-Page or were stored at -80°C for further analysis. Prior to electrophoresis, samples were diluted with 4x Laemmli buffer (62.5 mM Tris-HCl, pH 6.8, 20% (v/v) glycerol, 2% (w/v) SDS, 5% (v/v) β-mercaptoethanol, 0.025% (w/v) bromophenol blue) and denaturated at 95°C for 5 min.

4.4.2 SDS-PAGE

For protein separation according to their size, SDS-PAGE was used. In brief, whole cellular lysates were prepared as described in section 4.4.1 and 20 µl of each sample were loaded onto a 4% stacking gel, an 8% gel was used for separating the proteins by size. Gels were prepared as described in Table 4-4.

Gel electrophoresis was performed in the Mini Protean® Tetra Cell System using running buffer (25 mM Tris, 192 mM glycine, 3.5 mM SDS) at 60 V for 20 min followed by 125 V for 75 min. Precise Plus Protein Dual Color Standard was used as molecular weight standard.

Table 4-4. Gel formulations for SDS-PAGE

Components	Stacking gel (4%) Volume [ml]	Separating gel (8%) Volume [ml]
0.5 M Tris-HCl, ph 6.8	0.375	-
1.5 M Tris-HCl, ph 8.8	-	1.875
SDS (10% (w/v))	0.015	0.075
30% acrylamide/bis-acrylamide solution, 37,5:1	0.200	2.0
Ammonium persulfate (10% (w/v); APS)	0.025	0.050
Tetramethylethylenediamine (TEMED)	0.010	0.010
H_2O	0.875	3.5
Σ	1.5	7.5

4.5 Western blotting

For detection, proteins separated by SDS-PAGE were transferred to Immobilon™-P PVDF membranes (Millipore) using the Mini Trans-Blot® Electrophoretic Transfer Cell System and blotting buffer (25 mM Tris, 192 mM glycine, 0.9 mM SDS, 10% (v/v) methanol, pH 8.3) at 100 V, constant, 350 mA for 1 hour. Following transfer, membranes were blocked with SuperBlock® T20 (TBS) Blocking Buffer for 1 hour at RT and incubated with the indicated primary antibodies (see section 3.5), diluted in SuperBlock®, over night at 4°C on a shaker. Membranes were washed three times with washing buffer (145 mM NaCl, 10 mM Tris-HCL, ph 7.4, 0.05% Tween-20) and incubated with peroxidase-conjugated sec. mAbs, diluted in washing buffer, for 1 hour at RT on the shaker. Membranes were washed again, and proteins were visualized using Immobilon™ Western Chemiluminescent HRP Substrate, Amersham Hyperfilm™ ECL™ and Kodak M35 X-OMAT processor. If necessary, membranes were stripped with Restore™ Plus Western Blot Stripping Buffer according to manufacturer's instructions and further proteins were analyzed as described above.

4.6 Immunofluorescence microscopy

To visualize the subcellular distribution of Coro1a and Coro1b in conjugated and unconjugated IL-15-expanded NK cells, confocal microscopy was used. 6 x 10^4 NK cells were transferred in 30 µl NK medium containing 5 ng/ml IL-15 into a channel of an ibiTreat µ-Slide VI$^{0.4}$ and allowed to attach to the bottom for 30 min at 37°C and 5% CO_2 in the incubator. For the analysis of single cells, NK cells were fixed immediately using 4% PFA in PBS for 45 min at RT. To form NK cell-YAC-1-conjugates, slides were washed with NK medium and YAC-1 cells were added in a NK-YAC-1-ratio of 1:3. Cells were co-cultured for 30 min at 37°C, 5% CO_2 in the incubator and fixed as described before. After

permeabilization with 0.2% Triton X-100 in PBS for 5 min at RT, cells were blocked with blocking buffer and immunofluorescence labeling was performed as described before (4.3.2). Specificity of the coronin-staining was confirmed by using *Coro1a*$^{-/-}$*Coro1b*$^{-/-}$ NK cells as controls. In addition, cells were incubated with phalloidin and 4',6-Diamidino-2-Phenylindole, Dihydrochloride (DAPI) to visualize F-actin and DNA. Slides were mounted with Ibidi Mounting Medium and stored at 4°C.

To investigate granule polarization, IL-15-expanded NK cells were cultured in NK medium supplemented with 5 ng/ml IL-15 and 10 µM LysoTracker® Red DND-99 or LysoTracker® Green DND-26 in a ibiTreat µ-Slide VI$^{0.4}$ for 2 hours at 37°C and 5% CO_2 in the incubator. Conjugates were generated as described before, cells were fixed and permeabilized by incubation with ice cold methanol (5 min at -20°C) followed by treatment with ice cold acetone for 1 min at -20°C. DNA was visualized by staining with bisbenzimide H 33342 trihydrochloride (Hoechst 33342). Specificity of the LysoTracker®-labeling was confirmed by staining with fluorochrome-conjugated mAbs against CD107a, as control. Cells were analyzed using a scanning confocal microscope (TSC SP5). Image analysis was performed using Leica LAS AF Lite software.

4.7 Transwell migration assay

To assess chemokine-mediated migration of IL-15-expanded NK cells a transwell system was used. In brief, NK cells were washed twice with serum free NK medium (RPMI 1640 supplemented with 5 ng/ml IL-15 and 0.5% BSA and adjusted to a concentration of 1.3 x 10^6 cells/ml. 235 µl serum free NK medium with or without recombinant mouse chemokine (C-X-C motif) ligand (CXCL)-10 or CXCL12 in different concentrations were added to the reservoir plate of a HTS Transwell®-96 permeable supports plate with 5 µm pore size. In addition, some wells of the reservoir plate were filled with 25 µl NK cell suspension (33% of the input) and 210 µl serum free NK medium as input control. Finally, 75 µl of the NK cell suspension were added to the 96-well permeable support inserts and the plate was incubated for 4 hours at 37°C and 5% CO_2. For each condition, triplicates were performed. Subsequent to the incubation, the 96-well permeable support inserts were removed, cells were resuspended thoroughly and transferred into FACS tubes. Cells were counted using an LSRII flow cytometer by measuring for a period of 45 sec. The amount of cells, which migrated towards the chemokines was calculated as percentage of the input.

4.8 *In vitro* lactate dehydrogenase (LDH)-based killing assay

To measure cytotoxicity of IL-15-expanded NK cells *in vitro*, CytoTox 96® Non-Radioactive Cytotoxicity Assay was performed according to a standard protocol provided by the company. In brief, YAC-1 cells were plated at a density of 1 x 10^4 cells/well in a volume of

50 µl NK medium supplemented with 5% FCS and 5 ng/ml IL-15 in a 96-well round bottom plate. NK cells, adjusted to effector-target-ratios of 4:1 to 1:1 were added in a volume of 50 µl medium, composed as described before, in triplicates. As controls, wells containing only indicated numbers of NK cells or YAC-1 cells or only medium were prepared. The plate was centrifuged at 250 x g for 3 min and incubated for 4 hours at 37°C and 5% CO_2. Forty-five min prior to harvesting cell free supernatants, 10 µl of 10x lysis solution, provided with the kit, was added to the corresponding wells to obtain target cell maximum LDH release. Following incubation, plate was centrifuged at 250 x g for 3 min and 50 µl of supernatant was transferred into a 96-well flat bottom plate. To assess release of cytoplasmic LDH as a measure of cytotoxicity colorimetric, 50 µl of reconstituted LDH Substrate Mix, provided with the kit, was added and plates were incubated for 30 min at RT in the dark. The reaction was stopped and absorbance at 490 nm was recorded using an Infinite® M200 reader. Cytotoxicity was calculated as suggested by the manufacturer according to the following formula: % specific lysis = (experimental lysis - effector spontaneous lysis - target spontaneous lysis)/(target maximum lysis - target spontaneous lysis) x 100.

4.9 Flow cytometric conjugate assay

Intercellular conjugate formation of IL-15-expanded NK cells was investigated by two-color flow cytometry as described previously [272]. Briefly, 4 x 10^6 NK cells were labeled with 0.25 µM carboxyfluorescein diacetate succinimidyl ester (CFDA-SE, Molecular Probes) and 15 x 10^6 YAC-1 cells with 2 µM eFluor® 670, according to manufacturer's instructions. Labeled cells were adjusted to a concentration of 1 x 10^6 cells/ml (NK cells) and 2 x 10^6 cells/ml (YAC-1) with NK medium supplemented with 5% FCS and 5 ng/ml IL-15 and stored for 15 min on ice. 100 µl NK- and YAC-1 cell suspension were added to a FACS round bottom tube, respectively. Cells were mixed and immediately centrifuged at 20 x g for 1 min at 4°C. Tubes were incubated at 37°C in a water bath for the indicated time points. Following incubation, cells were mixed at 2500 rpm for 3 s on a vortexer and immediately fixed by adding 300 µl ice-cold 0.5% PFA in PBS. For each time point triplicates were performed. Flow cytometric analysis of intercellular conjugates was performed using an LSRII flow cytometer. Data were analyzed as described in 4.3.1. Single labeled NK- and YAC-1 cells were used to set up the gates. To assess the specificity of the assay, NK cells were co-cultured with labeled BMMCs or A20 cells as described above for YAC-1.

4.10 Cytoskeleton-rich fraction isolation

For the isolation of the cytoskeleton-containing detergent-insoluble and the cytosolic detergent-soluble fraction, stimulated IL-15-expanded NK cells were subjected to subcellular fractionation as previously described by Gatfield *et al*. [215]. In brief, NK cells (1 x 10^6 cells)

were stimulated with bead-bound mAbs against NK1.1 (2, 5, 20 and 60 min), PMA/ionomycin (20 min) or left untreated as described in 4.1.10. Alternatively cells were treated with 10 µM latrunculin B for 30 min to depolymerize the cellular F-actin. Cell pellets were suspended in 0.3 ml ice-cold cytoskeleton isolation buffer (1% (v/v) TritonX-100 in 80 mM Pipes, pH 6.8, 5 mM ethylene glycol tetraacetic acid (EGTA) and 1 mM $MgCl_2$) and immediately centrifuged at 3000 x g for 3 min to obtain the detergent-insoluble cytoskeleton-containing fraction (P) and the detergent-soluble cytosolic fraction (S). Equal cell equivalents were subjected to SDS-PAGE and Western blotting (see 4.4 and 4.5).

4.11 CD107a-degranulation assay

To assess NK cell degranulation, the surface expression of the lysosome-associated membrane protein 1 (LAMP-1, CD107a) upon activation was measured by flow cytometry. In resting cells, CD107a is predominantly expressed intracellularly on the membrane of secretory lysosomes and endosomes. Upon activation, secretory lysosomes are released and CD107a becomes accessible for antibody-binding on the surface of NK cells due to fusion of the lysosomal membrane with the outer cell membrane [273]. Therefore, CD107a was used as a marker for NK cell degranulation.

1 x 10^5 IL-15-expanded NK cells were co-cultured with or without 2 x 10^4 YAC-1 cells in 100 µl NK medium supplemented with 5% FCS, 5 ng/ml IL-15 and 2 µg/ml AlexaFluor 647-labeled anti-mouse CD107a mAbs within a 96-well round bottom plate for 3 hours at 37°C and 5% CO_2 in the incubator. The plate was centrifuged at 250 x g for 3 min after all components had been added. Following incubation, the reaction was stopped by adding cold FACS buffer. Surface staining of NK1.1 and CD3 was performed as described in 4.3.1 and degranulation of $NK1.1^+/CD3^-$ NK cells was analysed by flow cytometry using an LSRII flow cytometer as mentioned before.

To investigate the role of the actin cytoskeleton during degranulation, 1 x 10^5 IL-15-expanded NK cells were co-cultured with or without 5 x 10^4 YAC-1 cells in the presence of 10 µM latrunculin B for depolymerization of F-actin, 1 µM jasplakinolide for stabilizing actin filaments or left untreated for 2 hours and analyzed as described above. Drugs were added directly or after 10 min of incubation. As control, cells were treated with carrier (ethanol (EtOH) for latrunculin B and DMSO for jasplakinolide).

4.12 Cytokine measurement by ELISA

For the analysis of cytokine secretion, 1 x 10^6 IL-15-expanded NK cells were stimulated with plate-bound mAbs against NK1.1 and NKG2D, PMA/ionomycin or left untreated for 20 hours as described in 4.1.10. Cell free supernatants were collected and subjected to ELISA. For

this, DuoSet ELISA Development Kits were used and IFN-γ and CCL5 (RANTES) concentration was measured according to manufacturer's instructions.

4.13 Statistical analysis

All parametric data are presented as mean ± standard error of the mean (SEM) for pooled data from at least three independent experiments or mean ± standard deviation (SD) for representative experiments, performed in duplicates or triplicates, as indicated in the legends. One experiment includes data from at least one mice of each genotype. FACS data from one representative experiment of at least three are shown. The Mann-Whitney test was used for statistical analysis, unless stated otherwise. A p-value of <0.05 was considered statistically significant. (* $p < 0.05$; ** $p < 0.01$).

5 Results

Coro1a and Coro1b are members of the evolutionary highly conserved family of actin-regulatory coronin proteins. Both proteins have been implicated in various actin-mediated cellular functions in leukocytes like cell migration and motility [187,204], degranulation [222] and phagocytosis [187,248,250,252]. The loss of Coro1a-function in humans and mice as consequence of mutation or deletion results in a SCID, which is associated with defective actin-regulation in T lymphocytes [204,259–262]. SCIDs are a heterogeneous group of inborn genetic disorders which are mainly characterized by impaired T-, B- and NK cell development and function leading to opportunistic infections and early death unless treated [274,275]. Furthermore, Coro1a is also required for the survival of mycobacteria in phagosomes of infected macrophages [252,265]. However, up to now little is known about the impact of *coronin*-deficiency on NK cell development and function. Therefore, in the present study, the role of Coro1a and Coro1b in the biology and function of NK cells was investigated utilizing as a model *Coro1a*- and/or C*oro1b*-deficient mice.

5.1 Coro1a and Coro1b are co-expressed in NK cells

Coronins exhibit heterogeneous expression patterns. While Coro1a is mainly expressed in cells of the hematopoietic lineage and has been described in neutrophils, macrophages, dendritic cells, T- and B cells as well as mast cells [184,187,204,222,248,253,256–258], Coro1b shows ubiquitous expression and likely assumes a more general regulatory function within and outside the hematopoietic cell lineage [187,212,222–225].

To investigate the impact of Coro1a and Coro1b on NK cell function, the expression patterns of both proteins were analyzed. As a first step, real-time PCR analysis was performed to determine gene expression levels in NK cells (see section 4.2). Levels of *Coro1a*- and *Coro1b* gene expression were measured and normalized to the expression of the housekeeping gene *hypoxanthine phosphoribosyltransferase* (*Hprt)* in each sample. To evaluate the level of *Coro1a*- and *Coro1b* mRNA expression in NK cells, other immune cell types were used for comparison. *Coro1a*- as well as *Coro1b* mRNA was detected in *wild type* NK cells (gray bars) and in all other *wild type* immune cells investigated (Figure 5-1, left panel). As expected, the analysis of *Coro1a*$^{-/-}$ (green bars), *Coro1b*$^{-/-}$ (blue bars) and *Coro1a*$^{-/-}$*Coro1b*$^{-/-}$ NK cells (red bars) revealed no expression of either *Coro1a*- or *Coro1b* mRNA in the corresponding knockout NK cells (Figure 5-1, right panel), demonstrating the specificity of the assay. The expression levels of *Coro1a* mRNA in *Coro1b*-deficient NK cells and *Coro1b* mRNA in *Coro1a*-deficient NK cells were comparable to *wild type* amounts. The additional analysis of *Coro7* gene expression, a further member of the coronin-family, used

as internal control, revealed similar mRNA expression levels for all genotypes of NK cells (data not shown).

Together these data indicate the co-expression of *Coro1a* and *Coro1b* in NK cells, at least at the mRNA level.

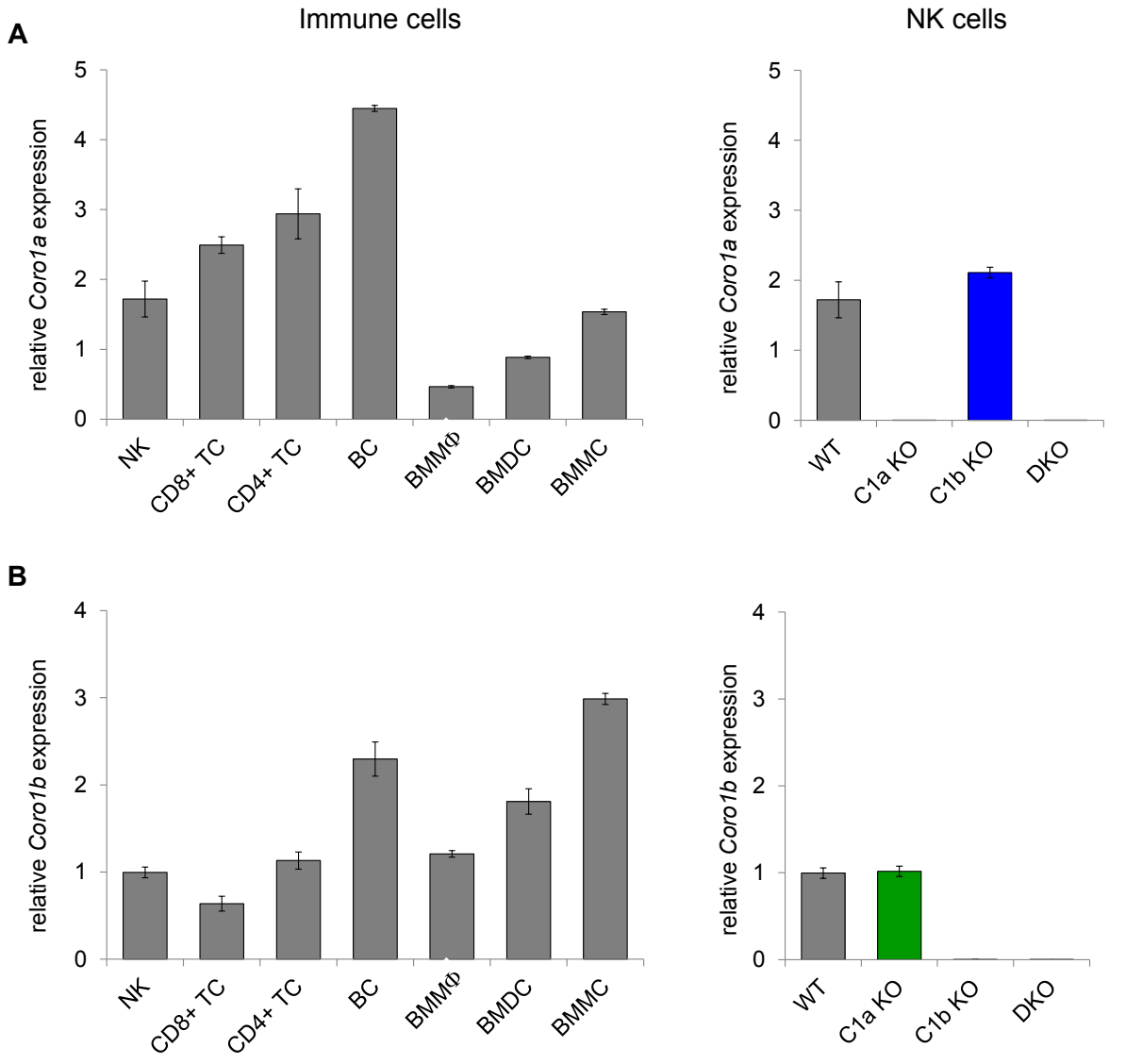

Figure 5-1. Expression of *Coro1a*- and *Coro1b* mRNA in NK cells and other immune cells.
RNA from *wild type* IL-15-expanded NK cells (NK), purified mouse primary $CD8^+$- ($CD8^+$ TC) and $CD4^+$ T cells ($CD4^+$ TC) as well as B cells (BC) and bone marrow-derived macrophages (BMMΦ), dendritic cells (BMDC) and mast cells (BMMC) (left panels) as well as from *wild type* (WT), *Coro1a*$^{-/-}$ (C1a KO), *Coro1b*$^{-/-}$ (C1b KO) and *Coro1a*$^{-/-}$*Coro1b*$^{-/-}$ (DKO) IL-15-expanded NK cells (right panels) was isolated and cDNA was synthesized. Quantitative real-time PCR analysis using *Coro1a*- and *Coro1b* specific primers was performed to investigate *Coro1a*- (A) and *Coro1b* mRNA (B) expression. Data are relative to *Hprt* and show the mean ± SD of one representative experiment in duplicate out of three experiments performed for the NK cells or one experiment for the other immune cells.

In the next step, the cellular Coro1a- and Coro1b protein content in NK cells was investigated. To this end, two different approaches were used. The protein levels were either assessed by flow cytometry after intracellular staining for Coro1a or Coro1b, as described in

section 4.3. (Figure 5-2 A) or by an immunoblot assay of whole NK cell lysates (see section 4.4 and 4.5) as shown in Figure 5-2 B.

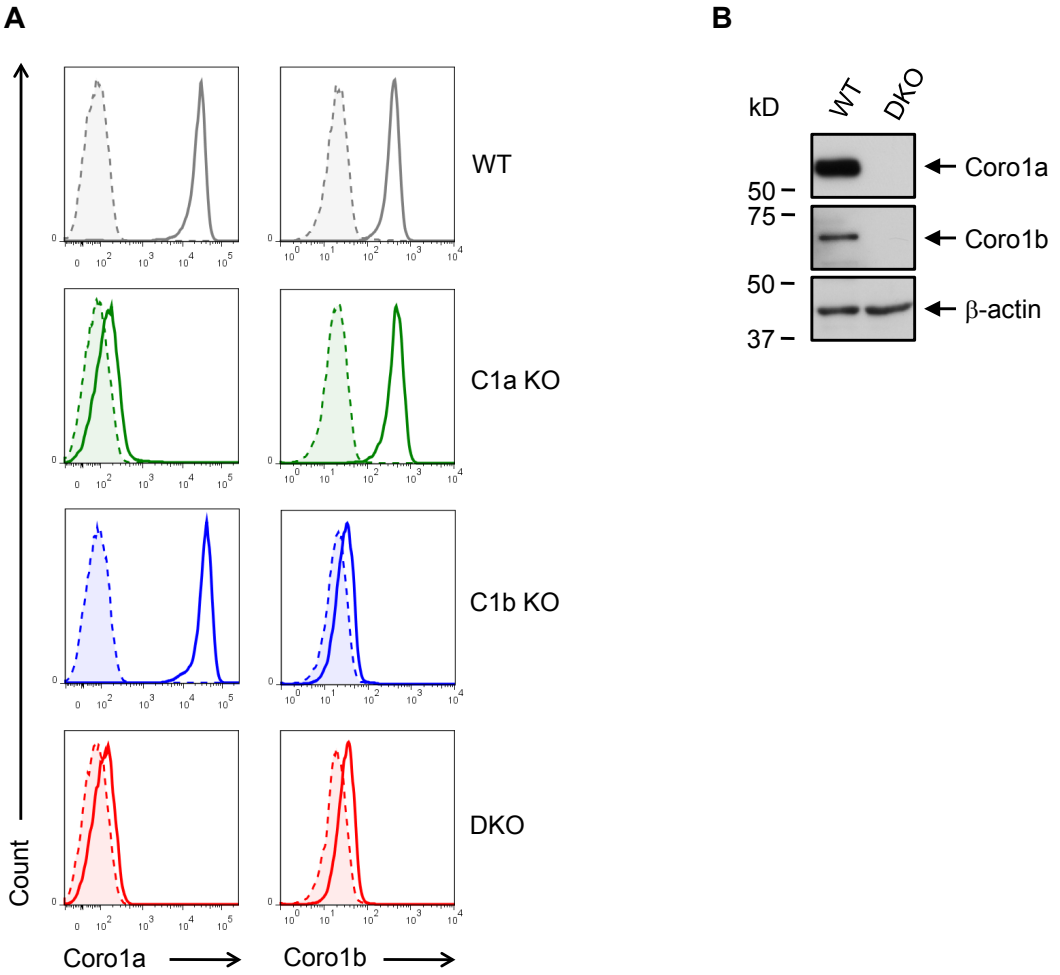

Figure 5-2. Coro1a and Coro1b protein expression in NK cells.
(A) Cellular Coro1a or Coro1b content of IL-15-expanded *wild type* (WT, gray), *Coro1a*$^{-/-}$ (C1a KO, green), *Coro1b*$^{-/-}$ (C1b KO, blue) and *Coro1a*$^{-/-}$*Coro1b*$^{-/-}$ (DKO, red) NK1.1^{+}/CD3^{-} NK cells was assessed by flow cytometry. NK cells were fixed, permeabilized and stained with specific antibodies for either Coro1a (left panel) or Coro1b (right panel). Data shown are representative of at least three independent experiments. Solid lines show protein staining and filled histograms with dashed lines show either the matching isotype control (Coro1a) or single staining with the secondary antibody (Coro1b).
(B) Immunoblot analysis of Coro1a (upper panel) and Coro1b expression (middle panel) in IL-15-expanded NK cells of the indicated genotype. Data are representative for at least three independent experiments. Protein loading was assessed by analysis of β-actin expression (lower panel).

Results from these studies confirmed the expression of Coro1a and Coro1b in *wild type* NK cells (WT), as shown by the gray histograms in Figure 5-2 A (upper panel) and the corresponding protein bands in Figure 5-2 B (upper and middle panel). In addition, Coro1a or Coro1b were detected in *wild type* amounts in the non-corresponding NK cell knockout genotypes shown by the green (*Coro1a*$^{-/-}$) and blue histograms (*Coro1b*$^{-/-}$) of Figure 5-2 A, thus indicating the absence of a compensatory counter-regulation. No protein expression of

Coro1a or Coro1b was found in the corresponding NK cell knockout genotypes (Figure 5-2 A). Furthermore, neither Coro1a nor Coro1b was detected in *Coro1a*$^{-/-}$*Coro1b*$^{-/-}$ NK cells (DKO) by flow cytometry (Figure 5-2 A, red histograms) or Western blotting (Figure 5-2 B).
In conclusion, these data confirmed the co-expression of Coro1a and Coro1b at the protein level in NK cells and thus suggest a potential role of both proteins in the regulation of actin-dependent processes in NK cell development and function.

5.2 Subcellular localization of Coro1a and Coro1b in NK Cells

Subject to the various functions, coronins have been described to be localized at different sites within mammalian cells. Coro1a colocalizes with the F-actin surrounding phagocytic vesicles in neutrophils and macrophages, as well as the F-actin-rich cortex of T cells and mast cells and accumulates at the leading edge of migrating neutrophils [187,203,204,222,252,255]. In contrast to Coro1a, only little is known about the subcellular localization of Coro1b. It localizes with the Arp2/3-complex to the leading edge of migrating fibroblast, however, further data indicate a distribution which is distinct from the one of Coro1a [212,222,224]. Since no information is available on the subcellular distribution of Coro1a and Coro1b in NK cells, the cellular localization of both proteins was investigated by confocal microscopy. NK cells were fixed, permeabilized and stained for either Coro1a or Coro1b and treated with phalloidin to stain F-actin as described in materials and methods (section 4.6). Confocal microscopy revealed that Coro1a was mainly localized at the cortex of NK cells, where it colocalized with F-actin as indicated by the yellow color in the overlay image (Figure 5-3 A, left panel). Additionally, Coro1a also exhibits some punctate cytoplasmic staining. As depicted in the left panel of Figure 5-3 B, Coro1b staining resulted in a more punctate staining distributed throughout the entire cytoplasm with only minor colocalization with the F-actin-rich cell cortex. No Coro1a- and Coro1b staining was detected in *Coro1a*$^{-/-}$*Coro1b*$^{-/-}$ NK cells, which were used as negative control (Figure 5-3, A and B, right panel).
In summary, these data indicate a differential subcellular distribution of Coro1a and Coro1b in NK cells. Coro1a was mainly localized to the F-actin-rich cell cortex, while Coro1b was found throughout the entire cytoplasm.
In addition, confocal microscopy analysis interestingly revealed that the loss of Coro1a and Coro1b resulted in a more pronounced phalloidin (F-actin) staining, indicating a role of the coronins in actin-regulation in NK cells.

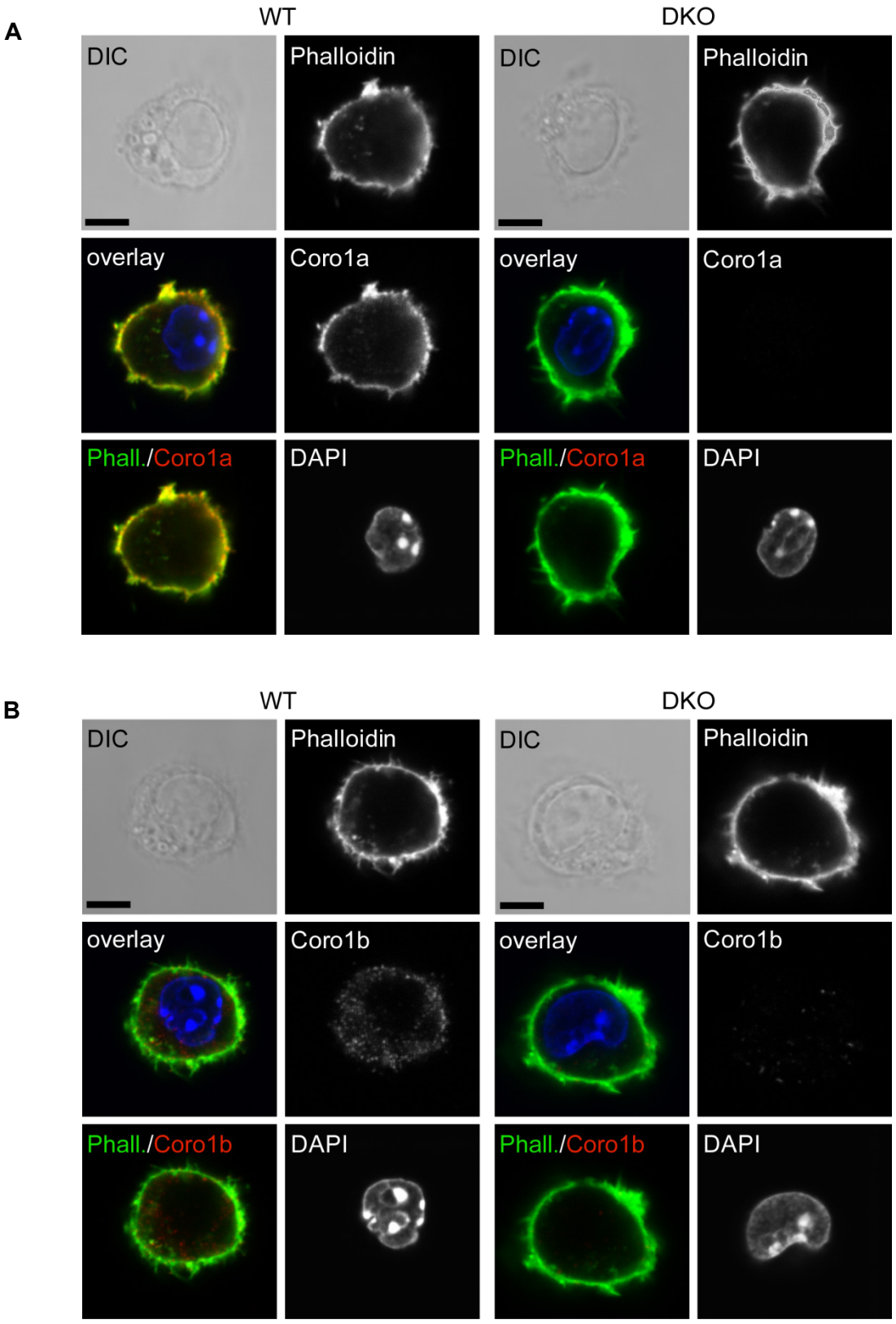

Figure 5-3. Subcellular localization of Coro1a and Coro1b in NK cells.
Subcellular localization of Coro1a or Coro1b was revealed in *wild type* (WT) and *Coro1a*$^{-/-}$*Coro1b*$^{-/-}$ (DKO) IL-15-expanded NK cells by confocal microscopy. NK cells were stained for either Coro1a (A, red) or Coro1b (B, red), F-actin (phalloidin, green) and DNA (DAPI, blue) after fixation and permeabilization. Representative individual or overlay fluorescence and DIC images of at least three independent experiments are shown. Bars, 5 µm.

5.3 Increased cellular F-actin levels in *Coro1a*-deficient NK cells

As loss of Coro1a greatly affects basal F-actin contents in T cells but only minimally affects them in mast cells, coronin-driven actin-regulation seems to be cell type and/or context dependent [204,222,259,260]. This is true for mammalian but has also been described for yeast coronins [233]. In accordance to T cells, the steady-state F-actin level in *Coro1a*$^{-/-}$*Coro1b*$^{-/-}$ NK cells appeared to be notably increased as observed by confocal microscopy and described in the previous section.

To gain further insights on the quantitative differences, the basal F-actin levels in *wild type* (WT) and *Coro1a*- and/or *Coro1b*-deficient NK cells were analyzed in greater detail. NK cells were fixed, permeabilized and incubated with phalloidin (stains F-actin) as described in section 4.3.2. After that, cellular F-actin levels were assessed by flow cytometry. As shown in Figure 5-4 A and B, the analysis revealed a significant, at least two-times higher steady-state level of F-actin in *Coro1a*$^{-/-}$ (green, C1a KO) and *Coro1a*$^{-/-}$*Coro1b*$^{-/-}$ NK cells (red, DKO) compared to *wild type* (gray). Only slight differences in cellular F-actin levels were observed between *wild type* and *Coro1b*$^{-/-}$ NK cells (blue, C1b KO, Figure 5-4, A and B).

In summary, these findings confirmed the accumulation of F-actin in *Coro1a*$^{-/-}$ and *Coro1a*$^{-/-}$*Coro1b*$^{-/-}$ NK cells, indicating the actin-regulatory role of Coro1a in these cells.

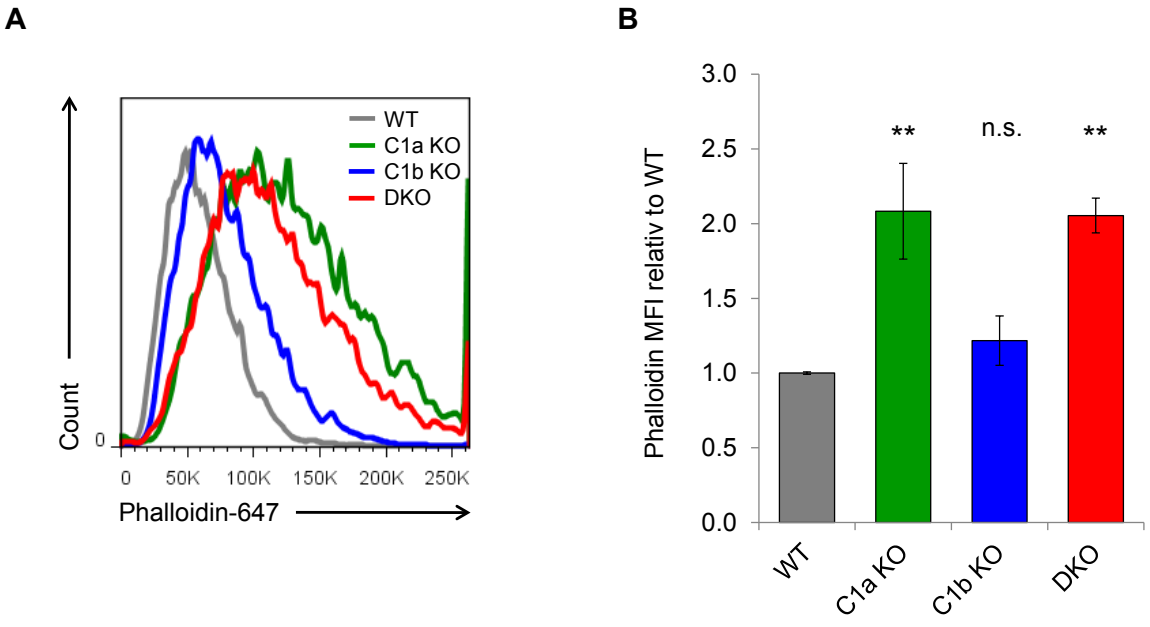

Figure 5-4. Increased cellular F-actin levels in *Coro1a*$^{-/-}$ and *Coro1a*$^{-/-}$*Coro1b*$^{-/-}$ NK cells.
Cellular F-actin content of IL-15-expanded *wild type* (WT, gray), *Coro1a*$^{-/-}$ (C1a KO, green), *Coro1b*$^{-/-}$ (C1b KO, blue) and *Coro1a*$^{-/-}$*Coro1b*$^{-/-}$ (DKO, red) NK1.1^{+}/CD3^{-} NK cells was assessed by flow cytometry. NK cells were fixed, permeabilized and treated with phalloidin to stain F-actin. Data show a representative FACS staining (A) and results from at least 4 independent experiments (B) (Mean ± SEM; WT n=7, C1a KO n=4, C1b KO n=4, DKO n=6), ** p<0,01, n.s. - not significant.

5.4 CXCL10 and CXCL12- induced migration of *Coro1a*$^{-/-}$ and *Coro1a*$^{-/-}$*Coro1b*$^{-/-}$ NK cells is impaired by the loss of Coro1a

One important property of immune cells, which has been directly linked to the actin cytoskeleton, is cell migration [276]. Since early days of coronin research it is known that Coro1a is required for cellular motility of *D. discoideum* [194]. Furthermore, it has been shown that the loss of Coro1a-function in T cells results in defective chemokine-mediated migration and impaired thymic egress [204]. Thus, the functional impact of *Coro1a*- and/or *Coro1b*-deficiency on NK cell migration was analyzed.

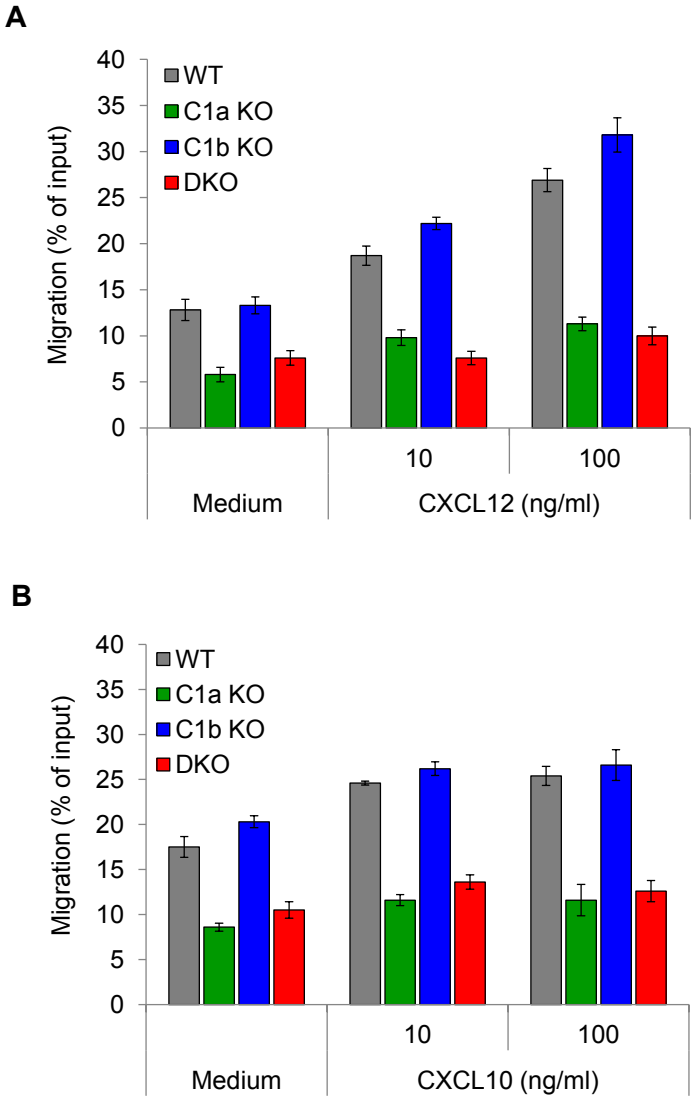

Figure 5-5. Defective migration of *Coro1a*$^{-/-}$ and *Coro1a*$^{-/-}$*Coro1b*$^{-/-}$ NK cells.
Migratory response of w*ild type* (gray bars), *Coro1a*$^{-/-}$ (green bars), *Coro1b*$^{-/-}$ (blue bars) and *Coro1a*$^{-/-}$*Coro1b*$^{-/-}$ (red bars) IL-15-expanded NK cells was investigated using a transwell assay. NK cells were incubated with either CXCL12 (A) or CXCL10 (B) at the indicated concentrations for 4 hours. The numbers of migrated cells were counted by flow cytometry. Data shown (Mean ± SD) are representative of at least three independent experiments in triplicates.

The chemokine-mediated migratory response of NK cells was assessed using a classical transwell migration assay as described in section 4.7. NK cells were exposed to the indicated concentrations of CXCL10 and CXCL12 chemokines or left untreated (Figure 5-5). After 4 hours of incubation, cells which migrated through the transwell-membrane towards the chemokines were recovered from the lower reservoir of the plate and were counted. Migration was calculated as percentage of cells originally seeded in the transwell-insert (input). Results from this study revealed a defective chemokine-mediated migration of *Coro1a*$^{-/-}$ (green bars) and *Coro1a*$^{-/-}$*Coro1b*$^{-/-}$ NK cells (red bars) as shown in Figure 5-5 A and B. Both genotypes showed a more than 50% decreased migratory response towards CXCL12 and CXCL10 compared to *wild type* levels (gray bars). Spontaneous migration was equally impaired as shown in Figure 5-5 (Medium-control). While in *wild type* NK cells the migratory response to chemokines strongly increased in a dose-dependent manner (Figure 5-5 A), the dose-dependent effect of the chemokines on the migration of *Coro1a*$^{-/-}$ and *Coro1a*$^{-/-}$*Coro1b*$^{-/-}$ NK cells was only minimal. Chemokine-mediated- and spontaneous migration of *Coro1b*$^{-/-}$ NK cells (blue bars) was almost comparable to *wild type* levels, suggesting no major role of Coro1b in the regulation of actin-dependent processes during chemotaxis in NK cells.

Together these findings demonstrate a critical role of Coro1a in chemokine-mediated NK cell migration which correlates with an actin-regulatory function of Coro1a in these cells. In contrast, Coro1b seems to play only a minor role in these processes.

5.5 *Coro1a*-deficiency affects absolute numbers of naïve NK cells in the bone marrow but not in the spleen

In humans and mice, loss of Coro1a-function results in a strong reduction in the number of peripheral T cells, while only a limited amount of data suggests that NK cell numbers seem to be unaffected [204,259–262]. Hence, absolute numbers of naïve NK cells in the bone marrow and in the spleen of *Coro1a*- and/or *Coro1b*-deficient mice were analyzed in greater detail.

To this end, freshly isolated single cells from bone marrow and spleen of six to ten weeks old mice, were stained for NK1.1 and CD3 (see section 4.1.1 and 4.3.1) and percentages of naïve NK cells, defined as NK1.1^{+}/CD3^{-} cell population, were assessed by flow cytometry (Figure 5-6 A). In addition, total numbers of viable bone marrow- and spleen cells were determined and absolute cell numbers were calculated by multiplying the total viable cell number by the percentage of NK1.1^{+}/CD3^{-} cells. Low percentages of naïve NK cells were present in the bone marrow (BM), which increased in the spleen in all genotypes (Figure 5-6 A). Interestingly, the percentage and absolute number of naïve NK cells, was higher in the bone marrow of *Coro1a*$^{-/-}$ mice (C1a KO), compared to *wild type* (WT) controls (Figure 5-6, A

and B, BM). A similar increase of NK cells was also observed in the bone marrow of *Coro1a*$^{-/-}$*Coro1b*$^{-/-}$ mice (DKO), while the analysis of the bone marrow from *Coro1b*$^{-/-}$ mice (C1b KO) revealed no differences to *wild type*s (Figure 5-6, A and B, BM).

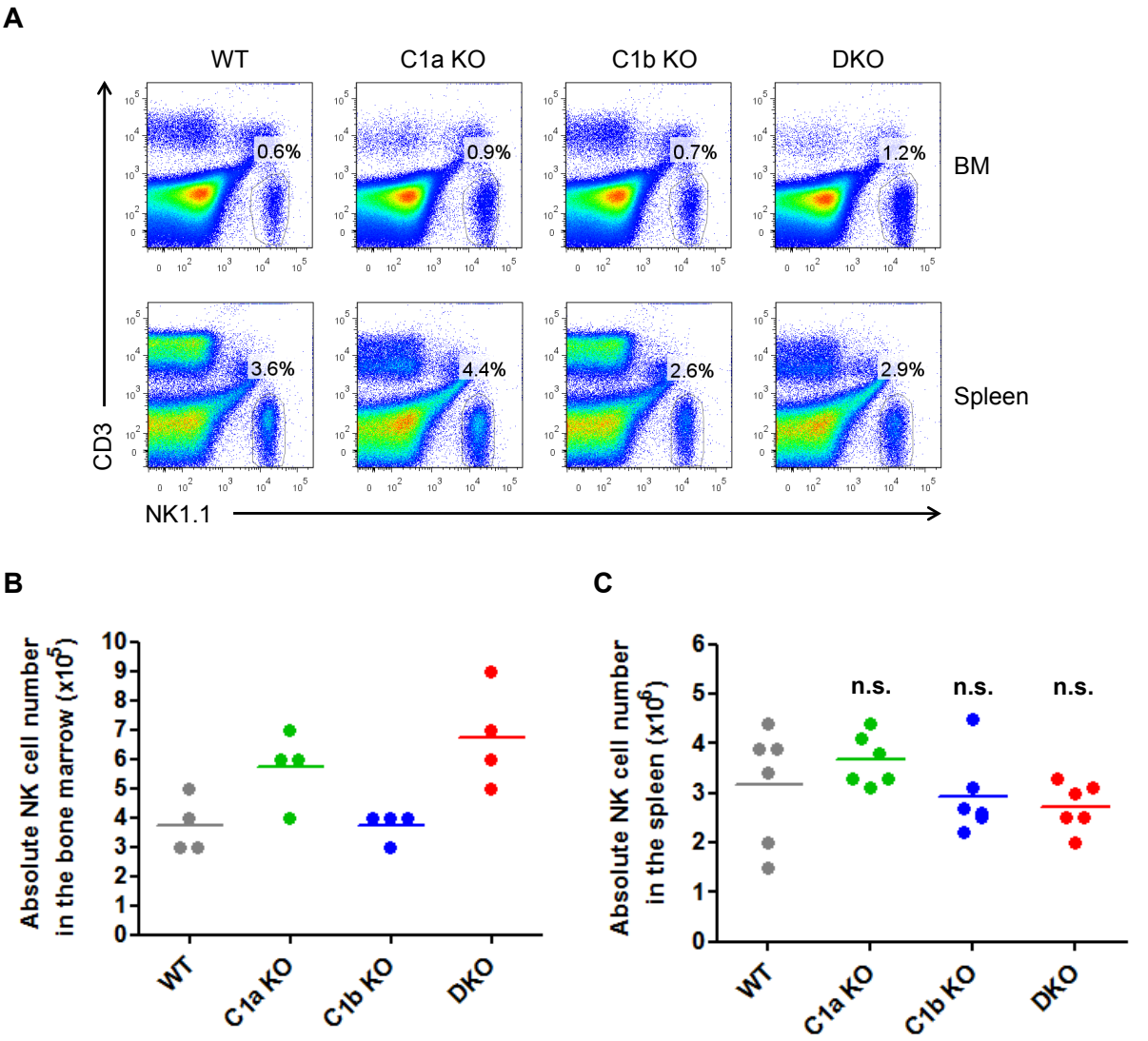

Figure 5-6. Absolute naïve NK cell numbers in bone marrow and spleen.
Total cell numbers of viable freshly isolated bone marrow- and spleen cells from 6 to 10 weeks old *wild type* (WT), *Coro1a*$^{-/-}$ (C1a KO), *Coro1b*$^{-/-}$ (C1b KO) and *Coro1a*$^{-/-}$*Coro1b*$^{-/-}$ (DKO) mice were determined by cell counting after trypan blue staining. In addition, bone marrow and spleen cells were stained with antibodies directed against NK1.1 and CD3. (A) Percentages of NK1.1$^+$/CD3$^-$ naïve NK cells in the bone marrow (BM) and in the spleen were assessed by FACS analysis. Absolute naïve NK cell numbers in the bone marrow (B) or in the spleen (C) were calculated by multiplying the total viable cell number by the percentage of NK1.1$^+$/CD3$^-$ cells. Plots show the absolute naïve NK cell numbers from four (bone marrow) or six (spleen) individual mice of each genotype. Horizontal bars show the mean values. n.s. – not significant.

Remarkably, the observed differences in NK cell numbers in the bone marrow did not translate into differences in the number of peripheral NK cells in the spleen. Although, increased numbers of naïve NK cells were detected in the bone marrow of *Coro1a*$^{-/-}$ and *Coro1a*$^{-/-}$*Coro1b*$^{-/-}$ mice, absolute NK cell numbers in the spleen were not significantly altered

in *Coro1a*$^{-/-}$ and/or *Coro1b*$^{-/-}$ mice, as compared to controls (Figure 5-6 B, Spleen), despite slightly reduced or heightened percentages of splenic NK cells in these mice, respectively (Figure 5-6 A).

In summary, the analysis of absolute NK cell numbers in the bone marrow and in the spleen of *Coro1a*$^{-/-}$ and/or *Coro1b*$^{-/-}$ mice revealed normal splenic NK cell numbers, despite differences in the bone marrow, where increased numbers were found in *Coro1a*- and *Coro1aCoro1b*-deficient mice.

5.6 Impaired NK cell maturation in *Coro1a*- and *Coro1aCoro1b*-deficient mice

NK cells derive from a CLP in the bone marrow, however, NKPs and iNKs were also found in lymphoid organs as well as the liver, indicating other potential sites of differentiation or access to the circulation [85–89,92,93,103,277]. NK cell differentiation and maturation is a multistep process accompanied by changes in the expression of various surface molecules [95,103]. Since the loss of Coro1a seems to influence NK cell development in mice, as indicated by increased numbers of NK cells in the bone marrow, NK cell maturation in *Coro1a*$^{-/-}$ and/or *Coro1b*$^{-/-}$ mice was analyzed in further detail.

To this end, the surface expression of selected maturation- and activation markers, as well as activating and inhibitory NK cell receptors on naïve bone marrow-, spleen- and liver NK cells was assessed by flow cytometry as described in section 4.3.1.

In the murine system, CD11b and CD27 surface expression is used to characterize NK cell developmental stages [89,97,110,111]. It has been proposed that NK cell maturation in mice occurs from the CD11b^{low}/CD27^{high} (immature) over CD11b^{high}/CD27^{high} (double-positive; DP) to the CD11b^{high}/CD27^{low} (mature) stage, as schematically shown in Figure 5-7 A [91,104,110]. The flow cytometric analysis of CD11b and CD27 surface expression on naïve NK1.1^{+}/CD3^{-} bone marrow- (BM), spleen- (Spleen) and liver NK cells (Liver) from *wild type* (WT), *Coro1a*$^{-/-}$ (C1a KO), *Coro1b*$^{-/-}$ (C1b KO) and *Coro1a*$^{-/-}$*Coro1b*$^{-/-}$ mice (DKO), pointed out differences in the maturation status of the NK cell populations located in the analyzed tissues/organs (Figure 5-7 B). In accordance to previous reports [91,110], NK cells in the bone marrow of *wild type* mice were found primarily immature or showed characteristics of the intermediate (DP) stage. In spleen and liver the percentage of immature *wild type* NK cells was relatively lower and accompanied by an increase of mature NK cells (Figure 5-7 B, WT). Interestingly, *Coro1a*$^{-/-}$*Coro1b*$^{-/-}$ NK cells consistently showed a more immature phenotype compared to controls, as indicated by an increase of CD11b^{low}/CD27^{high} and a decrease of DP and CD11b^{high}/CD27^{low} NK cells in all tissues/organs investigated (Figure 5-7 B). Similar to *Coro1a*$^{-/-}$*Coro1b*$^{-/-}$, *Coro1a*-deficient NK cells displayed a more immature phenotype, as shown in Figure 5-7 B. However, the relative shift in CD11b and

CD27 surface expression on *Coro1a*$^{-/-}$ NK cells was not as pronounced as observed for *Coro1a*$^{-/-}$*Coro1b*$^{-/-}$ NK cells and therefore the maturation status of *Coro1a*$^{-/-}$ NK cells ranged somewhere in between *wild type* and *Coro1a*$^{-/-}$*Coro1b*$^{-/-}$ NK cells.

Consistent with these data, both, bone marrow and splenic NK cells from *Coro1a*$^{-/-}$ and *Coro1a*$^{-/-}$*Coro1b*$^{-/-}$ mice showed an increased expression of early maturation markers which are the stem cell growth factor receptor (CD117), the IL-7 receptor-α (CD127) and CD51 [95], compared to *wild type* NK cells (Figure 5-8, bone marrow and spleen). The single loss of Coro1b in *Coro1b*$^{-/-}$ NK cells had no significant impact on the maturation status compared to *wild type* NK controls as shown in Figure 5-7 B and 5-8 for all tissues/organs. In addition to the maturation markers described above, the level of CD49b surface expression, which is highly expressed on NK cells starting from late developmental stages [103], was increased on *Coro1a*$^{-/-}$ and *Coro1a*$^{-/-}$*Coro1b*$^{-/-}$ bone marrow and splenic NK cells (Figure 5-8, bone marrow and spleen), as well as liver NK cells (Figure 5-11 B) compared to *wild type* and *Coro1b*$^{-/-}$ levels. Remarkably, two subsets of NK cells, one with low and one with high CD49b expression were detected in the liver (Figure 5-11 B). The CD49b^{low} subset was unique for the liver and likely represents remaining fetal NK cells [94,97] since this population was not present in the bone marrow or the spleen. These restricted CD49b^{low} NK cells were increased in *Coro1a*$^{-/-}$ and *Coro1a*$^{-/-}$*Coro1b*$^{-/-}$ mice compared to *wild type* and *Coro1b*$^{-/-}$ mice (Figure 5-11 B). In contrast to CD11b and CD49b, the expression of CD43, another adhesion receptor expressed on later developmental stages, was comparable between bone marrow and splenic NK cells of all genotypes (Figure 5-8, bone marrow and spleen).

The further analysis of selected activating and inhibitory NK cell receptors as well as activation markers on naïve bone marrow-, spleen- and liver NK cells revealed a comparable tissue-/organ-specific expression for the majority of investigated receptors on NK cells of all genotypes. The activating respectively inhibitory NK cell receptors NKG2D, Ly49H and NKG2A, -C and -E, the IL-2 receptor α-, β-chain as well as the common γ-chain (CD25, CD122 and CD132, respectively) and CD45R (B220) were either equally expressed or only minor differences were detected on bone marrow- an splenic NK cells isolated from *Coro1a*$^{-/-}$, *Coro1b*$^{-/-}$ and *Coro1a*$^{-/-}$*Coro1b*$^{-/-}$ mice compared to *wild type* controls (Figures 5-9 and 10, bone marrow and spleen).

Contrary to the majority of analyzed receptors, which were equally expressed on *Coro1a*$^{-/-}$ and *Coro1a*$^{-/-}$*Coro1b*$^{-/-}$ NK cells, expression of the activating NK cell receptor NKp46 was normal on *Coro1a*$^{-/-}$ and *Coro1b*$^{-/-}$ NK cells, but significantly increased on *Coro1a*$^{-/-}$*Coro1b*$^{-/-}$ NK cells isolated from bone marrow, spleen and liver (Figure 5-9 and 5-11 B). The killer cell lectin-like receptor 1 (KLRG1) is generally expressed at higher levels on later developmental NK cell stages [95]. In accordance with the maturation status of the analyzed NK cells, lower expression of KLRG1 was detected on *Coro1a*$^{-/-}$ and

Coro1a$^{-/-}$*Coro1b*$^{-/-}$ NK cells, while higher expression was found on *wild type* and *Coro1b*$^{-/-}$ NK cells (Figure 5-9, bone marrow and spleen). Finally, bone marrow NK cells from *Coro1a*$^{-/-}$ and *Coro1a*$^{-/-}$*Coro1b*$^{-/-}$ mice showed an increased expression of CD69 compared to *wild type* and *Coro1b*$^{-/-}$ NK cells, while no differences in CD69 expression of splenic NK cells were detected for all analyzed genotypes (Figure 5-10, bone marrow and spleen).

In summary, the analysis of maturation- and activation markers as well as activating and inhibitory NK cell receptors defined a more immature phenotype of *Coro1a*$^{-/-}$ and *Coro1a*$^{-/-}$*Coro1b*$^{-/-}$ bone marrow-, spleen- and liver NK cells compared to *wild type* and *Coro1b*$^{-/-}$ NK cells, suggesting a role of Coro1a in the regulation of NK cell maturation.

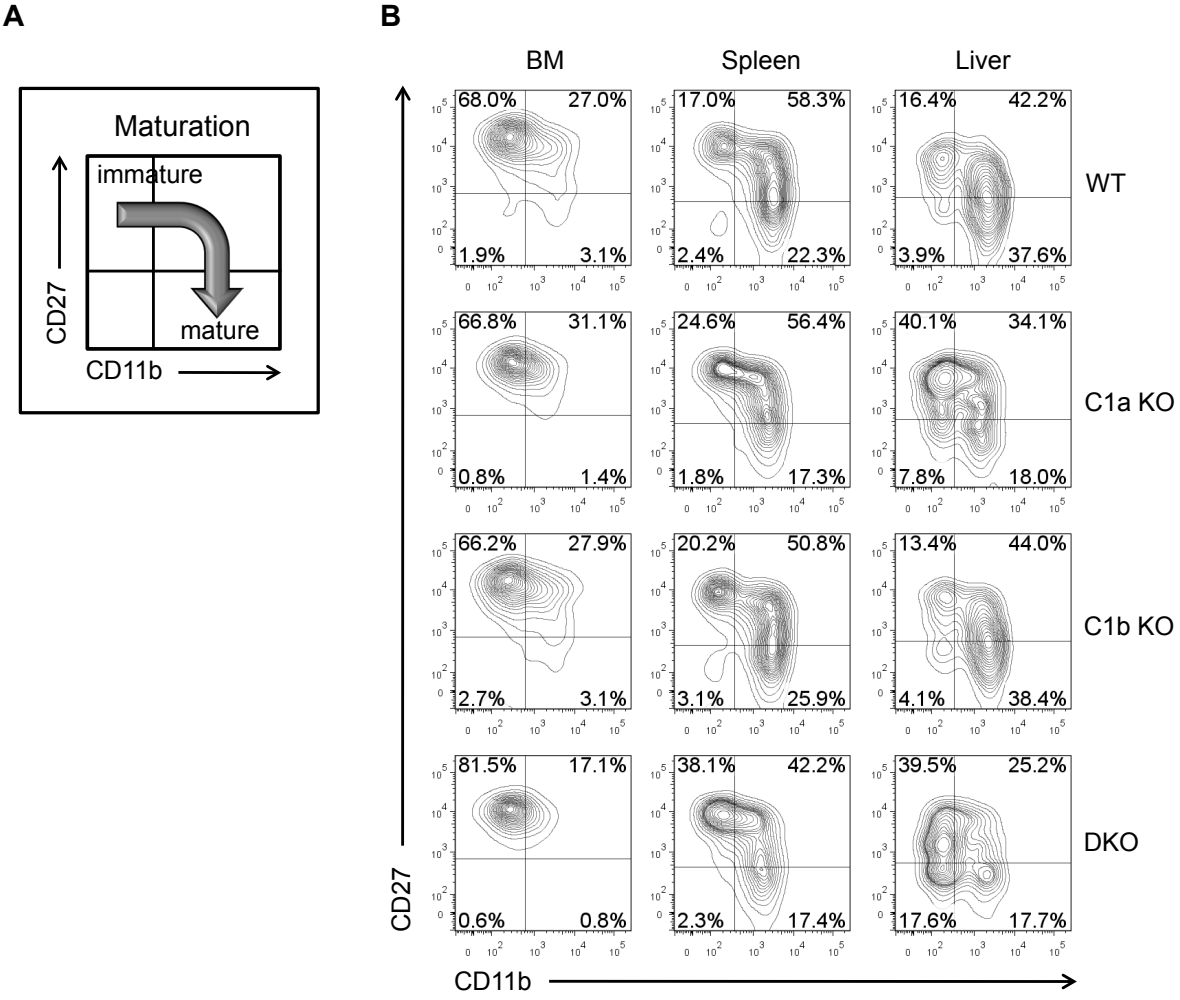

Figure 5-7. Naïve *Coro1a*$^{-/-}$ and *Coro1a*$^{-/-}$*Coro1b*$^{-/-}$ NK cells display a less mature phenotype. Surface expression of CD11b and CD27 on naïve *wild type* (WT), *Coro1a*$^{-/-}$ (C1a KO), *Coro1b*$^{-/-}$ (C1b KO) and *Coro1a*$^{-/-}$*Coro1b*$^{-/-}$ (DKO) NK1.1^{+}/CD3^{-} NK cells from bone marrow (BM), spleen or liver was assessed by flow cytometry. Shown are: (A) A scheme illustrating CD27 and CD11b surface expression on NK cells during maturation and (B) representative contour plots depicting CD27 and CD11b expression of at least three (bone marrow), ten (spleen) and four (liver) independent experiments. Numbers indicate the percentage of cells within the quadrant.

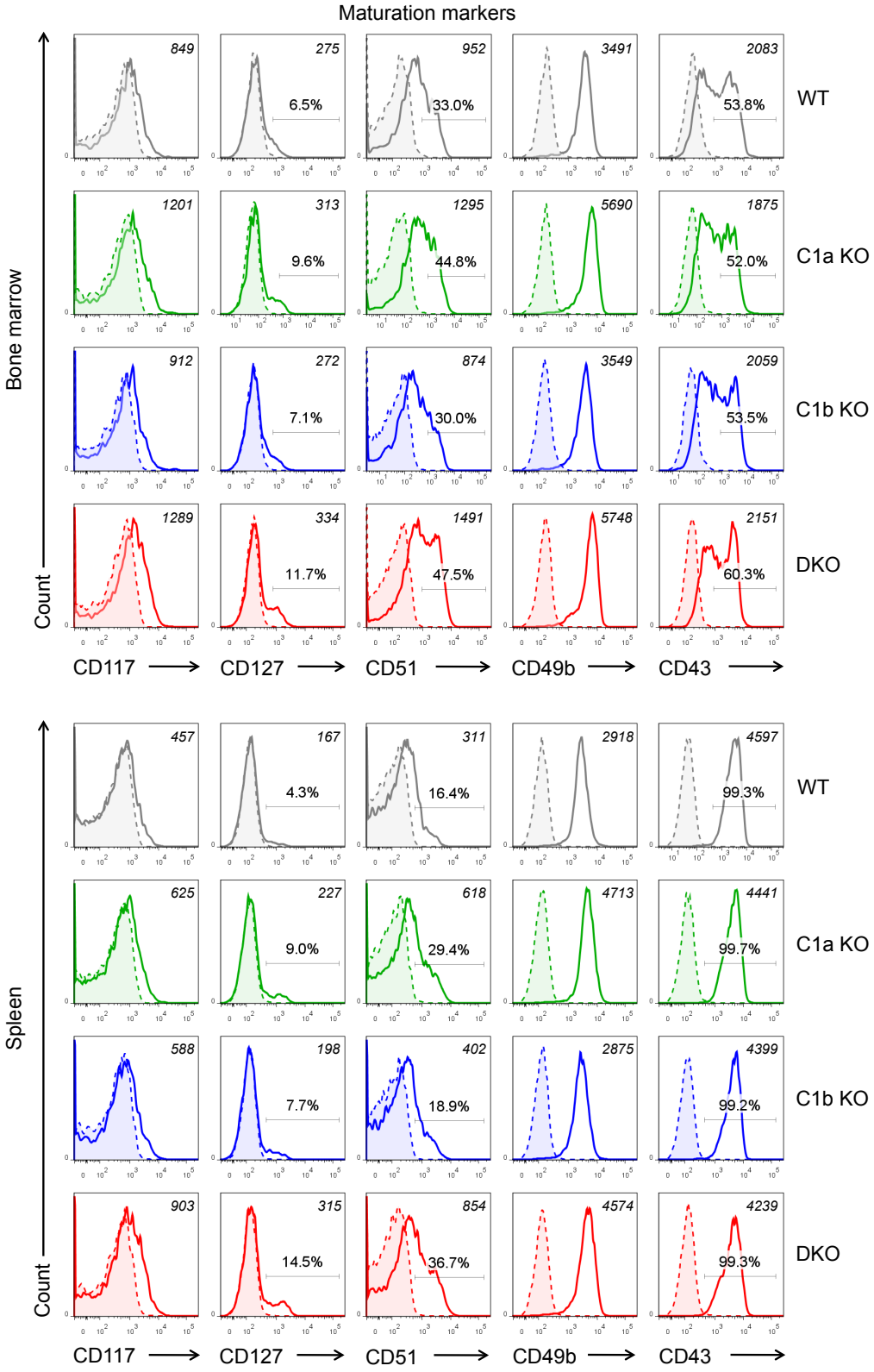

Figure 5-8. Surface expression of maturation markers on naïve NK cells.
Surface expression of the indicated molecules on naïve *wild type* (WT, gray), *Coro1a*$^{-/-}$ (C1a KO, green), *Coro1b*$^{-/-}$ (C1b KO, blue) and *Coro1a*$^{-/-}$*Coro1b*$^{-/-}$ (DKO, red) NK1.1^{+}/CD3^{-} NK cells either from the bone marrow (upper panel) or the spleen (lower panel) was assessed by flow cytometry. Shown histograms are representative of at least three independent experiments. Solid lines show receptor staining and filled histograms with dashed lines depict staining with matching isotype controls. Numbers in the histograms indicate the mean of fluorescence intensity (MFI, italic) or the percentage of positive cells.

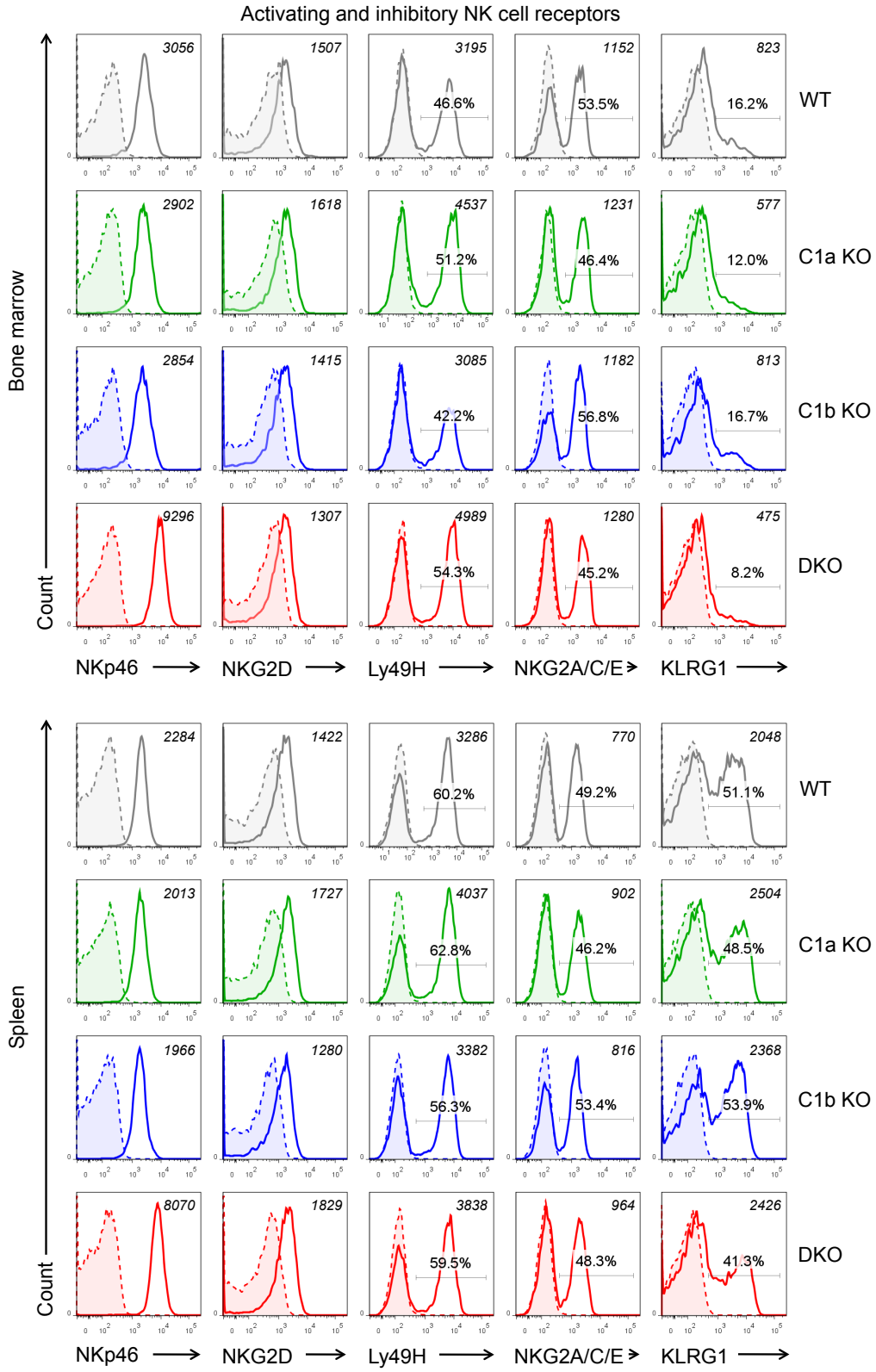

Figure 5-9. Surface expression of activating and inhibitory NK cell receptors on naïve NK cells. Surface expression of the indicated molecules on naïve *wild type* (WT, gray), *Coro1a*$^{-/-}$ (C1a KO, green), *Coro1b*$^{-/-}$ (C1b KO, blue) and *Coro1a*$^{-/-}$*Coro1b*$^{-/-}$ (DKO, red) NK1.1^{+}/CD3^{-} NK cells either from the bone marrow (upper panel) or the spleen (lower panel) was assessed by flow cytometry. Shown histograms are representative of at least three independent experiments. Solid lines show receptor staining and filled histograms with dashed lines depict staining with matching isotype controls. Numbers in the histograms indicate the MFI (italic) or the percentage of positive cells.

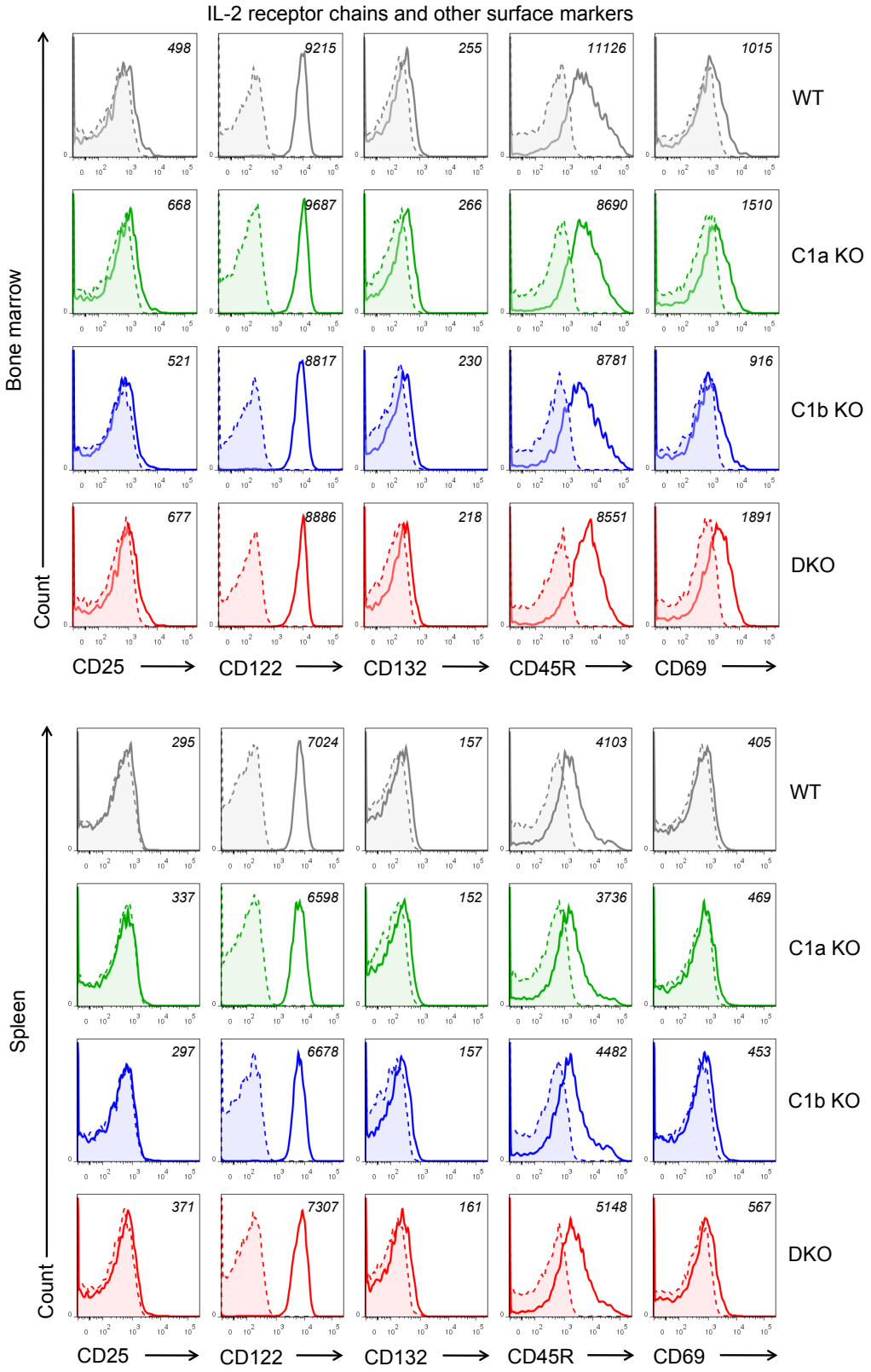

Figure 5-10. Surface expression of IL-2 receptor chains and other molecules on naïve NK cells. Surface expression of the indicated molecules on naïve *wild type* (WT, gray), *Coro1a*$^{-/-}$ (C1a KO, green), *Coro1b*$^{-/-}$ (C1b KO, blue) and *Coro1a*$^{-/-}$*Coro1b*$^{-/-}$ (DKO, red) NK1.1^{+}/CD3^{-} NK cells either from the bone marrow (upper panel) or the spleen (lower panel) was assessed by flow cytometry. Shown histograms are representative of at least three independent experiments. Solid lines show receptor staining and filled histograms with dashed lines depict staining with matching isotype controls. Numbers in the histograms indicate the MFI (italic).

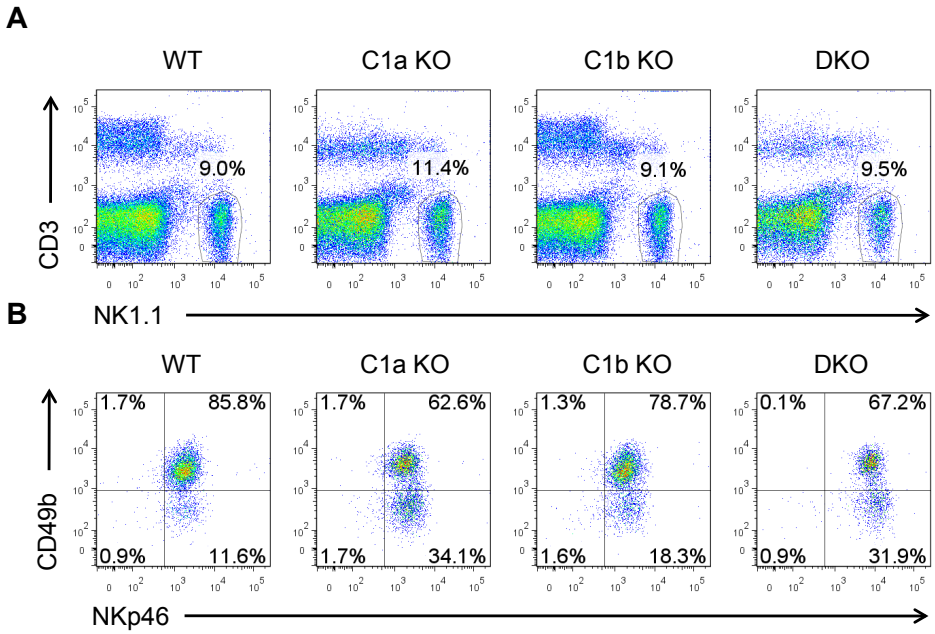

Figure 5-11. Expression of NK1.1, NKp46 and CD49b on naïve liver NK cells.
Surface expression of CD3, NK1.1, CD49b and NKp46 on naïve *wild type* (WT), *Coro1a*$^{-/-}$ (C1a KO), *Coro1b*$^{-/-}$ (C1b KO) and *Coro1a*$^{-/-}$*Coro1b*$^{-/-}$ (DKO) NK1.1^{+}/CD3^{-} NK cells isolated from the liver was assessed by flow cytometry. Shown dot blots depict percentages of NK1.1^{+}/CD3^{-} NK cells in the liver (A) and the surface expression of NKp46 and CD49b on NK1.1^{+}/CD3^{-} NK cells (B). Data are representative of four independent experiments. Numbers shown are the percentage of NK1.1^{+}/CD3^{-} NK cells (A) or the percentages of cells within the quadrant (B).

5.7 IL-15-expanded *wild type*, *Coro1a*$^{-/-}$ and/or *Coro1b*$^{-/-}$ NK cells show a similar phenotype

Cytokines, such as IL-2 or IL-15 are important for NK cell development and function [101,102,278–282]. Studies on cancer immunotherapy revealed that IL-15 promotes NK cell activation as well as proliferation [283–285]. As the purification of NK cells from the spleen results in only a limited number of cells, purified NK cells were expanded and activated with IL-15. This is a widely used and well established method to obtain sufficient numbers of activated NK cells for functional *in vitro* studies [286] (see section 4.1.3). As shown in Figure 5-12, purity of IL-15-expanded *wild type* (WT), *Coro1a*$^{-/-}$ (C1a KO), *Coro1b*$^{-/-}$ (C1b KO) and *Coro1a*$^{-/-}$*Coro1b*$^{-/-}$ NK cells (DKO) was routinely >95%, as assessed by flow cytometric analysis of NK1.1 and CD3 surface expression (upper left figure). Since the ratio of mature versus immature NK cell populations was significantly shifted towards more immature NK cells in *Coro1a*- and *Coro1aCoro1b*-deficient mice, the phenotype of IL-15-expanded NK cells was investigated in greater detail. To this end, the surface expression of CD11b, CD27 and selected maturation- and activation markers as well as activating and inhibitory NK cell receptors was investigated by flow cytometry as described in the previous section (Figure 5-12).

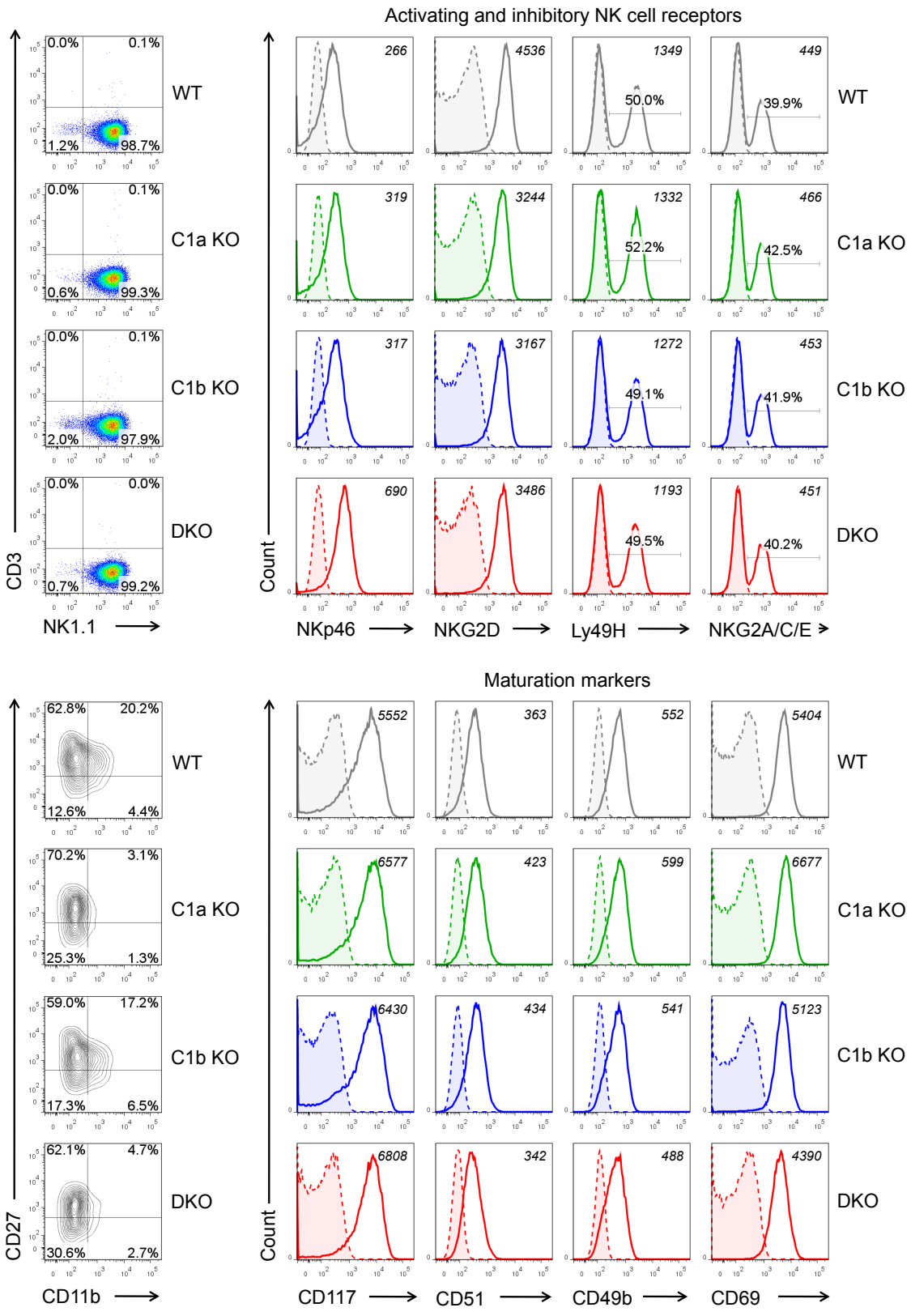

Figure 5-12. IL-15-expanded NK cells have a similar phenotype.
Surface expression of the indicated surface molecules on IL-15-expanded *wild type* (WT, gray), *Coro1a*$^{-/-}$ (C1a KO, green), *Coro1b*$^{-/-}$ (C1b KO, blue) and *Coro1a*$^{-/-}$*Coro1b*$^{-/-}$ (DKO, red) NK1.1^{+}/CD3^{-} NK cells was assessed by flow cytometry. Shown dot blots or histograms are representative of at least three independent experiments. Solid lines show receptor staining and filled histograms with dashed lines depict staining with the matching isotype control. Numbers in the dot blots show percentages of cells within the quadrant, numbers in the histograms indicate the MFI (italic) or the percentage of positive cells.

The analysis of CD11b and CD27 surface expression on cytokine expanded NK cells revealed only slight differences in the maturation status between the different genotypes (Figure 5-12, lower left figure). The majority of *wild type* (WT), *Coro1a*$^{-/-}$ (C1a KO), *Coro1b*$^{-/-}$ (C1b KO) and *Coro1a*$^{-/-}$*Coro1b*$^{-/-}$ NK cells (DKO) showed an immature phenotype, as indicated by the expression of low levels of CD11b and high levels of CD27. Noteworthy, mature DP NK cells were found in higher numbers in *wild type* and *Coro1b*$^{-/-}$ NK cell cultures compared to the *Coro1a*$^{-/-}$ and *Coro1a*$^{-/-}$*Coro1b*$^{-/-}$ ones. Here, DP NK cells were almost absent. However, it is noteworthy that the expression of selected activating and inhibitory NK cell receptors (Figure 5-12, upper right figure) as well as maturation- or activation markers (lower right figure), with exception of NKp46, was comparable between all NK cell genotypes. IL-15-expanded NK cells expressed NKG2D, high levels of CD117, CD51, CD49b and high levels of CD69 (Figure 5-12, upper and lower right panel). About 50% of the cells were positive for Ly49H and almost 40% expressed NKG2A, -C or -E (Figure 5-12, upper right panel). NKp46 expression patterns were similar to those detected on naïve NK cells (Figure 5-9 and 11) and were indistinguishable between *wild type*, Coro1a$^{-/-}$ and Coro1b$^{-/-}$ NK cells, while heightened levels of NKp46 were detected on *Coro1a*$^{-/-}$*Coro1b*$^{-/-}$ NK cells (Figure 5-12, upper right figure).

In summary, despite the observed differences in the maturation state of naïve NK cells, *wild type*, *Coro1a*$^{-/-}$, *Coro1b*$^{-/-}$ and *Coro1a*$^{-/-}$*Coro1b*$^{-/-}$ IL-15-expanded NK cells display a similar and relatively homogeneous phenotype.

5.8 *Coro1a*$^{-/-}$ and *Coro1a*$^{-/-}$*Coro1b*$^{-/-}$ NK cells show decreased cytotoxicity

Major NK cell activity is the killing of virus/bacteria-infected or transformed cells [9,11,23,37–41]. NK cell cytotoxicity is the result of a complex process, which includes the formation and stabilization of the lytic synapse and the initiation of the cytolytic response, promoted by various signaling and scaffolding proteins [115,148,165,287]. Since in human cells the actin cytoskeleton plays a critical role in the stabilization of the lytic synapse [288], the contribution of the actin-regulatory proteins Coro1a and Coro1b in this process was studied.

To this purpose, the cytotoxicity of IL-15-expanded NK cells was investigated by measuring the release of Lactate dehydrogenase (LDH) from target cells. YAC-1 cells were co-cultured with NK cells at the indicated ratios (Figure 5-13) and release of cytoplasmic LDH as a measure of cytotoxicity was quantified by colorimetric means as described in section 4.8.

As shown in Figure 5-13, *Coro1a*$^{-/-}$ NK cells (green line) exhibited a decreased cytotoxicity compared to *wild type* controls. This was further lowered by the additional loss of *Coro1b* in *Coro1a*$^{-/-}$*Coro1b*$^{-/-}$ NK cells (red line). Depending on the ratio of effector- to target cells, the specific lysis of target cells was reduced from 30.4% to 36.1% of *wild type* levels for

Coro1a$^{-/-}$*Coro1b*$^{-/-}$ NK cells and from 40.3% to 57.3% of *wild type* levels for *Coro1a*$^{-/-}$ NK cells. In contrast, NK cell cytotoxicity was only slightly reduced in *Coro1b*$^{-/-}$ cells compared to *wild type* controls (69.5% to 97.8% of *wild type* levels, suggesting a possible compensatory function of Coro1b in *Coro1a*$^{-/-}$ NK cells.

Thus, these findings point out the critical role of the actin-regulatory proteins Coro1a and Coro1b for NK cell cytotoxicity.

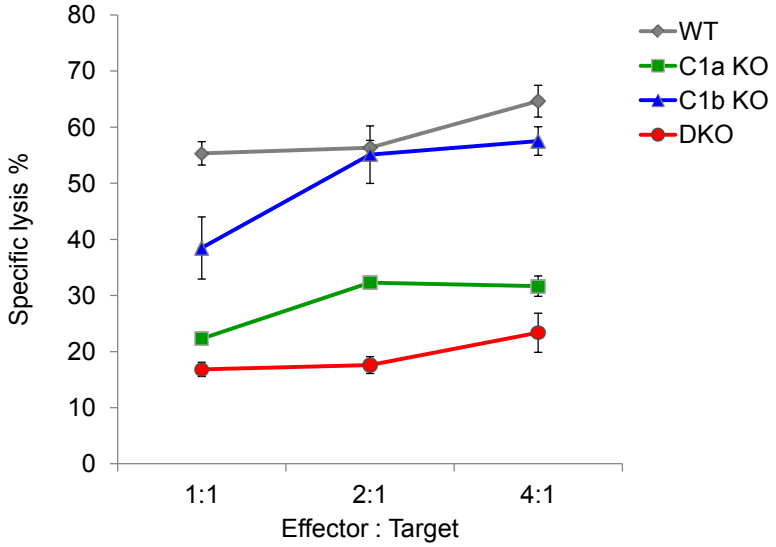

Figure 5-13. Impaired cytotoxicity of *Coro1a*$^{-/-}$ and *Coro1a*$^{-/-}$*Coro1b*$^{-/-}$ NK cells.
IL-15-expanded NK cells from *wild type* (gray line), *Coro1a*$^{-/-}$ (green line), *Coro1b*$^{-/-}$ (blue line) and *Coro1a*$^{-/-}$*Coro1b*$^{-/-}$ (red line) mice were co-cultured with Yac-1 target cells at the indicated ratios. NK cell-mediated lysis of YAC-1 cells was determined by colorimetric measurement of LDH-release. Data shown are representative of at least four independent experiments with triplicates. (Mean ± SD).

5.9 The impact of *Coro1a*- and *Coro1b*-deficency on NK cell activities and their modulators

Since *Coro1a*- and *Coro1b*-deficiency was shown to affect NK cell cytotoxicity the mechanism of action of the proteins was investigated.

5.9.1 Intercellular conjugate formation is not affected by the loss of *Coro1a* or *Coro1b*

The formation of a stable intercellular conjugate between an NK cell and its target is required for NK cell activation and the initiation of the cytolytic response [130,287]. Since remodeling of F-actin is critical for the stabilization of the lytic synapse [115], the impact of *Coro1a*- and *Coro1b*-deficiency on conjugate formation was investigated.

To this purpose, a previously described two-color-flow cytometry assay was used [272]. Due to the defective motility of *Coro1a*$^{-/-}$ and *Coro1a*$^{-/-}$*Coro1b*$^{-/-}$ NK cells, a setup which largely avoids the contribution of motility-dependent processes was chosen as described in section 4.9. To assess conjugate formation, CFDA-SE labeled NK cells and eFluor® 670-labeled YAC-1 target cells were co-cultured for the indicated time points (Figure 5-14 A) at a ratio of 1:2 and adhesion was analyzed upon fixation by flow cytometry as shown by the dot-blots in Figure 5-14 A. To measure conjugate formation, percentages of NK-YAC-1-conjugates (Figure 5-14 A, upper right quadrants) of total NK cells (Figure 5-14 A, lower right + upper right quadrants) were calculated (Figure 5-14, B and C). The flow cytometric analysis of co-cultured NK- and YAC-1 cells revealed a time dependent increase of NK-YAC-1-conjugates for all genotypes, as indicated by the representative dot blots in Figure 5-14 A for *wild type* (WT) and *Coro1a*$^{-/-}$*Coro1b*$^{-/-}$ NK cells (DKO). For instance, on average, 17.9% ± 2.1 (*wild type*, gray line), 20.3% ± 1.4 (*Coro1a*$^{-/-}$, green line), 16.6% ± 1.3 (*Coro1b*$^{-/-}$, blue line) and 19.9% ± 1.5 (*Coro1a*$^{-/-}$*Coro1b*$^{-/-}$, red line) of the NK cells were found conjugated after 15 min of co-culture (Figure 5-14 B). Importantly, no significant differences in the ability to form intercellular conjugates were detected in *Coro1a*$^{-/-}$ and/or *Coro1b*$^{-/-}$ NK cells compared to *wild type* counterparts (Figure 5-14, A and B).

To confirm the specificity of the assay, *wild type* NK cells were co-cultured with YAC-1 target cells, the cancer cell line A20 or BMMCs derived from C57BL6 mice with the same genetic background (used here as control). As indicated in Figure 5-14 C, specific intercellular conjugates were formed by the NK cells with the two cancer cell lines and 34.3% ± 0.7 (A20) and 29.4% ± 2.3 (YAC-1) of the NK cells were found conjugated after 15 min of co-culture. In contrast, only minor percentages of conjugated NK cells were found after co-culture with BMMCs, bearing the same MHC molecules as the NK cells (4.1% ± 0.1, for 15 min), confirming the specificity of the assay.

In conclusion, these data indicate that the formation of intercellular conjugates is not dependent on Coro1a and Coro1b.

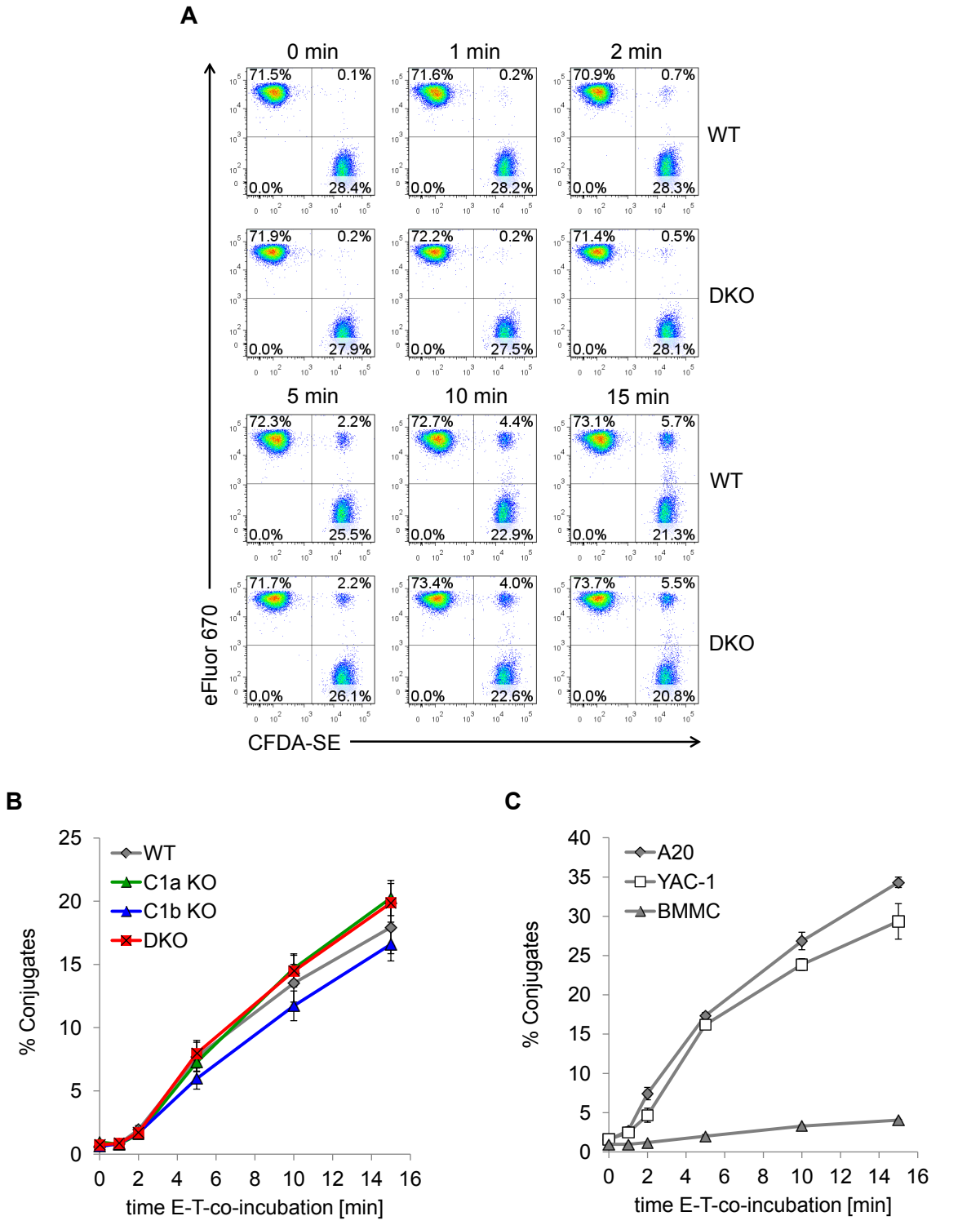

Figure 5-14. Comparable intercellular conjugate formation of *wild type* and *Coro1a*$^{-/-}$and/or *Coro1b*$^{-/-}$ NK cells.
NK cell-YAC-1-conjugate formation of *wild type* (WT, grey line), *Coro1a*$^{-/-}$ (C1a KO, green line), *Coro1b*$^{-/-}$ (C1b KO, blue line) and *Coro1a*$^{-/-}$*Coro1b*$^{-/-}$ (DKO, red line) IL-15-expanded NK cells was assessed by flow cytometry. CFDA-SE stained NK cells were co-cultured with eFluor® 670 stained YAC-1 cells at a ratio of 1:2 for the indicated time points. Shown are: (A) Flow cytometric data of one representative experiment, numbers indicate the percentage of cells within the quadrant. (B) calculated percentages of NK-YAC-1-conjugates to total NK cells from at least 4 independent experiments (Mean ± SEM; WT n=6, C1a KO n=4, C1b KO n=4, DKO n=6) and (C) percentages of NK-YAC-1-, NK-A20- and NK-BMMC-conjugates to total NK cells (Mean ± SD) of one experiment.

5.9.2 Akt and Erk phosphorylation in *Coro1a*$^{-/-}$ and/or *Coro1b*$^{-/-}$ NK cells upon cellular activation

Engagement of activating- and inhibitory NK cell receptors by cognate ligands results in signaling events which determine the further outcome of NK cell responses and thereby decide on the fate of the target cell. These processes require the clustering of involved receptors at the site of the forming synapse, which strictly depends on the rearrangement of the actin cytoskeleton [115,124,151–154]. In this context, among others, the initiation of the MAPK-cascade and the PI3K-pathway are crucial for the cytolytic response [129,289–292].

To study whether a defect in cellular activation may explain the impaired cytolytic response of *Coro1a*$^{-/-}$ and *Coro1a*$^{-/-}$Coro1b$^{-/-}$ NK cells, cells were stimulated for the indicated time via crosslinking the activating NK cell receptor NK1.1 as described in section 4.1.10 (Figure 5-15). Immunoblot analysis of whole NK cell lysates was performed to assess protein kinase Akt and extracellular signal-regulated kinase (Erk) 1 and -2 phosphorylation, activated via the PI3K- and MAPKs-pathway, respectively. Figure 5-15 shows Akt phosphorylation, Akt expression, which was used as loading control (upper two panels), MAPKs Erk1 and -2 phosphorylation as well as total Erk2 as loading control (two middle panels). As shown, activation of *wild type* NK cells (WT) via crosslinking the NK1.1 receptor results in a transient phosphorylation of Akt and the MAPKs Erk1 and -2 (Figure 5-15, WT). The phosphorylation was highest after 5 min of stimulation and decreased over time. After 20 min of stimulation, only low levels of Akt and Erk1 and -2 phosphorylation were detectable. While *Coro1b*$^{-/-}$ NK cells (C1b KO) showed Akt and Erk phosphorylation kinetics and levels similar to *wild type* NK cells, subtle differences in Akt, Erk1 and -2 phosphorylation in *Coro1a*$^{-/-}$ (C1a KO) and *Coro1a*$^{-/-}$*Coro1b*$^{-/-}$ (DKO) NK cells compared to *wild type* controls were detected. In contrast to *wild* type NK cells, phosphorylation of Akt was longer sustained in *Coro1a*$^{-/-}$ and *Coro1a*$^{-/-}$*Coro1b*$^{-/-}$ NK cells (Figure 5-15, p-Akt), while the induction of early Erk1 and -2 phosphorylation was slightly impaired in these cells (Figure 5-15, p-Erk1 and -2). In this context, Erk1 and -2 phosphorylation levels in *Coro1a*$^{-/-}$ and *Coro1a*$^{-/-}$*Coro1b*$^{-/-}$ NK cells were lower after 5 min of stimulation, but were similar at 20 min compared to *wild type* controls. In addition, total Erk1 protein expression was a little lower in *Coro1a*- and *Coro1aCoro1b*-deficient NK cells compared to *wild type* cells (Figure 5-15, Erk2). The lower panel of Figure 5-15 shows that the expression of β-actin, used here as additional loading control, was comparable in all samples.

Altogether, the activation of the PI3K-pathway and the MAPK-cascade in *wild type*, *Coro1a*$^{-/-}$, *Coro1b*$^{-/-}$ or *Coro1a*$^{-/-}$*Coro1b*$^{-/-}$ NK cells upon crosslinking of the NK1.1 receptor show minimal differences.

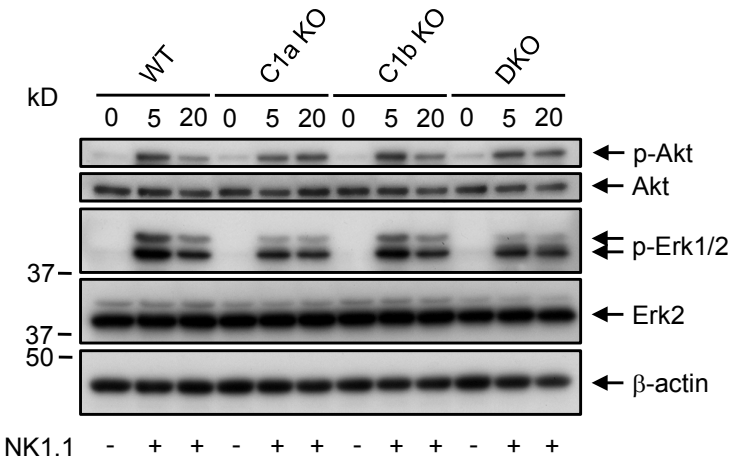

Figure 5-15. NK cell activation upon NK1.1-crosslinking.
Wild type (WT), *Coro1a*$^{-/-}$ (C1a KO), *Coro1b*$^{-/-}$ (C1b KO) and *Coro1a*$^{-/-}$*Coro1b*$^{-/-}$ (DKO) IL-15-expanded NK cells were stimulated with streptavidin-microspheres coated with specific antibodies against NK1.1 at a ratio of 1:2 for the indicated time points. Immunoblot analysis of whole cell lysates was performed using specific antibodies against p-Akt, Akt, p-Erk1/2 and Erk2. Data are representative for at least three independent experiments. Protein loading was assessed by β-actin expression (lower panel).

5.9.3 Subcellular localization of Coro1a and Coro1b in NK cells upon cellular activation.

Recent studies show that activation of MCs or MΦs initiates a transient subcellular relocation of Coro1a and Coro1b upon phosphorylation [222,250]. Therefore, the subcellular distribution of Coro1a and Coro1b upon NK cell activation was investigated next by biochemical fractionation of activated NK cells.

To this purpose, *wild type* NK cells were stimulated via crosslinking of the activating NK cell receptor NK1.1, with PMA/ionomycin or left untreated (see section 4.1.10) for the indicated time (Figure 5-16) and were subjected to subcellular fractionation as described in section 4.10. In non-stimulated NK cells, Coro1a and Coro1b were mainly detected in the cytoskeleton-containing detergent-insoluble fraction (P, cytoskeleton-rich fraction, Figure 5-16, Coro1a and Coro1b). Interestingly, no major changes in the subcellular distribution of Coro1a were detected upon activation of NK cells by PMA/ionomycin (P/I) or crosslinking of NK1.1 (NK1.1) (Figure 5-16, Coro1a). Only a minor relocation of Coro1a from the cytoskeleton-rich- into the cytosolic detergent-soluble fraction (S, cytosolic fraction) was observed after activation via NK1.1 for 5 or 20 min. In contrast, stimulation of NK cells with PMA/ionomycin or crosslinking of NK1.1 resulted in a transient relocation of Coro1b from the cytoskeleton-rich- into the cytosolic fraction, particularly at later time points (Figure 5-16, Coro1b). Furthermore, activation of NK cells resulted in a long-lasting phosphorylation of Coro1b on Ser2, which was detectable early upon activation and showed the highest levels between 5 and 20 min of stimulation (Figure 5-16, p-Ser2-Coro1b). In addition, the analysis revealed that phosphorylated Coro1b was mainly located in the cytosolic fraction. The

depolymerization of cellular F-actin by latrunculin B resulted in the relocation of Coro1a, Coro1b and β-actin from the cytoskeleton-rich- into the cytosolic fraction as shown in Figure 5-16 (Coro1a, Coro1b and β-actin), indicating an association of the coronins with F-actin in NK cells. The subcellular localization of vimentin, glyceraldehyde-3-phosphate dehydrogenase (GAPDH) and total Erk2 was assessed to control the purity of the single fractions and loadings. Vimentin, as constituent of the cytoskeleton, was detected exclusively in the cytoskeleton-rich fraction and GAPDH was found in the cytosolic fraction, revealing a proper separation of the fractions (Figure 5-16). To verify the activation of NK cells, Erk1 and -2 phosphorylation was also investigated. Both, stimulation via crosslinking of NK1.1 or with PMA/ionomycin, were sufficient to activate NK cells, as indicated by the phosphorylation of Erk1 and -2 (Figure 5-16, p-Erk1/2 and Erk2).

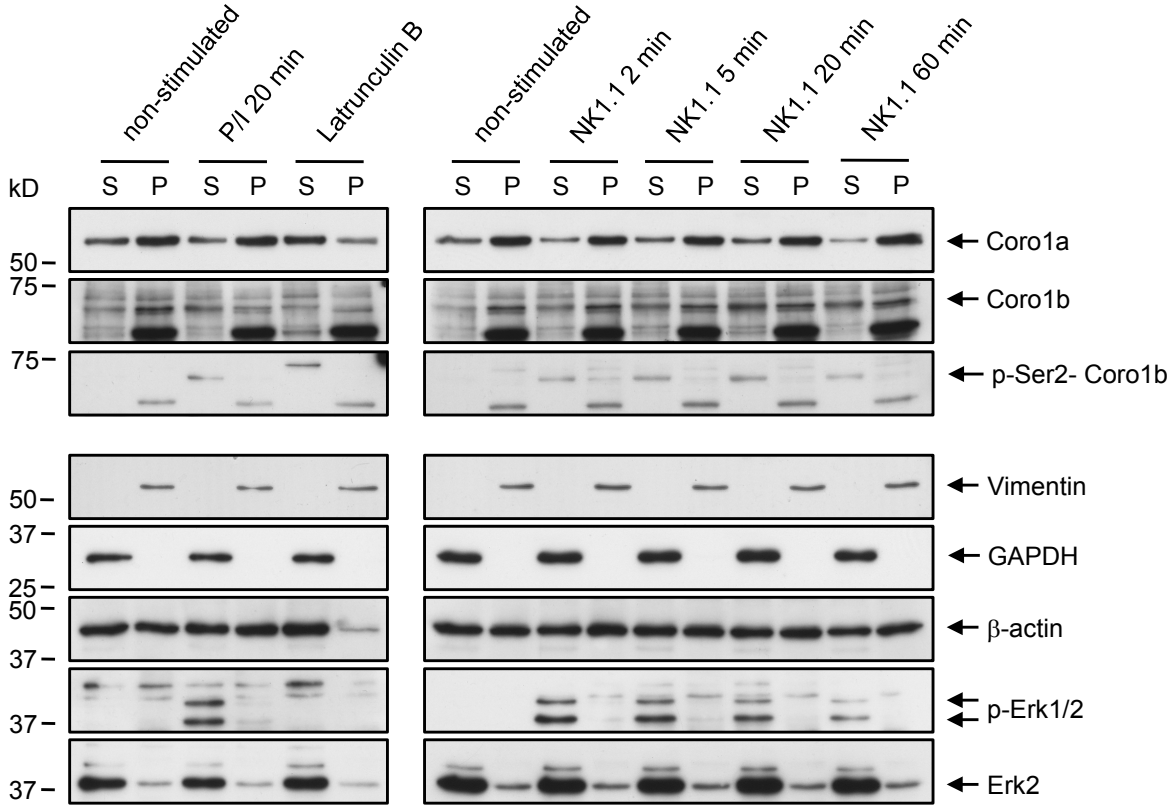

Figure 5-16. Subcellular distribution of Coro1a and Coro1b upon stimulation.
Wild type IL-15-expanded NK cells, were stimulated with PMA/ionomycin (P/I, left panel), beads coated with mAbs against NK1.1 (right panel) at a ratio of 1:2 for the indicated time points or left untreated. Subsequently, samples were fractionated with cytoskeleton isolation buffer as described in methods. Detergent-soluble fraction (S, cytosolic fraction) and detergent-insoluble precipitate (P, cytoskeleton-containing fraction) were analyzed by immunoblotting using the indicated antibodies. As control, NK cells were treated with latrunculin B (30 min). Protein loading was assessed by β-actin expression. Purity of the fractions was controlled by GAPDH (S) and vimentin (P) expression. Shown data are representative of two independent experiments.

In summary, Coro1a as well as Coro1b were found to be primarily associated with the cytoskeletal fraction in non-stimulated NK cells. The cellular activation by crosslinking of the activating NK cell receptor NK1.1 led to a relocation of Coro1b from the cytoskeleton-rich- into the cytosolic fraction correlating with a long-lasting phosphorylation of the protein. In contrast, only minor changes in the localization of Coro1a were detected upon cellular activation.

5.9.4 Coro1a and Coro1b localize to F-actin-rich areas in the pSMAC of the cytolytic synapse

As described previously, the activation of NK cells by crosslinking of NK1.1 led not only to minor changes in the subcellular distribution of Coro1a and Coro1b, but also resulted in a long-lasting phosphorylation of Coro1b on Ser2. Since Ser2 phosphorylation of coronin is known to be important for the actin regulatory function of Coro1a and Coro1b [204,212,222], the contribution of both coronins in the actin-dependent formation of a stable cytolytic synapse was investigated.

To this end, the cellular localization of both proteins was investigated in NK cells upon conjugation with target cells by confocal microscopy. NK cell-YAC-1-conjugates were generated and stained for either Coro1a or Coro1b and treated with phalloidin to stain F-actin subsequent to fixation and permeabilization as described in materials and methods (see section 4.6). As shown in Figure 5-17, confocal microscopy revealed no considerable changes in the subcellular distribution of Coro1a and Coro1b compared to unconjugated NK cells in NK cell areas which were not directly connected to target cells (A and B and previously described in section 5.2). In these areas, Coro1a was mainly localized at the cortex of NK cells, where it colocalized with F-actin (Figure 5-17 A, left panel). In contrast, Coro1b showed a more punctate distribution throughout the entire cytoplasm with only marginal colocalization with the F-actin-rich cell cortex (Figure 5-17 B, left panel). Interestingly, changes in the subcellular distribution of Coro1a and Coro1b were found at the site of the lytic synapse, compared to unconjugated areas. Coro1a and Coro1b were enriched in the actin-rich pSMAC region where they colocalized with the F-actin as shown in the overlay image (Figure 5-17, A and B, left panels). In contrast, almost no Coro1a was found in the largely actin-dim cSMAC region, the inner part of the lytic synapse as shown in Figure 5-17 A (Coro1a and phalloidin). At the site of the cSMAC, Coro1b was present in the cytoplasm but appeared to be decreased at the cell cortex of the NK cells (Figure 5-17 B, Coro1b and phalloidin). No Coro1a- and Coro1b staining was detected in *Coro1a*$^{-/-}$*Coro1b*$^{-/-}$ NK cells which were used as negative control (Figure 5-17, A and B, right panel).

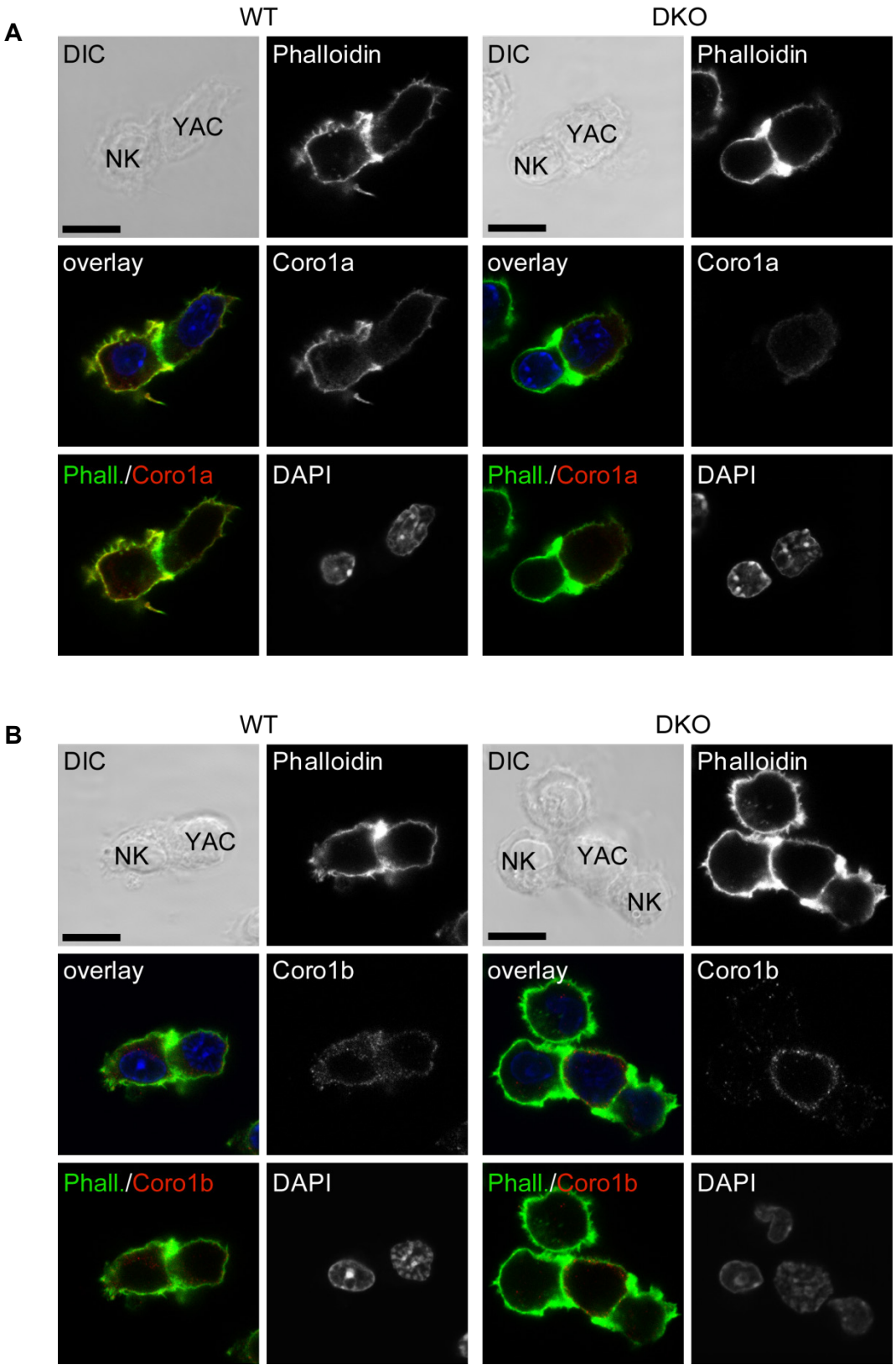

Figure 5-17. Localization of Coro1a and Coro1b in the cytolytic synapse.
Subcellular localization of Coro1a or Coro1b upon contact with target cells was revealed in *wild type* (WT) and *Coro1a*$^{-/-}$*Coro1b*$^{-/-}$ (DKO) IL-15-expanded NK cells by confocal microscopy. NK cells were co-cultured with Yac-1 cells at a ratio of 1:3 for 30 min and were stained for either Coro1a (A, red) or Coro1b (B, red), F-actin (phalloidin, green) and DNA (DAPI, blue) after fixation and permeabilization. Representative individual or overlay fluorescence and DIC images of at least three independent experiments are shown. Bars, 10 µm.

In accordance with my previously described finding that conjugate formation is unaffected by the loss of Coro1a and Coro1b (Figure 5-14, A and B), also no major differences in the morphology of lytic synapses formed by *wild type* or *Coro1aCoro1b*-deficient NK cells (Figure 5-17, A and B) were observed by confocal microscopy.

In conclusion, Coro1a and Coro1b were both found in the actin-rich pSMAC region of the lytic synapse where they colocalized with F-actin and only minor amounts were detected in the largely actin-dim cSMAC region. Furthermore, synapse formation seems to be unaffected by the loss of Coro1a and Coro1b, given that no morphological differences between synapses formed by *wild type* or *Coro1aCoro1b*-deficient NK cells were found by confocal microscopy.

5.9.5 Granule content is not affected by the loss of Coro1a or Coro1b

NK cell cytotoxicity is mediated by the release of granules containing the pore-forming protein perforin and cytotoxic serine proteases named granzymes [137–142]. Since the altered cytolytic response found in coronin-deficient NK cells could be due to abnormal granule contents, the cellular contents of granzyme A (GrzA) or –B (GrzB) and perforin of *Coro1a*- and/or *Coro1b*-deficient NK were investigated by flow cytometry after intracellular staining or immunoblot analysis of whole NK cell lysates.

For this purpose, resting IL-15-expanded NK cells were fixed, permeabilized and intracellularly stained for GrzA or GrzB (see section 4.3.2) or lysates were prepared and subjected to immunoblot analysis as described in section 4.4 and 4.5. Flow cytometry revealed no differences in the cellular content of GrzA (left panel) or GrzB (right panel) between *wild type* (gray histograms), *Coro1a*$^{-/-}$ (green histograms), *Coro1b*$^{-/-}$ (blue histograms) and *Coro1a*$^{-/-}$*Coro1b*$^{-/-}$ NK cells (red histograms) as shown in Figure 5-18 A (solid lines). Both proteases were detected in at least 97% of the analyzed NK cells for all genotypes. Moreover, no differences in the cellular amounts of perforin were detected by immunoblot analysis as shown by the equal intensity of protein bands in Figure 5-18 B (upper panel). The lower panel of Figure 5-18 B shows that the expression of β-actin, used here as loading control, was comparable in all samples.

In summary, comparable GrzA, GrzB and perforin were found in all NK cell genotypes, thus, excluding alterations in the content of cytotoxic molecules as the underlying cause for the decreased cytotoxicity of *Coro1a*- and *Coro1aCoro1b*-deficient NK cells.

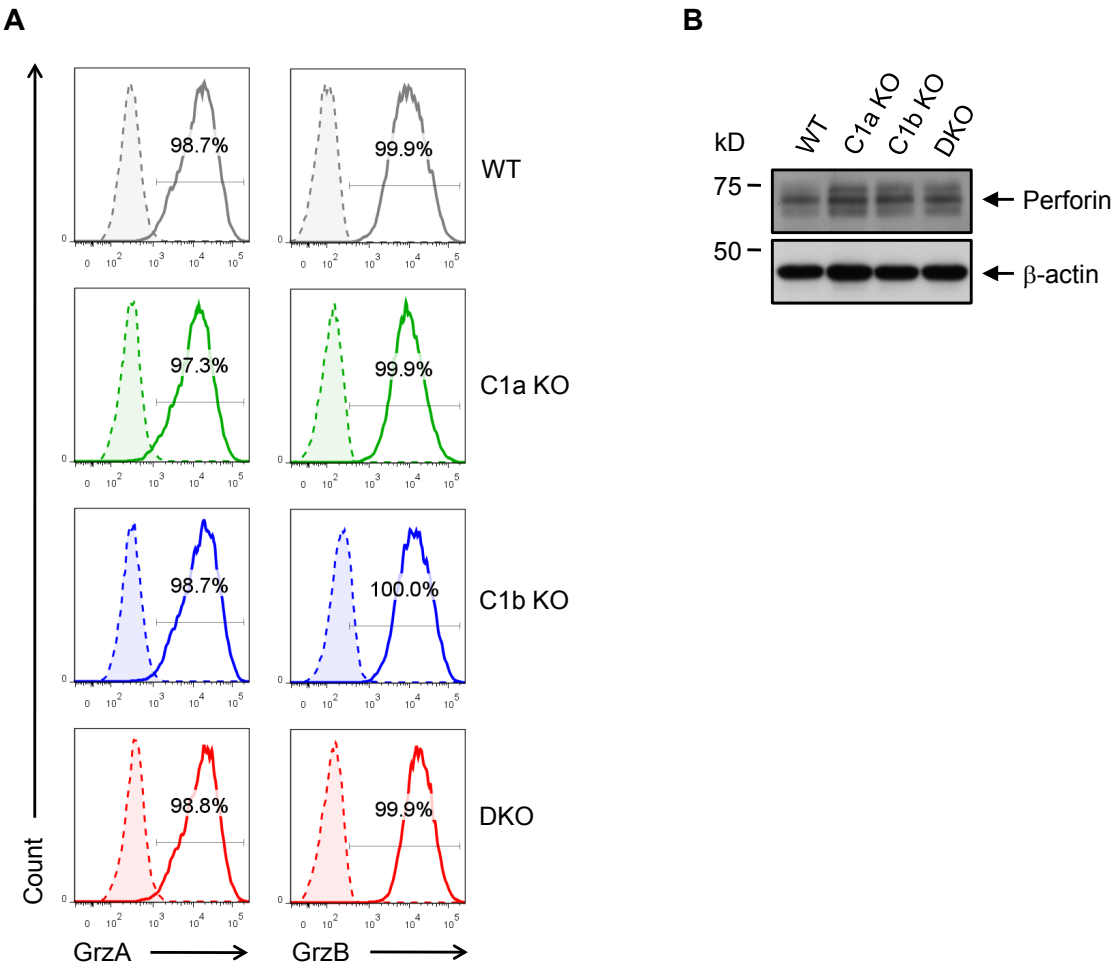

Figure 5-18. Normal granule content in WT, *Coro1a*$^{-/-}$, *Coro1b*$^{-/-}$ and *Coro1a*$^{-/-}$*Coro1b*$^{-/-}$ NK cells.
(A) Cellular granzyme A (GrzA) or granzyme B (GrzB) content of IL-15-expanded *wild type* (WT, gray), *Coro1a*$^{-/-}$ (C1a KO, green), *Coro1b*$^{-/-}$ (C1b KO, blue) and *Coro1a*$^{-/-}$*Coro1b*$^{-/-}$ (DKO, red) NK1.1^{+}/CD3^{-} NK cells was assessed by flow cytometry. NK cells were fixed, permeabilized and stained with specific antibodies for either GrzA (left panel) or GrzB (right panel). Data shown are representative of at least three independent experiments. Solid lines show protein staining and filled histograms with dashed lines shows the matching isotype. Numbers depicted are the percentage of GrzA-/GrzB-positive cells. (B) Immunoblot analysis of perforin expression (upper panel) in IL-15-expanded NK cells of the indicated genotype. Data are representative for at least five independent experiments. Protein loading was assessed by analysis of β-actin expression (lower panel).

5.9.6 Impaired granule polarization in *Coro1aCoro1b*-deficent NK cells

The activation of NK cells upon target cell recognition initiates cellular polarization, the second stage of the cytolytic response of NK cells. Polarization involves several steps including F-actin accumulation at the NK-target contact site and the reorientation of the microtubule-organizing center (MTOC), the Golgi apparatus and the cytotoxic granules toward the target cell [115,116,128,149,155,156]. For these processes, cytoskeletal remodeling is critical since inhibition of F-actin or microtubule dynamics by pharmacologic drugs blocks granule polarization and target cell lysis [115,116,288,293]. Since *Coro1a*-deficient NK cells exhibited dysregulated F-actin contents, which correlates with an impaired cytolytic response, I investigated whether coronins are involved in controlling NK

cell polarization. To this purpose, the reorientation of cytotoxic NK cell granules following conjugate formation was analyzed by confocal microscopy after labeling of granules with Lysotracker® Red DND-99 or -Green DND-26, which stains acidic cell compartments, as previously described [159,294,295]. As a first step, the specificity of the Lysotracker®-labeling was assessed (Figure 5-19). For this purpose, Lysotracker®-labeled *wild type* NK cells were fixed, permeabilized and stained for CD107a (LAMP-1) and DNA (Hoechst) as described in section 4.6. Confocal microscopy experiments revealed a colocalization of CD107a (LAMP-1), which is predominantly expressed intracellularly in the membrane of secretory lysosomes and endosomes in resting cells, with the Lysotracker® Green DND-26 staining (LTgreen), as shown by the overlay pictures in Figure 5-19 A or drawn to a larger scale in Figure 5-19 B. Almost all cytotoxic granules of the NK cells were efficiently labeled with Lysotracker® (Figure 5-19 A), thus, providing a valid experimental tool to investigate granule polarization in NK cells upon contact with target cells.

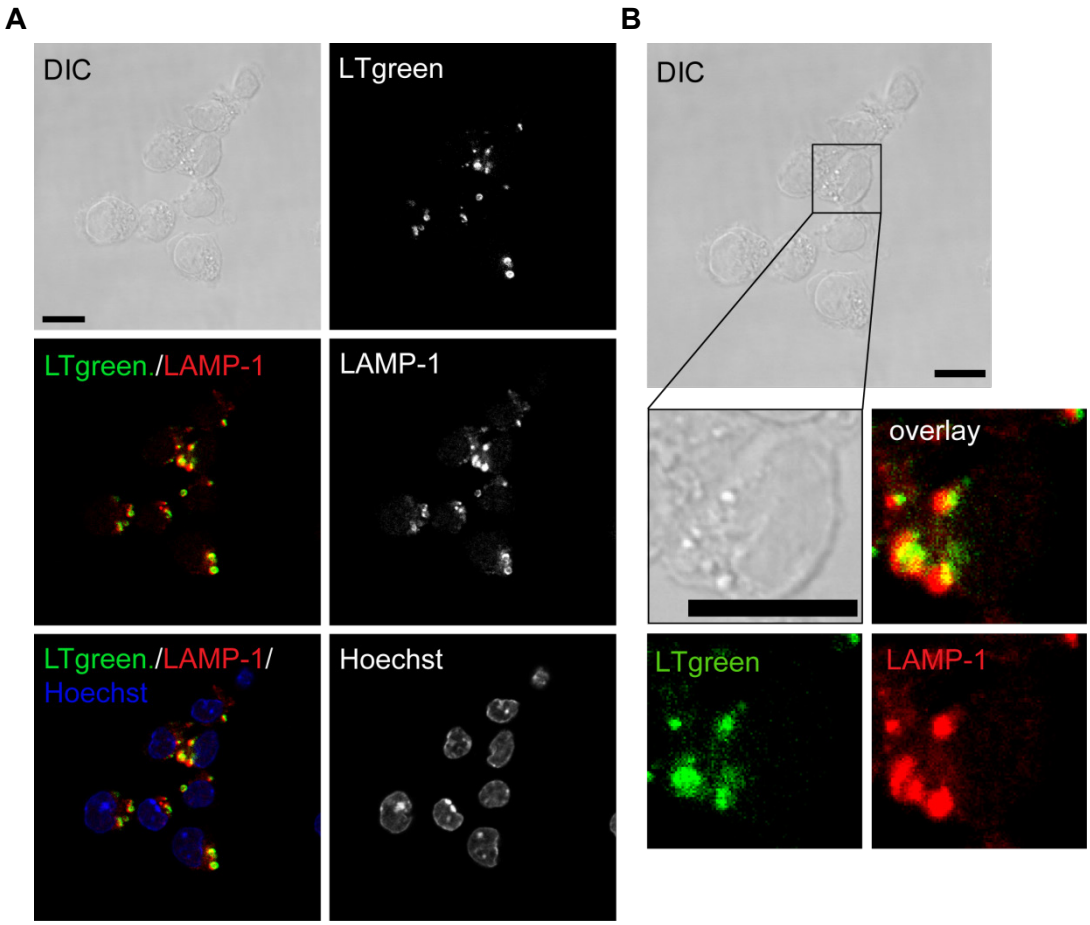

Figure 5-19. Colocalization of LysoTracker® Green and LAMP-1.
Subcellular localization of CD107a (LAMP-1, red) and cytotoxic granules (stained with LysoTracker® Green) was revealed in *wild type* IL-15-expanded NK cells by confocal microscopy. NK cells were loaded with LysoTracker® Green (LTgreen, green) for 2 hours. Cells were fixed with methanol/acetone and stained for CD107a and with Hoechst as DNA-marker (blue). Shown are individual or overlay fluorescence and DIC images (A) or a part of the image drawn to a larger scale (B). Bars, 10 µm.

Next, the reorientation of NK cell granules subsequent to NK-target-conjugation was investigated in detail. NK cells were labeled with Lysotracker® Red DND-99 (LTred) and co-cultured with YAC-1 target cells at a ratio of 1:3 for 30 min, followed by fixation, permeabilization and staining for DNA with Hoechst-dye as described in section 4.6. Different degrees of reorientation of the cytotoxic granules toward the site of the synapse were observed by confocal microscopy in *wild type* as well as in *Coro1a*$^{-/-}$*Coro1b*$^{-/-}$ NK cells. Figure 5-20 A exemplarily shows fully polarized *wild type* (WT) and *Coro1a*$^{-/-}$*Coro1b*$^{-/-}$ NK cell (DKO) granules of conjugated NK cells. Lysotracker® Red DND-99 labeled cytolytic granules are depicted by the red staining located at the site of the lytic synapse. For the quantification of the granule reorientation, conjugated NK cells were subdivided into areas, enabling a classification of NK cells in polarized or non-polarized stages as schematically shown in Figure 5-20 B. Fully polarized NK cells were calculated as percentages of total analyzed NK cell conjugates.

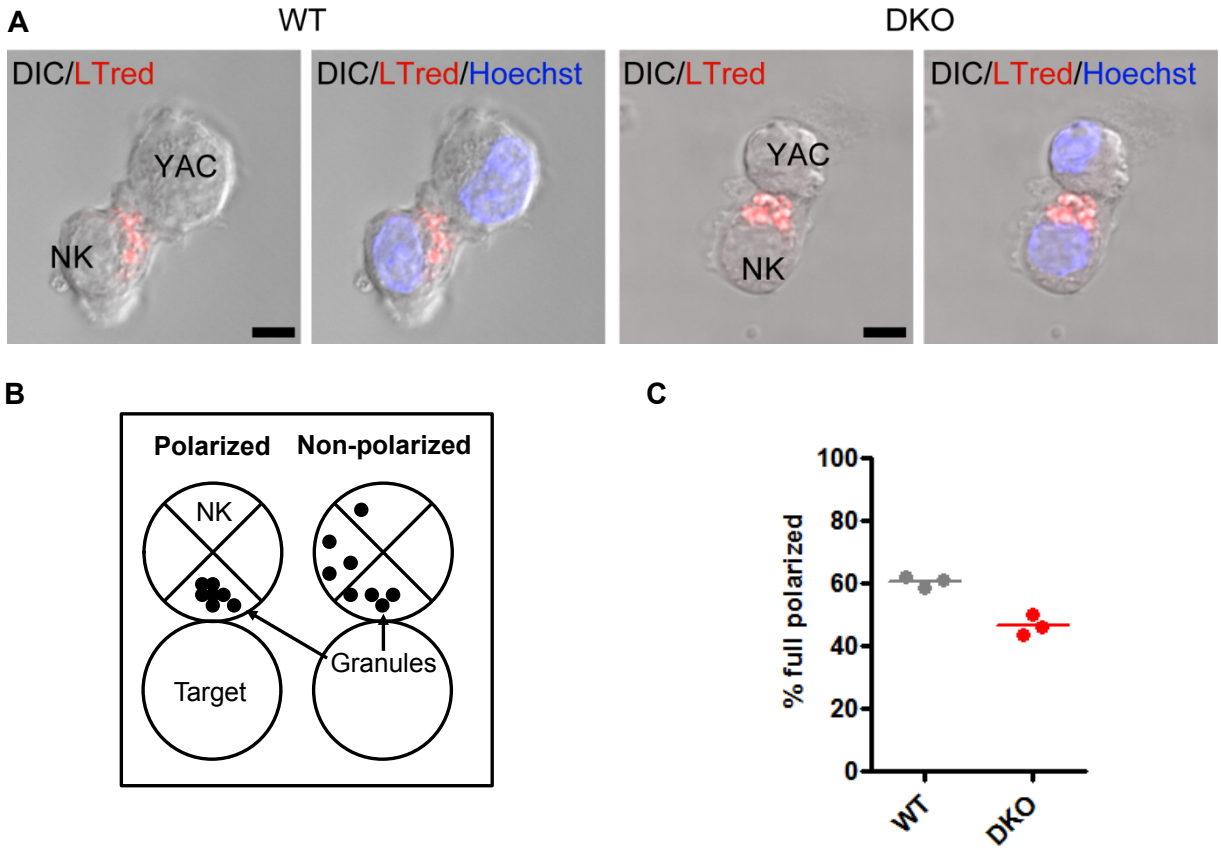

Figure 5-20. *Coro1a*$^{-/-}$*Coro1b*$^{-/-}$ NK cells show an impaired granules polarization.
Subcellular localization of cytotoxic granules was revealed in *wild type* (WT) and *Coro1a*$^{-/-}$*Coro1b*$^{-/-}$ (DKO) IL-15-expanded NK cells upon contact with target cells by confocal microscopy. NK cells were incubated with LysoTracker® Red (LTred, red) for 2 hours. Afterwards cells were co-cultured with Yac-1 cells at a ratio of 1:3 for 30 min, fixed and stained for DNA (Hoechst, blue). Shown are: Representative fluorescence and DIC overlay images of polarized cells (A), a scheme depicting characteristics of polarized versus non-polarized NK cells (B) and calculated percentage of fully polarized NK cells of three independent experiments (C). (Mean ± SEM; n=3 with 162 WT and 170 DKO conjugates analyzed in total; Bars, 5 µm.)

The analysis of 162 conjugated *wild type* (WT) and 170 conjugated *Coro1a*$^{-/-}$*Coro1b*$^{-/-}$ NK cells (DKO), originated from three independent experiments for granule polarization, revealed an impaired reorientation of the cytotoxic granules of *Coro1a*$^{-/-}$*Coro1b*$^{-/-}$ NK cells towards the target cell compared to *wild type* cells (Figure 5-20 C). While 60.7% ± 1.0 of the conjugated *wild type* NK cells were polarized, fully reoriented cytotoxic granules at the site of the cytolytic synapse were detected only in 46.6% ± 1.9 of the *Coro1a*$^{-/-}$*Coro1b*$^{-/-}$ NK cells. These observations provide a possible mechanistic explanation for the impaired cytotoxicity of *Coro1a*$^{-/-}$*Coro1b*$^{-/-}$ NK cells. In addition, the further subdivision of non-polarized NK cells into partially polarized and non-polarized cells showed no indication for a stagnation of the granules reorientation within a special stage of polarization, as no significant difference in the frequency of these subgroups were found between *wild type* and *Coro1a*$^{-/-}$*Coro1b*$^{-/-}$ NK (data not shown).

In conclusion, the analysis of granule polarization in NK cells subsequent to the conjugation with a target cell, revealed an impaired reorientation of cytotoxic granules in *Coro1aCoro1b*-deficient NK cells compared to *wild type* cells, possibly contributing to the decreased cytotoxicity of *Coro1a*$^{-/-}$ and *Coro1a*$^{-/-}$*Coro1b*$^{-/-}$ NK cells.

5.9.7 NK cell degranulation depends on F-actin remodeling and is impaired by the loss of Coro1a

The final stage of the cytolytic activity of NK cells is the secretion of cytotoxic granule contents at the site of the synapse to kill aberrant cells. The fusion of polarized granules with the plasma membrane and the associated release of perforin and granzymes occur in locally hypodense areas of the actin network and strictly require F-actin remodeling at the site of the cytolytic synapse [115,116,159]. In this context, the impact of the actin cytoskeleton on regulating NK cell degranulation was mainly demonstrated by employing actin-modulatory drugs [115,124,159,165,296]. Hence, only little is known about the impact of actin regulatory proteins on degranulation. To study to what extend F-actin remodeling and coronins in particular contribute to the regulation of NK cell degranulation, *Coro1a*- and/or *Coro1b*-deficient NK cells were investigated for their ability to degranulate.

To this end, *wild type* NK cells were co-cultured with target cells, to induce NK cell degranulation, in the presence of a mAb directed against CD107a (LAMP-1) and surface expression of CD107a was used as read-out. Cells were treated with drugs that prevented F-actin assembly (latrunculin B and cytochalasin D) or disassembly (jasplakinolide), with the respective carrier or left untreated and degranulation was assessed by flow cytometric analysis (see section 4.11). Since the remodeling of cortical F-actin is crucial for receptor clustering and the accumulation of F-actin at the site of the synapse, both early processes in the NK cell activation cascade, as well as for later steps, e.g. the degranulation of NK cells

[115,159], drug treatment was performed independently at two time points. The inhibitors were added at time zero to inhibit the activation and thereby later processes, or after 10 min of co-culture allowing activation but impairing degranulation by inhibiting cortical F-actin remodeling as shown by the time scale in Figure 5-21 A.

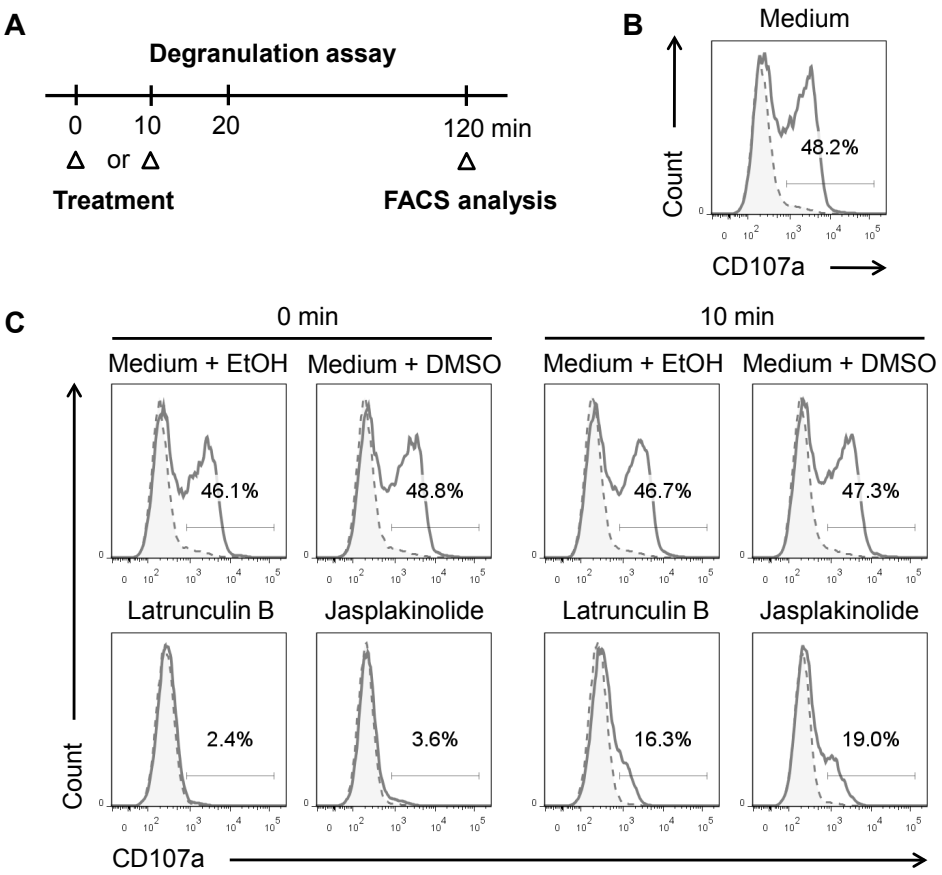

Figure 5-21. Pharmacologic manipulation of the actin cytoskeleton results in decreased degranulation.
Degranulation of *wild type* IL-15-expanded NK cells treated with actin-modulatory drugs was analyzed by flow cytometry. NK cells were cultured either without target cells (dashed line) or co-cultured with Yac-1 cells (solid line) at a ratio of 2:1 in the presence of a CD107a mAb for 2 hours. At time 0 or after 10 min of culture latrunculin B or jasplakinolide was added to destroy or stabilize the actin cytoskeleton of the cells, respectively. Carrier was added as control. Numbers shown are the percentage of CD107a-positive NK1.1^{+}/CD3^{-} cells. Data are representative of three independent experiments. (A) Time scheme of the experiment, (B) Medium-only control, (C) NK cell degranulation upon treatment with latrunculin B or jasplakinolide.

The addition of latrunculin B, cytochalasin D (data not shown) or jasplakinolide at time zero completely inhibited degranulation upon contact with the target cells (Figure 5-21 C). Only 4% of drug treated NK cells resulted CD107a-positive compared to circa 48% of the untreated control counterpart (Figure 5-21, B and C). In contrast, treatment with the corresponding control drug carrier had no impact on NK cell degranulation, as comparable percentages of degranulated cells were measured for treated and untreated conditions (Figure 5-21, B and C). Exposure of NK cells to actin-modulatory drugs 10 min after the activation (10 min, lower panel) still significantly reduced degranulation. The analysis

revealed frequencies of CD107a-positive cells below 20% upon treatment as shown in Figure 5-21 C. However, the inhibitory effect was not as strong as when actin modulatory drugs were added at time zero. Again carrier treatment at 10 min had no effect on degranulation (Figure 5-21, B and C, upper panel).

Altogether, these results provide additional evidence for the proposed requirement of an initial F-actin remodeling for the synapse formation and a crucial role for actin-reorganization during NK cell degranulation.

Since the loss of Coro1a results in increased cortical F-actin levels in NK cells, which potentially influence the exocytosis of cytolytic granules, the impact of *Coro1a*- and/or *Coro1b*-deficiency on NK cell degranulation was investigated next. To this end, NK cells were co-cultured for 3 hours with or without target cells and degranulation was assessed by CD107a staining and flow cytometry. As shown in Figure 5-22, the loss of Coro1a (C1a KO) resulted in a decreased degranulation compared to *wild type* (WT) levels (23% CD107a positive *Coro1a*$^{-/-}$ NK cells vs. 36% *wild type* NK cells). Interestingly, degranulation was unaffected in *Coro1b*$^{-/-}$ NK cells (C1b KO) and *Coro1a*$^{-/-}$*Coro1b*$^{-/-}$ NK cells (DKO) degranulated comparably to *Coro1a*-deficient NK cells (Figure 5-22) indicating a minor contribution of Coro1b in the degranulation processes.

In summary, the actin-regulatory protein Coro1a participates in modulating NK cell degranulation, possibly by influencing the remodeling of the actin cytoskeleton.

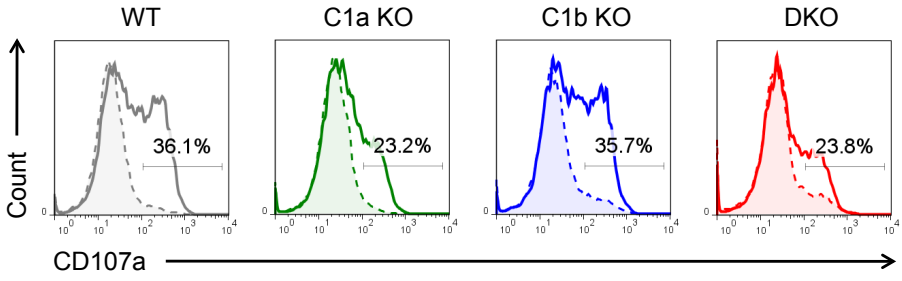

Figure 5-22. *Coro1a*$^{-/-}$ and *Coro1a*$^{-/-}$*Coro1b*$^{-/-}$ NK cells show decreased degranulation.
Degranulation of *wild type* (gray lines), *Coro1a*$^{-/-}$ (green lines), *Coro1b*$^{-/-}$ (blue lines) and *Coro1a*$^{-/-}$*Coro1b*$^{-/-}$ (red lines) IL-15-expanded NK cells was analyzed by flow cytometry. NK cells were cultured either without target cells (dashed line) or co-cultured with Yac-1 cells (solid line) at a ratio of 5:1 in the presence of a CD107a mAb for 3 hours. Numbers shown are the percentage of CD107a-positive NK1.1^{+}/CD3^{-} cells. Data are representative of at least five independent experiments.

5.10 Impaired cytokine secretion in *Coro1a*$^{-/-}$ and *Coro1a*$^{-/-}$*Coro1b*$^{-/-}$ NK cells

Besides being cytolytic, activated NK cells secrete a variety of different soluble mediators, including interleukins, interferons, growth factors and chemokines [52,57–60,65,66,297–301]. As the secretion of these mediators by NK cells is important for an adequate immune

response under several circumstances (e.g. a viral infection) [38,40,57,58,302], it is important to understand whether coronins are involved in the control of the NK cell cytokine expression and secretion.

To this end, NK cells were stimulated with plate-bound mAbs directed against NK1.1 or NKG2D, PMA/ionomycin or left untreated (see section 4.1.10) and used for further analysis. In a first step *IFN-γ* gene expression in stimulated NK cells was determined by real-time PCR analysis (see section 4.2). The level of *IFN-γ* gene expression was measured and normalized to the expression of the housekeeping gene *Hprt* in each sample. As shown in Figure 5-23 A, crosslinking of the activating NK cell receptor NK 1.1 (NK1.1), resulted in a comparable induction of *IFN-γ* mRNA in *wild type* (gray), *Coro1a*$^{-/-}$ (green), *Coro1b*$^{-/-}$ (blue) and *Coro1a*$^{-/-}$*Coro1b*$^{-/-}$ NK cells (red). Similar results were obtained upon PMA/ionomycin stimulation (data not shown). No *IFN-γ* gene expression was detected in non-stimulated cells (Figure 5-23 A, Medium), which were used as control, confirming an activation-specific induction of the *IFN-γ* mRNA.

Next, possible differences in the cellular IFN-γ protein content of *Coro1a*- and/or *Coro1b*-deficient NK cells were investigated. To this purpose, intracellular IFN-γ staining in stimulated NK cells was assessed by flow cytometry as described in section 4.3. and shown in Figure 5-23 B. Results from these studies demonstrate a comparable production of IFN-γ in *wild type* (gray), *Coro1a*$^{-/-}$ (green), *Coro1b*$^{-/-}$ (blue) and *Coro1a*$^{-/-}$*Coro1b*$^{-/-}$ NK cells (red) as shown by the percentages of IFN-γ-positive NK cells in the histograms (Figure 5-23 B). After 6 hours of stimulation, 78.8% of the *wild type*, 80.2% of the *Coro1a*$^{-/-}$, 82.0% of the *Coro1b*$^{-/-}$ and 75.3% of the *Coro1a*$^{-/-}$*Coro1b*$^{-/-}$ NK cells were positive for IFN-γ-staining (Figure 5-23 B, NK1.1). Similar results were obtained upon stimulation via NKG2D or with PMA/ionomycin (data not shown). Consistent with the data obtained on *IFN-γ* gene expression (Figure 5-23 A), no IFN-γ protein expression was detected in non-stimulated *wild type*, *Coro1a*$^{-/-}$, *Coro1b*$^{-/-}$ and *Coro1a*$^{-/-}$*Coro1b*$^{-/-}$ NK cells (Figure 5-23 B, Medium).

Altogether, these data indicate that the loss of Coro1a and/or Coro1b does not affect the IFN-γ-production in NK cells.

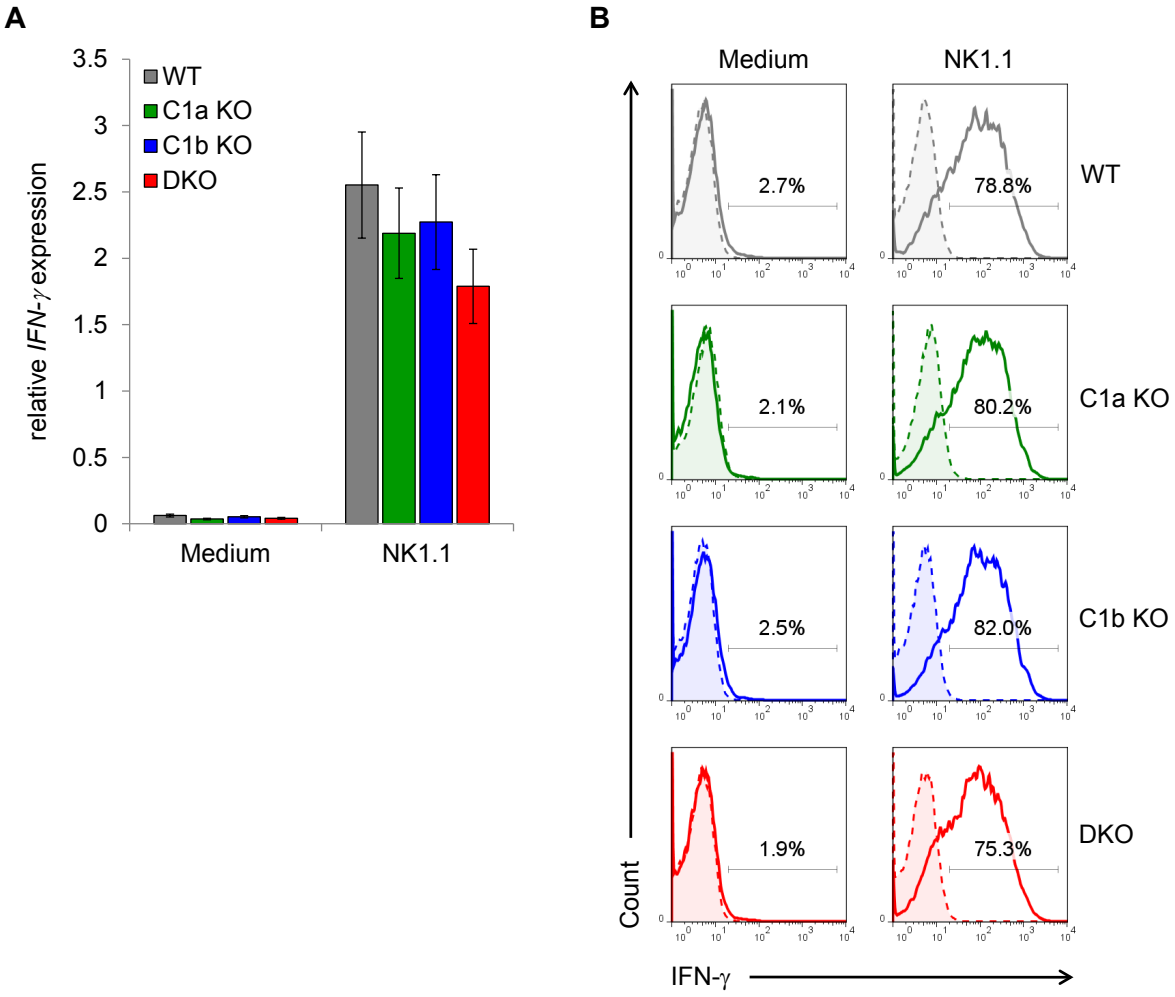

Figure 5-23. Normal IFN-γ production in *wild type*, *Coro1a*$^{-/-}$, *Coro1b*$^{-/-}$ and *Coro1a*$^{-/-}$*Coro1b*$^{-/-}$ NK cells.
IL-15-expanded NK cells from *wild type* (gray bars/line), *Coro1a*$^{-/-}$ (green line/bars), *Coro1b*$^{-/-}$ (blue line/bars) and *Coro1a*$^{-/-}$*Coro1b*$^{-/-}$ (red line/bars) mice were stimulated with plate-bound specific antibodies against NK1.1. or left untreated. (A) RNA was isolated after 1 hour of stimulation and cDNA was synthesized. Quantitative real-time PCR analysis using *IFN-γ* and *hprt* specific primers was performed to assess *IFN-γ* mRNA expression. Data are relative to *hprt* and show the mean ± SD from one representative experiment in duplicates. (B) Cellular IFN-γ content of NKp46^{+}/CD3^{-} NK cells was assessed by flow cytometry. NK cells were stimulated for 6 hours in the presence of Brefeldin A. Cells were fixed, permeabilized and stained with specific antibodies for either IFN-γ (solid lines) or the corresponding isotype (filled histograms with dashed lines). Numbers depicted are the percentage of IFN-γ-positive cells. Data are representative of three independent experiments.

Secretory processes are known to depend on the remodeling of the cytoskeleton [222,303,304]. To address the question whether loss of Coro1a- and/or Coro1b-function impairs the cytokine secretion in NK cells, release of IFN-γ and CCL5 upon activation of NK cells was assessed by ELISA. *Wild type* and *Coro1a*- and/or *Coro1b*-deficient NK cells were stimulated via crosslinking of NK1.1 (NK1.1) or NKG2D (NKG2D), with PMA/ionomycin (P/I) or left untreated for 20 hours as described in section 4.1.10 and supernatants were subjected to ELISA (Figure 5-24).

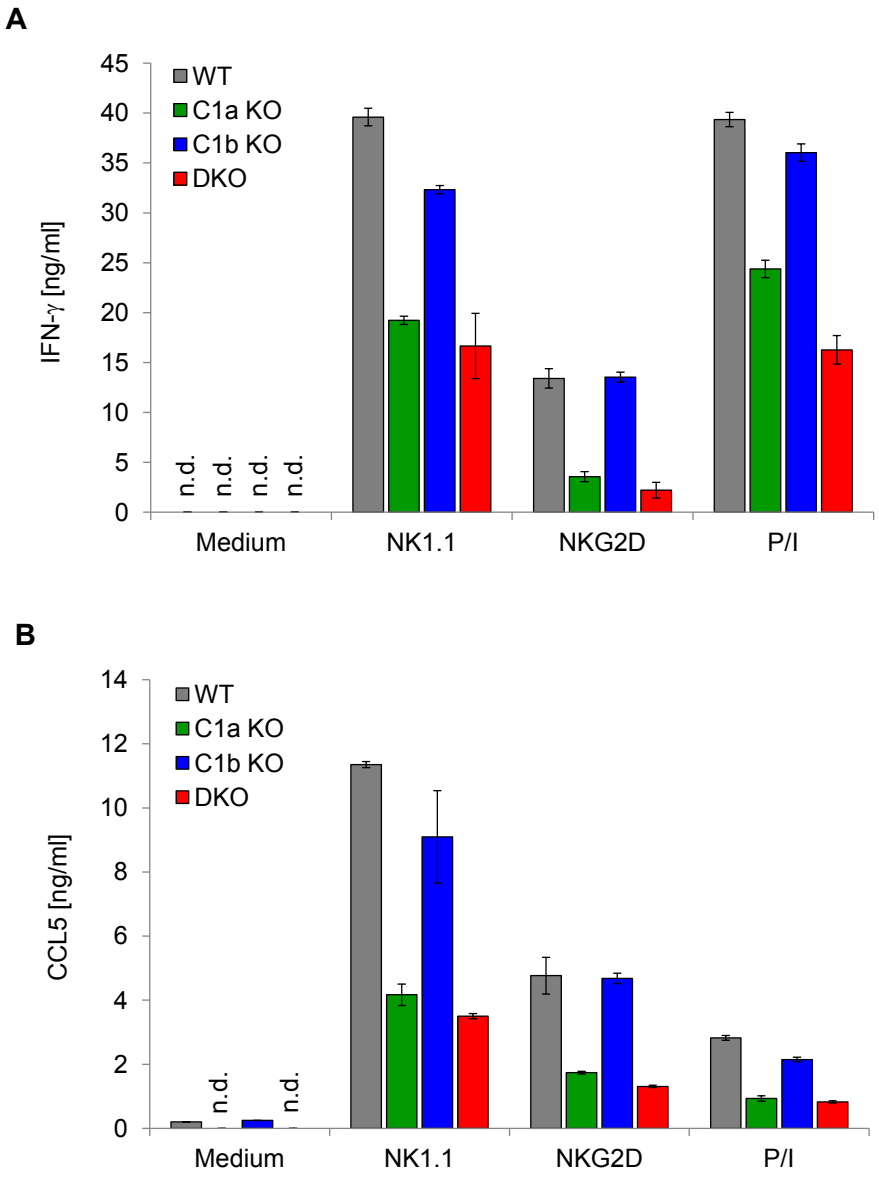

Figure 5-24. IFN-γ and CCL5 secretion is impaired in *Coro1a*$^{-/-}$ and *Coro1a*$^{-/-}$*Coro1b*$^{-/-}$ NK cells. *Wild type* (gray bars), *Coro1a*$^{-/-}$ (green bars), *Coro1b*$^{-/-}$ (blue bars) and *Coro1a*$^{-/-}$*Coro1b*$^{-/-}$ (red bars) IL-15-expanded NK cells were stimulated with plate-bound specific antibodies against either NK1.1 or NKG2D, PMA and ionomycin (P/I) for 20 hours or left untreated. The release of IFN-γ (A) and CCL5 (B) into the supernatant was measured by ELISA. Data (Mean ± SD) are representative of three independent experiments in triplicates. N.d. – not detectable.

Differently to the intracellular cytokine expression, the loss of Coro1a (green bars) resulted in a dramatically impaired secretion of IFN-γ (Figure 5-24 A) and CCL5 (Figure 5-24 B) compared to the release by *wild type* (gray bars) or *Coro1b*-deficient NK cells (blue bars) for all stimuli. Only minimal differences in the cytokine secretion were found between *wild type* and *Coro1b*$^{-/-}$ NK cells while cytokine release impairment was comparable between *Coro1a*$^{-/-}$ and *Coro1a*$^{-/-}$*Coro1b*$^{-/-}$ NK cells (red bars), indicating a marginal role of Coro1b in this process. It is known that cytokine-activated NK cells produce and secrete moderate amounts of CCL5 without further activation [66,67]. Consistent with these reports, low

concentrations of CCL5 were found in the supernatants of non-stimulated *wild type* and *Coro1b*$^{-/-}$ NK cells, while no CCL5 was detectable in the supernatants of *Coro1a*$^{-/-}$ and *Coro1a*$^{-/-}$*Coro1b*$^{-/-}$ NK cells, indicating a secretory defect of these cells even in the absence of a receptor-mediated activation, as shown in Figure 5-24 B for the medium control (Medium). In contrast to CCL5, no secreted IFN-γ was detected in the supernatants of non-stimulated NK cells of all genotypes (Figure 5-24 A, Medium).

In conclusion, *Coro1a*-deficient activated NK cells display a normal expression but an impaired secretion of IFN-γ and CCL5.

6 Discussion

NK cells have been attributed to the control of viral and intracellular bacterial infections as well as to tumor immune surveillance [9–12,23,37–41]. In addition, NK cells have also been implicated in the regulation of other immune cells, not only by the secretion of humoral factors but also via controlling their homeostasis [50,53,55]. In this context, a crucial role for dynamic actin reorganization has been described for various cellular processes required for NK cell functionality [165–171,183]. The dynamic reorganization of F-actin filaments is achieved by a variety of different actin nucleators and their associated regulators [172]. One part of the complex network of proteins involved in actin regulation is represented by coronins. These proteins constitute an evolutionary highly conserved family and representatives have been described in a variety of different species [185,193,198–207]. Coronins have been linked to diverse functions on actin filaments, including actin binding/bundling, actin disassembly and activation/inhibition of the Arp2/3-complex [185,186,229–233,242,244]. The mammalian genome encodes seven coronin family members [189]. Two of them, namely Coro1a and Coro1b, formed the primary focus of this work, as both proteins have been implicated in various actin-mediated cellular functions in leukocytes [187,204,222,248,250,252,253,265]. Importantly, loss of Coro1a-function in humans and mice results in a SCID, which so far has mainly been attributed to defective actin-regulation in T cells [204,259–262]. However, up to now almost nothing is known about the impact of *coronin*-deficiency on the development and function of NK cells. Therefore, in the present study the role of Coro1a and Coro1b in the biology and function of NK cells was investigated.

Utilizing a system of *Coro1a*- and/or C*oro1b*-deficient mice I demonstrated for the first time that Coro1a and, to a lesser degree, Coro1b are critically involved in the regulation of NK cell development and function. Coro1a and Coro1b are co-expressed in NK cells and the loss of Coro1a-function could be directly linked to altered F-actin regulation in NK cells. A detailed study of NK cell development revealed a generally impaired maturation of *Coro1a*$^{-/-}$ and *Coro1a*$^{-/-}$*Coro1b*$^{-/-}$ NK cells compared to *wild type* counterparts, which was associated with developmental alterations in the bone marrow. In addition, I could show that central NK cell functions like killing of aberrant cells, chemokine-mediated migration and cytokine secretion are impaired in IL-15-expanded *Coro1a*$^{-/-}$ and *Coro1a*$^{-/-}$*Coro1b*$^{-/-}$ NK cells. My data demonstrate that decreased cytotoxicity of *Coro1a*$^{-/-}$ and *Coro1a*$^{-/-}$*Coro1b*$^{-/-}$ NK cells was associated with an impaired polarization of cytolytic granules and a decreased capability of NK cells to degranulate, whereas early steps of the cytolytic response including the formation of the cytolytic synapse and the consequent activation of the NK cells appeared to be unaffected. Together, these data demonstrate a crucial role of coronins in the regulation of NK cell development and function.

Although coronins are known for more than 20 years the majority of mammalian coronins is poorly investigated. The limited number of studies investigating the role of mammalian coronins reported heterogeneous expression patterns of the various coronin family members (see Table 1-2). While *Coro1a* is mainly expressed in cells of the hematopoietic lineage and has been described in neutrophils, macrophages, T cells, B cells, dendritic cells and mast cells [187,204,222,248,253,255–258], *Coro1b* shows an ubiquitous expression and likely a more general regulatory function within and outside the hematopoietic cell lineage [212,222–225].

Since no expression data were available for NK cells, mRNA- as well as protein levels of Coro1a and -1b were examined first. Real-time PCR analysis revealed a co-expression of both coronins on the mRNA level in NK cells. Co-expression could be confirmed on protein level by immunoblot analysis and flow cytometry, indicating a potential role of these proteins in the regulation of actin-dependent processes in NK cells. No Coro1a or Coro1b protein expression was detected in the corresponding knockout genotypes, while normal amounts of either Coro1a or Coro1b were found in the non-corresponding knockout NK cell genotypes, indicating a successful knockout of the coronins and the absence of a compensatory counter-regulation upon knockout of either of them, respectively.

Consistent with previous reports on resting T cells, MCs, neutrophils, macrophages, B cells and HL60 cells [204,222,250,252,253,255,256], confocal microscopy of resting NK cells revealed that Coro1a primarily localizes to the F-actin rich cell cortex where it colocalizes with F-actin, but also exhibits some punctate cytoplasmic localization. In contrast to Coro1a, Coro1b showed a more punctate staining distributed throughout the entire cytoplasm of the NK cells with only minor colocalization with the F-actin-rich cell cortex. While a similar distribution of Coro1b was described for resting mast cells a more pronounced cortical Coro1b localization combined with a distribution throughout the entire cytoplasm was found in vascular smooth muscle cells, confirming the idea of cell type and/or context-specific differences in the actin-regulatory activities of coronins [222,225,233]. No Coro1a or Coro1b staining was detected in *Coro1a*$^{-/-}$*Coro1b*$^{-/-}$ NK cells, which served as a negative control, indicating a high specificity of the antibodies.

Additional to staining for Coro1a respectively Coro1b, NK cells were treated with phalloidin which stains F-actin. As first evidence of a potential actin-regulatory function of coronins in NK cells, cellular F-actin contents of *Coro1a*$^{-/-}$*Coro1b*$^{-/-}$ NK cells appeared to be more pronounced compared to *wild type* counterparts. Interestingly, recent studies linked Coro1a to the control of the cellular steady-state F-actin content in T cells but not in MCs [204,222,259,260]. Using an approach enabling the quantification of cellular F-actin contents in greater detail, I demonstrated that the steady-state level of F-actin in *Coro1a*$^{-/-}$ and *Coro1a*$^{-/-}$*Coro1b*$^{-/-}$ NK cells was at least two-times higher as in *wild type* controls. This

significant increase in the F-actin content was observed for *Coro1a*$^{-/-}$ and *Coro1a*$^{-/-}$*Coro1b*$^{-/-}$ NK cells but not for *Coro1b*$^{-/-}$ NK cells. Thus, these data demonstrate an important role of Coro1a but not of Coro1b in the regulation of the steady-state F-actin contents in NK cells and therefore link the effect observed in *Coro1a*$^{-/-}$*Coro1b*$^{-/-}$ NK cells to the loss of Coro1a-function. These data again support the idea of cell type and/or context-specific differences in the actin regulatory activities of coronins [233]. Both, NK- as well as T cells are dedicated to the lymphoid lineage of immune cells. All lymphocytes share common lymphoid characteristics and utilize common mechanisms to fulfill effector functions like the cytolytic activity of NK- and CD8^{+} T cells [100,305]. Hence, a common mechanism controlling F-actin remodeling in NK- and T cells is likely and may explain the similar actin-regulatory functions of Coro1a in these related cell types. In contrast, MCs are dedicated to the myeloid lineage and therefore other mechanisms may be involved in the regulation of the steady-state F-actin level in these cell types [306].

6.1 Coronins and NK cell development

NK cells arise from a CLP in the bone marrow [85–88]. While initial steps of NK cell development, including commitment to the NK cell lineage, early maturation processes as well as NK cell education, occur in the bone marrow, final maturation steps take place in the periphery [88–91]. However, NKPs and iNKs have been also found in the thymus, indicating other potential sites of differentiation or an access of early developmental NK cell stages to the circulation [89,92,93,95,98]. In humans and mice, mNKs are trackable in a number of different tissues and organs including spleen and liver [32–34,36]. In addition to mNKs, the liver maintains a fetal NK cell population into adulthood. These cells phenotypically differ from mNKs and the size of this population reduces over time [94,97]. So far, little is known about the impact of the actin cytoskeleton on NK cell development and maturation. In this context, limited data suggested normal numbers of peripheral NK cells in patients with an inborn defect of *Coro1a* and in *Coro1a*$^{-/-}$ mice [259,260,262]. Consistent with these reports, my analysis revealed that the loss of *Coro1a* had no impact on NK cell numbers in the periphery. In contrast, increased absolute NK cell numbers were detected in the bone marrow of *Coro1a*$^{-/-}$ and *Coro1a*$^{-/-}$*Coro1b*$^{-/-}$ mice compared to *wild type* counterparts, which in turn leads to the question about the underlying mechanisms responsible for this discrepancy. Up to now, it is unclear whether only early developmental NK cell stages, which have no access to the circulation, are increased upon loss of Coro1a-function or if there is a block in the egress of *Coro1a*-deficient NK cells from the bone marrow towards the periphery. Another possible explanation would be an increased susceptibility for apoptosis of circulating peripheral NK cells in *Coro1a*$^{-/-}$ and *Coro1a*$^{-/-}$*Coro1b*$^{-/-}$ mice as described for T cells [204,260,307]. However, data confirming one of these theories or providing further

explanations remain elusive so far. To this end, additional research is needed to dissolve this discrepancy. Contrary to Coro1a, loss of Coro1b-function had no impact on NK cell numbers in the bone marrow or the periphery. Thus, my data indicate that Coro1a and in turn likely the actin cytoskeleton are crucial for proper NK cell development in the bone marrow. An important role of the actin cytoskeleton in developmental processes is further supported by the fact that the loss of function of various actin-regulatory proteins is associated with early embryonic lethality [308–310]. Furthermore, effects on the integrity of the actin cytoskeleton as a consequence to the loss of function of diverse actin-regulatory proteins often affects numbers of peripheral immune cells including B- and T cells as reviewed by Wickramarachchi *et al.* [311].

NK cell development and maturation is a multistep process accompanied by changes in the expression of various surface molecules as well as changes in NK cell functionality [31,89,95,103,104]. The implied developmental steps resulting in mNKs are orchestrated by cell-intrinsic signals like transcription factors and environmental cues including activation via cytokines and other factors [95,100,312]. Interestingly, so far there is no evidence for an involvement of the actin cytoskeleton in developmental processes in NK cells as described for other immune cells [311]. As mentioned above, loss of Coro1a-function resulted in an increased number of *Coro1a*- and *Coro1a/Coro1b*-deficient NK cells in the bone marrow, therefore indicating a regulatory function of coronins and in turn of the actin cytoskeleton in early NK cell development. Further evidence for this theory came from a detailed analysis of various maturation- and activation markers as well as activating- and inhibitory receptors expressed on naïve NK cells located in the bone marrow but also in the periphery. In this context, the analysis of CD11b- and CD27-surface expression is a well-established method to determine the maturation status of murine NK cells [89,91,97,110,111]. By analyzing CD11b/CD27-surface expression on *Coro1a*$^{-/-}$ and/or *Coro1a*$^{-/-}$*Coro1b*$^{-/-}$ NK cells I could show, that loss of Coro1a-function impairs not only the NK cell development in the bone marrow but also in the periphery. Independent of their tissue origin (bone marrow, spleen or liver), *Coro1a*$^{-/-}$ NK cells showed a more immature phenotype compared to *wild type* counterparts. This could be concluded from the expression levels of CD11b and CD27 and other cell surface markers including stem cell growth factor receptor (CD117), IL-7 receptor-α (CD127) and the integrin alpha chain-V (CD51), all markers that are exclusively expressed on early developmental stages [95]. Interestingly, loss of Coro1a-function had no effect on the expression level of CD43, a surface molecule which is known to be gradually upregulated in the course of maturation of CD11b^{+} NK cells [81,89,91]. However, Coro1a-deficiency resulted in an increased expression of another integrin alpha subunit, CD49b. In this context, it should be noted that loss of *Coro1a* had practically no effect on the expression levels of various other receptors that have been analyzed, including activating- and inhibitory NK cell

receptors as well as IL-2-receptor-chains. In contrast to Coro1a, the single loss of Coro1b-function had no impact on NK cell development and maturation, however the immature phenotype of *Coro1a*$^{-/-}$ NK cells was further strengthened by the additional loss of *Coro1b* in *Coro1a*$^{-/-}$*Coro1b*$^{-/-}$ mice. Thus, my data likely implicate a counter regulation or a compensatory effect of Coro1a in *Coro1b*$^{-/-}$ NK cells. As mentioned above, so far the actin cytoskeleton has not been implicated in developmental processes in NK cells. Thus, the observation that *Coro1a*$^{-/-}$ and *Coro1a*$^{-/-}$*Coro1b*$^{-/-}$ NK cells exhibit developmental/maturation defects represents a novel finding, as it suggests a crucial role of coronins and likely of the actin cytoskeleton in maturation processes in NK cells. Though, the underlying mechanisms remain elusive so far. As NK cell development and maturation strictly depends on the proper regulation via transcription factors [93,313–316], a dysregulated activation of these factors due to impaired signaling events is a potential explanation for the developmental defects of NK cell observed in the context of *Coro1a*- and *Coro1a/Coro1b*-deficiency. Furthermore, recent work demonstrated that NK cells require a special bone marrow microenvironment and contact to stromal cells for initial developmental steps [100,103,317,318] and are localized to restricted areas of the spleen and liver under steady-state conditions [319,320]. However, so far the requirements for peripheral NK cell maturation are still poorly investigated. In this context, an alternative explanation for the developmental impairment of *Coro1a*- and *Coro1a/Coro1b*-deficient NK cells may be defects in cell migration and/or cell adhesion that could result in limited maturation signals. Defective migratory responses of *Coro1a*$^{-/-}$ and *Coro1a*$^{-/-}$*Coro1b*$^{-/-}$ NK cells are described in this thesis. Furthermore, observed alterations of actin cytoskeletal structures in these cells may affect adhesion to developmental niches, as this activity strictly depends on a proper F-actin reorganization [321].

As different maturation stages of NK cell have been linked to differences in NK cell effector functions, including cytotoxicity and cytokine production [31,89,104,110], it is tempting to speculate that the reduced maturation status of *Coro1a*- and *Coro1a/Coro1b*-deficient NK cells may be associated with differences in NK cell responsiveness and/or function.

Altogether, my data demonstrate that although loss of coronin-function had no impact on peripheral NK cell numbers, *Coro1a*$^{-/-}$ and *Coro1a*$^{-/-}$*Coro1b*$^{-/-}$ spleen- and liver NK cells exhibit a developmental impairment indicated by a more immature phenotype compared to *wild type* controls which potentially affects their functionality.

6.2 The role of Coro1a and -1b in the regulation of NK cell functions

The encounter of an NK cell with a target cell lacking adequate inhibitory ligands initiates different signaling cascades leading to the release of cytolytic granules and in turn to the death of the target cell and additionally induces the secretion of cytokines [116,126–

129,322]. Various studies have linked NK cell activation with F-actin remodeling at the cell-cell contact site and pointed out a critical role of Arp2/3-complex-mediated F-actin polymerization for NK cell cytotoxicity [124,151,165,167,170,171,181,182]. Class I coronins like Coro1a and -1b co-sediment with components of the Arp2/3-complex and are known to negatively interfere with its function [184,186,187,204,241]. Since loss of Coro1a-function increased steady-state F-actin level in NK cells, adverse effects on NK cell functionality appeared possible. As the purification of murine NK cells from the spleen results in only a limited number of suitable cells, purified NK cells were expanded and activated with IL-15 as previously described by Salagianni *et al.* to obtain sufficient numbers of activated NK cells for functional *in vitro* studies [286]. In contrast to naïve NK cells, IL-15-expanded *Coro1a*$^{-/-}$ and/or *Coro1b*$^{-/-}$ NK cells displayed a similar and relatively homogeneous phenotype concerning the expression of selected maturation markers including CD11b and CD27 as well as activating and inhibitory NK cell receptors. Since NK cell functionality is strongly determined by the maturation status of the cell [31,89,91,104,110], IL-15-expanded cells were utilized to examine potential functional impairments of *Coro1a*- and/or *Coro1b*-deficient NK cells, as those cells showed a relatively comparable maturation phenotype between all genotypes as compared to freshly isolated naïve NK cells.

Since early days of coronin research, coronins have been linked to cellular motility [194]. Mammalian class I coronins have been implicated in both, the impairment as well as the promotion of cellular motility in distinct cell types. For NK cells, I demonstrated that the loss of Coro1a-function resulted in a dramatically decreased spontaneous- as well as chemokine-mediated migration of *Coro1a*$^{-/-}$ and *Coro1a*$^{-/-}$*Coro1b*$^{-/-}$ NK cells, while the disruption of only *Coro1b* expression had no effect on the cellular motility. These data are consistent with the observation that loss of Coro1a-function results in a defective chemokine-mediated migration and an impaired thymic egress of T cells and impaired chemotaxis of human neutrophils [187,204,263]. Moreover, in vascular smooth muscle cells the down regulation of *Coro1b* resulted in increased platelet-derived growth factor-induced migration [225]. While the silencing of *Coro1c* had no impact on vascular smooth muscle cell-migration, an increased cellular motility, cell-matrix adhesion and enhanced cell spreading was observed in intestinal epithelial cells, whereas overexpression of *Coro1c* antagonized cell adhesion and spreading in intestinal epithelial cells [225,323]. Together, my data on the impact of *Coro1a*- and/or *Coro1b*-deficiency on cellular motility of NK cells provide further evidence for cell type and/or context-specific differences in the actin-regulatory activities of coronins as postulated by Gandhi *et al*. [233]. Recent work has linked Coro1b with the inhibition of Arp2/3-complex-mediated F-actin assembly as well as the regulation of cofilin-activity by recruiting SSH1L at the leading edge of rat fibroblasts [186,230]. Similar regulatory functions and properties have been also reported for Coro1a

[187,204,229,246,260]. In this context, a dysregulated F-actin reorganization at the leading edge as result of the regulatory function of Coro1a likely explains the impaired cellular motility of *Coro1a*$^{-/-}$ and *Coro1a*$^{-/-}$*Coro1b*$^{-/-}$ NK cells.

As reported for other regulators of the Arp2/3-complex including WASp, WIP and HS1 [165,167,170], loss of Coro1a-function resulted in decreased NK cell cytotoxicity indicated by a reduced killing of YAC-1 target cells. Cytotoxicity was further diminished upon additional loss of *Coro1b* in *Coro1a*$^{-/-}$*Coro1b*$^{-/-}$ NK cells. However, the single loss of Coro1b-function had no effect on the capability of *Coro1b*$^{-/-}$ NK cells to kill target cells. These data implicate an overlapping role of Coro1a and Coro1b in NK cells. Since NK cell cytotoxicity is a tightly regulated process which strictly depends on early as well as late actin-mediated mechanisms [115,152–154,159], the functional impairment of NK cell cytotoxicity by the loss of coronins could have several reasons that are further discussed in the next paragraphs:

Coro1a- as well as Coro1b-function is dispensable for intercellular conjugate formation and cellular activation of NK cells.

The initial step of NK cell cytotoxicity following the recognition of a target is the formation of a stable conjugate between NK- and target cell [115]. This process requires the segregation of adhesion molecules like LFA-1 into the outer region of the cytolytic synapse known as pSMAC [115,130,151]. There, they mediate the formation of a tight conjugate and initiate various signaling cascades which, among others, stimulate F-actin reorganization [115,124,127,150,151]. Recent work demonstrates that loss of Arp2/3-function as well as disruption of expression of HS1, an NPF linked to the activation of the Arp2/3-complex, negatively affects NK cell adhesion [170,171]. In contrast to Arp2/3 or HS1, I demonstrated that Coro1a- and/or Coro1b-function seems to be dispensable for the formation of a stable intercellular conjugate given that no differences in the ability to form intercellular conjugates were detected between *wild type*, *Coro1a*- and/or *Coro1b*-deficient NK cells. This idea was further supported by the fact that no apparent differences in the morphology of cytolytic synapses formed upon conjugation of *wild type* or *Coro1a*$^{-/-}$*Coro1b*$^{-/-}$ NK cells with YAC-1 target cells were revealed by microscopy indicating an expendable role of both proteins for this process.

NK cell activation initiates F-actin accumulation at the site of the pSMAC likely in a WASp- and Vav-1-dependent manner [115,118,124,165,322,324]. In contrast, F-actin is almost cleared from the inner region of the cytolytic synapse known as cSMAC upon activation [156,157,159]. By utilizing confocal microscopy I demonstrated that the localization of Coro1a as well as Coro1b at the site of the cytolytic synapse resembles the distribution of F-actin. Both coronins were found enriched in the actin-rich pSMAC-region where they colocalized with F-actin and were almost cleared from the largely actin-dim cSMAC-region. In

contrast, localization of both proteins was not altered in unconjugated NK cell areas, thus linking potential coronin-regulatory functions upon NK cell activation to processes at the cell-cell contact site.

Further evidence for coronin-regulatory events following NK cell activation and a tight interaction of Coro1a as well as Coro1b with the actin cytoskeleton came from biochemical fractionation experiments. While in non-stimulated NK cells, Coro1a and -1b were mainly recovered in the cytoskeleton-rich fraction, β-actin and both coronins were mainly located in the cytosolic fraction upon treatment of the cells with the actin-modulatory drug latrunculin B, which disrupts the actin cytoskeleton. Furthermore, activation of the cells via crosslinking of the activating NK cell receptor NK 1.1 leads to a long-lasting phosphorylation of Coro1b on Ser2 correlating with a relocation of the protein from the cytoskeleton-rich- into the cytosolic fraction. Comparable effects on Coro1b but also on Coro1a were previously reported for MCs following FcεRI-mediated activation [222]. However, in contrast to Coro1b only minor changes in the localization of Coro1a were detected upon cellular activation of NK cells not only subsequent to NK1.1 mediated stimulation but also upon treatment with PMA/ionomycin that resulted in a substantial relocation of the protein in MΦs and MCs [222,250]. Importantly, the described differences between NK cells and MCs with respect to Coro1a may be the result of the different strategies used to activate cells as well as general differences between these cell types. While the stimulation of MCs with Abs and the associated antigen affects the whole cell surface and in turn the underlying cortical F-actin cytoskeleton, stimulation of NK cells utilizing beads mimics the interaction with a target cell and therefore involves cell polarization processes which limit activating events to restricted areas. Thus, coronin-regulatory events in NK cells upon stimulation with bead-bound Abs are likely located to the site of activation as demonstrated for NK cell-YAC-1-conjugates and therefore affect only minor portions of the overall cellular coronin content. As demonstrated for fibroblasts, T cells and MΦs, phosphorylation of coronins strictly regulates the interaction of Coro1a and Coro1b with the Arp2/3-complex as well as F-actin and in turn F-actin reorganization [204,212,222,250,251]. Thus, even minor effects on coronins located at the site of activation could be crucial for NK cell function. Nevertheless, it should be mentioned that enrichment of Coro1a and -1b in the pSMAC-region is possibly only a side effect provoked by the F-actin-binding activity of both proteins upon F-actin accumulation in these area. Furthermore, clearance of coronins from the cSMAC-region may be the result of F-actin disassembly during synapse formation. However, independent of the question about the underlying mechanisms leading to the changes in the localization of Coro1a and Coro1b at the site of the forming cytolytic synaps, my data indicate a dispensable role of both coronins for intercellular conjugate formation and the subsequent NK cell activation.

In contrast to adhesion and co-stimulatory molecules which are found in the pSMAC-region, activating- and inhibitory NK cell receptors accumulate in the cSMAC-region of the cytolytic synapse [118,119,152–154]. The formation of microclusters of NK cell receptors strictly depends on actin-mediated lipid raft reorganization and for this reason might be influenced by the loss of *Coro1a* and/or *Coro1b* [124,158,325,326]. The engagement of cognate ligands by activating NK cell receptors initiates the recruitment of various molecules involved in signal transduction like PI3K, PLCγ, PKC or Vav-1 and in turn leads to the activation of the MAPK- and JNK-pathway which are involved in the regulation of the cytolytic response [118,119,126–129]. In this context, I could demonstrate that loss of Coro1a-function only minimally affects the activation of the PI3K-pathway and the MAPK-cascade in *Coro1a*$^{-/-}$ and *Coro1a*$^{-/-}$*Coro1b*$^{-/-}$ NK cells upon activation via crosslinking of NK1.1 as indicated by immunoblot analysis of Akt- and Erk1/2-phosphorylation. In contrast to Coro1a, loss of Coro1b-function had no impact on signaling events. Despite the slight alterations in the Akt- and Erk1/2 phosphorylation levels and kinetics that were observed in *Coro1a*- and *Coro1aCoro1b*-deficient NK cells compared to *wild type* controls, the activation of NK cells of all genotypes via NK1.1 crosslinking resulted in a comparable induction of *IFN-*γ mRNA and following protein production. Thus, the small effects of Coro1a on NK cell signaling seem to be functionally irrelevant, at least in regards to IFN-γ-production.

Loss of coronin-function results in impaired polarization of cytotoxic granules.

NK cell cytotoxicity is mainly mediated by the release of granules containing the pore-forming protein perforin and cytotoxic serine proteases named granzymes, including GrzA and -B [137–142]. Comparable amounts of GrzA, GrzB and perforin were found in all NK cell genotypes, thus excluding alterations in the content of cytotoxic molecules as the underlying cause for the decreased cytotoxicity of *Coro1a*- and *Coro1aCoro1b*-deficient NK cells. In response to the engagement of NK cell-activating receptors and the induction of signaling events linked to the MAPK- and JNK-pathway, cytotoxic granules translocate to the site of the cytolytic synapse [115,128,149,155]. The translocation occurs in two steps including the initial dynein-mediated transport of the cytotoxic granules along the microtubules directed to the MTOC and the following polarization of both, MTOC as well as the granules, towards the cytolytic synapse [115,149,155]. A critical role of the actin cytoskeleton for MTOC polarization has been pointed out by various studies. In this context, the loss of function of proteins involved in the F-actin regulation including WASp or WIP as well as proteins which link microtubules and the actin cytoskeleton like CIP4, IQGAP1 and hDia1 or the inhibition of F-actin dynamics by utilizing pharmacologic drugs, blocks MTOC-polarization and in turn severely impairs NK cell cytotoxicity [115,116,171,183,327,328]. In contrast to the dispensable role of coronins for early steps of the NK cell cytolytic response, loss of

Coro1a/Coro1b-function visually impaired the translocation of cytotoxic granules towards the cell-cell contact site. While 61% of conjugated *wild type* NK cells were polarized, fully reoriented cytotoxic granules at the site of the synapse were only detected in 47% of the *Coro1a*$^{-/-}$*Coro1b*$^{-/-}$ NK cells. As mentioned above, the integrity of the actin network at the site of the cytolytic synapse seems to be indispensable for the polarization of the MTOC and in turn polarization of the cytotoxic granules towards the cell-cell contact site. Although obviously no major differences in the morphology of cytolytic synapses and in particular of the distribution of F-actin within the synapse formed by *wild type* or *Coro1a/Coro1b*-deficient NK cells were revealed by confocal microscopy, non-visible differences in the architecture of the actin cytoskeleton are likely. Thus, a potentially disturbed interaction of the microtubules with the actin cytoskeleton may explain the reduced polarization of cytotoxic granules upon loss of *Coro1a/Coro1b* in *Coro1a*$^{-/-}$*Coro1b*$^{-/-}$ NK cells.

NK cell degranulation is impaired upon loss of Coro1a.

Studies on various types of secretory cells have suggested that the actin cytoskeleton acts as a barrier to exocytosis. However, in many of these cells it became apparent that F-actin additionally acts as a facilitator of secretion [329–334]. A barrier function of the actin cytoskeleton on secretory processes was also described in MCs and neutrophils [222,304]. In T- as well as NK cells the polarized MTOC docks at the synapse membrane within the cSMAC region, however recent work of Rak *et al.* as well as Brown *et al.* demonstrate that release of cytotoxic granules in NK cells, in contrast to T cells, occurs through locally hypodense areas of a pervasive F-actin network within the cSMAC-region in an myosin IIA-dependent manner [156–162,335]. Since the impairment of the integrity of the F-actin network by utilizing pharmacological drugs leads to decreased secretion of cytotoxic granules in human NK cells rather than an increase, Rak *et al.* suggested that F-actin in NK cells acts as a facilitator of secretion rather than a barrier [159]. Consistent with this idea, my data strongly indicate an indispensable role of the actin cytoskeleton for the cytotoxicity of murine NK cells. The inhibition of actin polymerization utilizing latrunculin B or cytochalasin D during NK cell activation resulted in an almost complete prevention of cytolytic granule release. Similar effects were observed upon treatment of cells with jasplakinolide, supporting a crucial role of F-actin reorganization for NK cell cytotoxicity. Further evidence for a contribution of the actin cytoskeleton and its reorganization not only in early but also in late events of NK cell cytotoxicity were provided by the effects of actin-modulatory drugs added following NK cell activation. However, the impact of the treatment with the actin-modulatory drugs subsequent to activation on NK cell degranulation was not as pronounced as for the treatment at the time of activation.

Although the loss of function of various actin-regulatory proteins in NK cells was linked to an impaired cytotoxicity, only little is known about the contribution of these proteins to NK cell degranulation. My studies on NK cell degranulation revealed a crucial role of Coro1a for this process. Specifically, *Coro1a*$^{-/-}$ and *Coro1a*$^{-/-}$*Coro1b*$^{-/-}$ NK cells exhibited decreased degranulation upon conjugation with YAC-1-target cells. In contrast, degranulation of *Coro1b*$^{-/-}$ NK cells was comparable to *wild type* counterparts. These observations are contrary to the previously described role of Coro1a and -1b in MC degranulation. Föger *et al.* recently demonstrated that in MCs the loss of Coro1a-function resulted in FcεRI-induced "hyperdegranulation" which was further increased upon the additional loss of *Coro1b* [222]. Indeed, this discrepancy is likely the result of the different functions of the cytoskeleton in the context of secretory processes. While in MCs, the cortical F-actin has been suggested to act as a barrier during exocytosis, supported by the fact that treatment of MCs with latrunculin B somehow mimics the "hyperdegranulation-phenotype" of *Coro1a*-deficient MCs [222], F-actin in NK cells operates as a facilitator of secretion rather than a barrier [159].

Prior to docking and fusion with the plasma membrane, cytolytic granules have to pass through locally hypodense areas of the pervasive F-actin network within the cSMAC-region of the NK cell [158,159]. However, up to now it remains unclear how these hypodense areas within the actin network are formed. One potential mechanism is a local reorganization of F-actin filaments by actin-regulatory proteins like cofilin that mediates F-actin depolymerization and severing [172,245]. This seems to be important for the exocytosis of glucose transporter-containing vesicles in muscle cells [336]. Interestingly, class I coronins were linked to the regulation of cofilin in yeast as well as in mammals [186,200,232,233,244]. However, in this context coronins have been linked to both, the promotion as well as the inhibition of cofilin-mediated actin disassembly [229,246]. Thus, further investigations are required to resolve this discrepancy. A more simple explanation for the impaired capability of *Coro1a*$^{-/-}$ and *Coro1a*$^{-/-}$*Coro1b*$^{-/-}$ NK cells to secrete cytolytic granules may be a disturbed integrity of the cortical actin network. A dysregulated F-actin organization in these cells has previously already been described for the steady-state F-actin content. Slight changes in the architecture of the cortical F-actin within the cSMAC may inhibit the myosin IIA-mediated transport of cytolytic granules or prevent the passage of granules through the pervasive actin network. In addition, docking of secretory vesicles to the plasma membrane strictly depends on the activity of docking and priming proteins like Rab27a [163,164]. Recent work demonstrated an interaction of Rab27a with Coro1a as well as Coro1c in HL-60 cells and pancreatic beta-cells, respectively [239,337]. However, so far there is no evidence for a Coro1a/Coro1b-Rab27a-interaction in NK cells. Thus, additional research is needed to clarify the role of coronins and in turn of the actin cytoskeleton in NK cell degranulation.

Besides their cytolytic function NK cells produce and secrete a variety of cytokines and other soluble factors, for instance IFN-γ and CCL5, which are important for the modulation of innate as well as acquired immune responses [57,58,300,302]. Despite their relevance, only little is known about the underlying mechanisms of cytokine secretion in NK cells. *Coro1a*$^{-/-}$ and/or *Coro1b*$^{-/-}$ NK cells showed a normal induction of *IFN-γ* mRNA and protein production upon activation. Importantly, however, the loss of Coro1a-function resulted in a dramatically impaired secretion of IFN-γ and CCL5 upon NK cell activation via crosslinking of the activating NK cell receptors NK1.1 as well as NKG2D or by treatment with PMA/ionomycin in *Coro1a*$^{-/-}$ and *Coro1a*$^{-/-}$*Coro1b*$^{-/-}$ NK cells. In contrast, the loss of Coro1b-function had no impact on the capability of NK cells to secrete cytokines. Taken together, my data indicate a regulatory function of Coro1a on cytokine exocytosis in NK cells. Similar observations have previously been made for IL-6 and TNF-α secretion in *Coro1a*-deficient MCs [222], thus suggesting a general role of Coro1a for cytokine exocytosis in immune cells.

Studies on various cell types revealed that the release of soluble factors may be mediated by prestored secretory vesicles or granules segregated from the Golgi in a regulated manner following activation or can occur rapidly upon their synthesis through recycling endosomes and small secretory vesicles through constitutive exocytosis with or without further regulation [338]. The cellular polarization of activated NK cells comprise not only the reorientation of cytolytic granules but also the translocation of the Golgi apparatus as well as recycling endosomes to the site of the cytolytic synapse [115,116,149,156,339]. Reefman *et al.* recently demonstrated that IFN-γ /TNF and perforin are located in separate structures upon cellular activation of NK cells and that the exocytosis of chemokines and perforin occurs in a distinct fashion. While perforin was released in a polarized manner through the cSMAC-region of the cytolytic synapse subsequent to conjugate formation, IFN-γ /TNF were recovered in the Golgi complex and the surrounding recycling endosome and were delivered to the site of the synapse but also to the periphery. Thus, demonstrating that release of these cytokines occurs all over the cell surface of NK cells [339]. Since cytokine secretion in NK cells seems to be carried out over the entire cell surface, the increased cortical F-actin levels observed in *Coro1a*- and *Coro1a*/*Coro1b*-deficient NK cells potentially impair the release of cytokines. In this context, the dysregulated cortical F-actin may act as a barrier which hampers the passage of vesicles and therefore inhibits cytokine secretion. This idea is supported by the observation that a disturbed F-actin reorganization impairs cytokine secretion in T cells [340].

In summary, my data demonstrate that Coro1a and to a lower extent Coro1b are strictly required for diverse cellular functions of NK cells and in turn implicates a crucial role of the actin cytoskeleton for the regulation of these processes

6.3 Conclusions and perspective

NK cells are potent effector cells which are basically capable to respond against stressed endogenous cells in the absence of prior sensitization [9–12,23,37–40]. For that reason, an adequate regulation of NK cell activities is strictly required to avoid the injury of the host organism [39,341,342]. In this study I provide genetic evidence for an important role of two actin-regulatory proteins of the coronin family, Coro1a and Coro1b, in the regulation of NK cell development and function. By utilizing gene-deficient mice I demonstrated that the loss of Coro1a-function was directly linked to dysregulated F-actin organization in NK cells. My data indicate a direct inhibitory role of Coro1a in the regulation of F-actin levels in NK cells and reinforce the significance of coronins as actin-regulators. Furthermore, so far unrecognized regulatory mechanisms of coronins were revealed in the context of NK cell development and maturation. Consistent with previous reports [259,261,262], loss of *Coro1a* had no impact on NK cell numbers in the periphery, however influenced NK cell development in the bone marrow. Additionally, the loss of coronin-function negatively affected NK cell maturation in *Coro1a*$^{-/-}$ mice, not only in the bone marrow but also in the periphery. In this context, naïve *Coro1a*$^{-/-}$ bone marrow-, spleen- and liver NK cells were characterized by a more immature phenotype compared to *wild type* counterparts. Contrary to Coro1a, loss of Coro1b-function had no impact on NK cell development and maturation in *Coro1b*$^{-/-}$ mice. However, the immature phenotype of *Coro1a*$^{-/-}$ NK cells was further strengthened by the additional loss of *Coro1b* in *Coro1a*$^{-/-}$*Coro1b*$^{-/-}$ mice. Thus, my data likely implicate a counter regulation or a compensatory effect of Coro1a in *Coro1b*$^{-/-}$ NK cells. Together, these data strongly indicate a so far unknown role of Coro1 as well as Coro1b and likely of the actin cytoskeleton in NK cell development and maturation. Though the underlying mechanisms still remains elusive, these findings open up a new interesting field for further research.

Importantly, loss of coronin-function affected not only NK cell development but also NK cell functionality. *In vitro*, IL-15-expanded *Coro1a*$^{-/-}$ and *Coro1a*$^{-/-}$*Coro1b*$^{-/-}$ NK cells matured comparably to *wild type* NK cells but exhibited clear defects in central NK cell functions like killing of tumor cells, chemokine-induced migration and cytokine secretion. All in all functions, that are also impaired upon loss of other proteins associated with actin regulation [165–171,183]. By contrast, loss of *Coro1b* had no effect on NK cell functionality. My data strongly indicate that decreased cytotoxicity of *Coro1a*$^{-/-}$ and *Coro1a*$^{-/-}$*Coro1b*$^{-/-}$ NK cells was associated with an impaired polarization of cytolytic granules and a reduced NK cell degranulation. By contrast, early steps of the cytolytic response, including the formation of the cytolytic synapse and the consequent activation of NK cells, seems to be unaffected by the loss of *Coro1a* and/or *Coro1b*. I further demonstrated that decreased cytokine secretion of *Coro1a*$^{-/-}$ and *Coro1a*$^{-/-}$*Coro1b*$^{-/-}$ NK cells was likely associated with an impairment of exocytic pathways, whereas no major defects were revealed for the cytokine production.

Thus, distinct actin-associated processes involved in NK cell activities likely have different requirements on coronin proteins and the actin cytoskeleton. Furthermore, my data confirm the particular significance of the actin cytoskeleton for the regulation of distinct NK cell activities as emphasized by various studies [165–171,183].

My *in vitro* data strongly suggest an important regulatory role of Coro1a in NK cell activities. However, so far the functional impact of *coronin*-deficiency in an *in vivo* setting still remains elusive. To this end, further research is needed regarding the verification of the here presented results. A T cell-independent tumor model should be the method of choice to verify the role of the coronins *in vivo* because of the reported peripheral T cell-deficiency of *Coro1a*$^{-/-}$ mice [204,259]. A possible approach is provided by the RMA/RMA-S-tumor model [343–346]. In this assay, differently labeled NK cell-resistant RMA cells and NK-susceptible RMA-S cells are injected into the peritoneal cavity of mice and recovered after two days by lavage of the peritoneum. Subsequently, the amount of remaining tumor cells can be easily revealed by flow cytometry. Due to the short period of disposition, the elimination of RMA-S cells should be primarily mediated by NK cells. As *Coro1a*$^{-/-}$ and *Coro1a*$^{-/-}$*Coro1b*$^{-/-}$ NK cells showed a decreased cytotoxicity *in vitro,* the prediction is that higher amounts of RMA-S cells should be recovered from these mice. This approach could also deliver important information about the role of the coronins in regard to the SCID-phenotype of patients with an inborn defect in *Coro1a* or of *Coro1a*$^{-/-}$ mice. So far, the pathological alterations observed in humans and mice resulting in the SCID phenotype, were mainly attributed to defective actin-regulation in T cells, since normal amounts of peripheral NK cells were assessed [204,259–262]. NK cells act as a first barrier against pathogens and are important regulators of adaptive immune responses [23,342]. Therefore, developmental- and functional impairments of NK cells upon loss of Coro1a-function as outlined above, may contribute to the establishment of the clinical symptoms observed in patients with an inborn defect of *Coro1a*.

The demonstrated regulatory role of coronins, especially of Coro1a in NK cell development and function, displays a new aspect of NK cell research. I could show for the first time that coronins are important regulators of NK cell development as well as NK cell maturation and are required for the proper regulation of distinct NK cell activities. In this context, an important role of the actin cytoskeleton in processes like killing of tumor cells, chemotaxis and cytokine secretion is emphasized by various studies and further reinforced by the demonstrated data. Importantly, however, the discovery of the role of coronins and likely of the actin cytoskeleton in NK cell development and especially maturation reveals a novel level of NK cell regulation.

Thus, this study opens up new approaches in NK cell biology and gathers first evidence on the possible role of NK cells in SCID patients with an inborn defect of *Coro1a*.

7 References

[1] S.N. Shishido, S. Varahan, K. Yuan, X. Li, S.D. Fleming, Humoral innate immune response and disease., Clin. Immunol. 144 (2012) 142–58.

[2] O.E. Sørensen, N. Borregaard, A.M. Cole, Antimicrobial peptides in innate immune responses., Contrib. Microbiol. 15 (2008) 61–77.

[3] H. Menezes, C. Jared, Immunity in plants and animals: common ends through different means using similar tools., Comp. Biochem. Physiol. C. Toxicol. Pharmacol. 132 (2002) 1–7.

[4] H.L. Twigg, Macrophages in innate and acquired immunity., Semin. Respir. Crit. Care Med. 25 (2004) 21–31.

[5] G.J. Clark, N. Angel, M. Kato, J.A. López, K. MacDonald, S. Vuckovic, et al., The role of dendritic cells in the innate immune system., Microbes Infect. 2 (2000) 257–72.

[6] S.D. Kobayashi, F.R. DeLeo, Role of neutrophils in innate immunity: a systems biology-level approach., Wiley Interdiscip. Rev. Syst. Biol. Med. 1 (2009) 309–33.

[7] S.N. Abraham, M. Arock, Mast cells and basophils in innate immunity., Semin. Immunol. 10 (1998) 373–81.

[8] R. Shamri, J.J. Xenakis, L.A. Spencer, Eosinophils in innate immunity: an evolving story., Cell Tissue Res. 343 (2011) 57–83.

[9] R.B. Herberman, M.E. Nunn, D.H. Lavrin, Natural cytotoxic reactivity of mouse lymphoid cells against syngeneic acid allogeneic tumors. I. Distribution of reactivity and specificity., Int. J. Cancer. 16 (1975) 216–29.

[10] R.B. Herberman, M.E. Nunn, H.T. Holden, D.H. Lavrin, Natural cytotoxic reactivity of mouse lymphoid cells against syngeneic and allogeneic tumors. II. Characterization of effector cells., Int. J. Cancer. 16 (1975) 230–9.

[11] R. Kiessling, E. Klein, H. Wigzell, “Natural” killer cells in the mouse. I. Cytotoxic cells with specificity for mouse Moloney leukemia cells. Specificity and distribution according to genotype., Eur. J. Immunol. 5 (1975) 112–7.

[12] R. Kiessling, E. Klein, H. Pross, H. Wigzell, “Natural” killer cells in the mouse. II. Cytotoxic cells with specificity for mouse Moloney leukemia cells. Characteristics of the killer cell., Eur. J. Immunol. 5 (1975) 117–21.

[13] S. Akira, S. Uematsu, O. Takeuchi, Pathogen recognition and innate immunity., Cell. 124 (2006) 783–801.

[14] R.V. Luckheeram, R. Zhou, A.D. Verma, B. Xia, $CD4^+$T cells: differentiation and functions., Clin. Dev. Immunol. 2012 (2012) 925135.

[15] M.A. Williams, M.J. Bevan, Effector and memory CTL differentiation., Annu. Rev. Immunol. 25 (2007) 171–92.

[16] T.W. LeBien, T.F. Tedder, B lymphocytes: how they develop and function., Blood. 112 (2008) 1570–80.

[17] K. Murphy, Janeway’s Immunobiology, 8th ed., Garland Science, 2011.

[18] M.D. Vesely, M.H. Kershaw, R.D. Schreiber, M.J. Smyth, Natural innate and adaptive immunity to cancer., Annu. Rev. Immunol. 29 (2011) 235–71.

[19] Y. Liu, G. Zeng, Cancer and innate immune system interactions: translational potentials for cancer immunotherapy., J. Immunother. 35 (2012) 299–308.

[20] H. Waldner, The role of innate immune responses in autoimmune disease development., Autoimmun. Rev. 8 (2009) 400–4.

[21] S.C. Eisenbarth, The innate and adaptive immune systems in allergy: a two-way street., Clin. Exp. Allergy. 36 (2006) 135–7.

[22] E. Narni-Mancinelli, E. Vivier, Y.M. Kerdiles, The “T-cell-ness” of NK cells: unexpected similarities between NK cells and T cells., Int. Immunol. 23 (2011) 427–31.

[23] E. Vivier, D.H. Raulet, A. Moretta, M.A. Caligiuri, L. Zitvogel, L.L. Lanier, et al., Innate or adaptive immunity? The example of natural killer cells., Science. 331 (2011) 44–9.

[24] Y. Shinkai, G. Rathbun, K.P. Lam, E.M. Oltz, V. Stewart, M. Mendelsohn, et al., RAG-2-deficient mice lack mature lymphocytes owing to inability to initiate V(D)J rearrangement., Cell. 68 (1992) 855–67.

[25] P. Mombaerts, J. Iacomini, R.S. Johnson, K. Herrup, S. Tonegawa, V.E. Papaioannou, RAG-1-deficient mice have no mature B and T lymphocytes., Cell. 68 (1992) 869–77.

[26] J.-P. de Villartay, A. Fischer, A. Durandy, The mechanisms of immune diversification and their disorders., Nat. Rev. Immunol. 3 (2003) 962–72.

[27] R.B. Herberman, J.R. Ortaldo, Natural killer cells: their roles in defenses against disease., Science. 214 (1981) 24–30.

[28] L.L. Lanier, NK cell receptors., Annu. Rev. Immunol. 16 (1998) 359–93.

[29] L.L. Lanier, NK cell recognition., Annu. Rev. Immunol. 23 (2005) 225–74.

[30] Y.T. Bryceson, M.E. March, H.-G. Ljunggren, E.O. Long, Activation, coactivation, and costimulation of resting human natural killer cells., Immunol. Rev. 214 (2006) 73–91.

[31] M.A. Cooper, T.A. Fehniger, M.A. Caligiuri, The biology of human natural killer-cell subsets., Trends Immunol. 22 (2001) 633–40.

[32] K. Nishikawa, S. Saito, T. Morii, K. Hamada, H. Ako, N. Narita, et al., Accumulation of CD16-CD56+ natural killer cells with high affinity interleukin 2 receptors in human early pregnancy decidua., Int. Immunol. 3 (1991) 743–50.

[33] B.A. Croy, H. He, S. Esadeg, Q. Wei, D. McCartney, J. Zhang, et al., Uterine natural killer cells: insights into their cellular and molecular biology from mouse modelling., Reproduction. 126 (2003) 149–60.

[34] F. Colucci, M.A. Caligiuri, J.P. Di Santo, What does it take to make a natural killer?, Nat. Rev. Immunol. 3 (2003) 413–25.

[35] T.A. Fehniger, M.A. Cooper, G.J. Nuovo, M. Cella, F. Facchetti, M. Colonna, et al., CD56bright natural killer cells are present in human lymph nodes and are activated by T cell-derived IL-2: a potential new link between adaptive and innate immunity., Blood. 101 (2003) 3052–7.

[36] C. Grégoire, L. Chasson, C. Luci, E. Tomasello, F. Geissmann, E. Vivier, et al., The trafficking of natural killer cells., Immunol. Rev. 220 (2007) 169–82.

[37] J.F. Bukowski, B.A. Woda, S. Habu, K. Okumura, R.M. Welsh, Natural killer cell depletion enhances virus synthesis and virus-induced hepatitis in vivo., J. Immunol. 131 (1983) 1531–8.

[38] C.A. Biron, K.S. Byron, J.L. Sullivan, Severe herpesvirus infections in an adolescent without natural killer cells., N. Engl. J. Med. 320 (1989) 1731–5.

[39] J.S. Orange, Human natural killer cell deficiencies and susceptibility to infection., Microbes Infect. 4 (2002) 1545–58.

[40] S.-H. Lee, T. Miyagi, C.A. Biron, Keeping NK cells in highly regulated antiviral warfare., Trends Immunol. 28 (2007) 252–9.

[41] A. Horowitz, K.A. Stegmann, E.M. Riley, Activation of natural killer cells during microbial infections., Front. Immunol. 2 (2011) 88.

[42] K. Kärre, H.G. Ljunggren, G. Piontek, R. Kiessling, Selective rejection of H-2-deficient lymphoma variants suggests alternative immune defence strategy., Nature. 319 (1986) 675–8.

[43] H.G. Ljunggren, K. Kärre, In search of the “missing self”: MHC molecules and NK cell recognition., Immunol. Today. 11 (1990) 237–44.

[44] D. Horst, M.C. Verweij, A.J. Davison, M.E. Ressing, E.J.H.J. Wiertz, Viral evasion of T cell immunity: ancient mechanisms offering new applications., Curr. Opin. Immunol. 23 (2011) 96–103.

[45] B. Seliger, U. Ritz, S. Ferrone, Molecular mechanisms of HLA class I antigen abnormalities following viral infection and transformation., Int. J. Cancer. 118 (2006) 129–38.

[46] M. Lucas, W. Schachterle, K. Oberle, P. Aichele, A. Diefenbach, Dendritic cells prime natural killer cells by trans-presenting interleukin 15., Immunity. 26 (2007) 503–17.

[47] E. Mortier, R. Advincula, L. Kim, S. Chmura, J. Barrera, B. Reizis, et al., Macrophage- and dendritic-cell-derived interleukin-15 receptor alpha supports homeostasis of distinct CD8+ T cell subsets., Immunity. 31 (2009) 811–22.

[48] S. Guia, C. Cognet, L. de Beaucoudrey, M.S. Tessmer, E. Jouanguy, C. Berger, et al., A role for interleukin-12/23 in the maturation of human natural killer and CD56+ T cells in vivo., Blood. 111 (2008) 5008–16.

[49] J. Chaix, M.S. Tessmer, K. Hoebe, N. Fuséri, B. Ryffel, M. Dalod, et al., Cutting edge: Priming of NK cells by IL-18., J. Immunol. 181 (2008) 1627–31.

[50] Y. Hayakawa, V. Screpanti, H. Yagita, A. Grandien, H.-G. Ljunggren, M.J. Smyth, et al., NK cell TRAIL eliminates immature dendritic cells in vivo and limits dendritic cell vaccination efficacy., J. Immunol. 172 (2004) 123–9.

[51] D. Tosi, R. Valenti, A. Cova, G. Sovena, V. Huber, L. Pilla, et al., Role of cross-talk between IFN-alpha-induced monocyte-derived dendritic cells and NK cells in priming CD8+ T cell responses against human tumor antigens., J. Immunol. 172 (2004) 5363–70.

[52] T. Walzer, M. Dalod, S.H. Robbins, L. Zitvogel, E. Vivier, Natural-killer cells and dendritic cells: “l’union fait la force”., Blood. 106 (2005) 2252–8.

[53] L. Lu, K. Ikizawa, D. Hu, M.B.F. Werneck, K.W. Wucherpfennig, H. Cantor, Regulation of activated CD4+ T cells by NK cells via the Qa-1-NKG2A inhibitory pathway., Immunity. 26 (2007) 593–604.

[54] S.H. Robbins, G. Bessou, A. Cornillon, N. Zucchini, B. Rupp, Z. Ruzsics, et al., Natural killer cells promote early CD8 T cell responses against cytomegalovirus., PLoS Pathog. 3 (2007) e123.

[55] U. Schulz, M. Kreutz, G. Multhoff, B. Stoelcker, M. Köhler, R. Andreesen, et al., Interleukin-10 promotes NK cell killing of autologous macrophages by stimulating expression of NKG2D ligands., Scand. J. Immunol. 72 (2010) 319–31.

[56] F.B. Thorén, R.E. Riise, J. Ousbäck, M. Della Chiesa, M. Alsterholm, E. Marcenaro, et al., Human NK Cells induce neutrophil apoptosis via an NKp46- and Fas-dependent mechanism., J. Immunol. 188 (2012) 1668–74.

[57] G. Alter, J.M. Malenfant, R.M. Delabre, N.C. Burgett, X.G. Yu, M. Lichterfeld, et al., Increased natural killer cell activity in viremic HIV-1 infection., J. Immunol. 173 (2004) 5305–11.

[58] C.J. Montoya, P.A. Velilla, C. Chougnet, A.L. Landay, M.T. Rugeles, Increased IFN-gamma production by NK and CD3+/CD56+ cells in sexually HIV-1-exposed but uninfected individuals., Clin. Immunol. 120 (2006) 138–46.

[59] W.M. Yokoyama, S. Kim, A.R. French, The dynamic life of natural killer cells., Annu. Rev. Immunol. 22 (2004) 405–29.

[60] D. Peritt, S. Robertson, G. Gri, L. Showe, M. Aste-Amezaga, G. Trinchieri, Cutting Edge: Differentiation of Human NK Cells into NK1 and NK2 Subsets, J. Immunol. 161 (1998) 5821–5824.

[61] C. Adam, S. King, T. Allgeier, H. Braumüller, C. Lüking, J. Mysliwietz, et al., DC-NK cell cross talk as a novel CD4+ T-cell-independent pathway for antitumor CTL induction., Blood. 106 (2005) 338–44.

[62] R. Wehner, K. Dietze, M. Bachmann, M. Schmitz, The bidirectional crosstalk between human dendritic cells and natural killer cells., J. Innate Immun. 3 (2011) 258–63.

[63] M. Mitrović, J. Arapović, L. Traven, A. Krmpotić, S. Jonjić, Innate immunity regulates adaptive immune response: lessons learned from studying the interplay between NK and CD8+ T cells during MCMV infection., Med. Microbiol. Immunol. 201 (2012) 487–95.

[64] M.J. Scott, J.J. Hoth, M.K. Stagner, S.A. Gardner, J.C. Peyton, W.G. Cheadle, CD40-CD154 interactions between macrophages and natural killer cells during sepsis are critical for macrophage activation and are not interferon gamma dependent., Clin. Exp. Immunol. 137 (2004) 469–77.

[65] M.C. Cuturi, I. Anegón, F. Sherman, R. Loudon, S.C. Clark, B. Perussia, et al., Production of hematopoietic colony-stimulating factors by human natural killer cells., J. Exp. Med. 169 (1989) 569–83.

[66] J.M. Roda, R. Parihar, C. Magro, G.J. Nuovo, S. Tridandapani, W.E. Carson, Natural killer cells produce T cell-recruiting chemokines in response to antibody-coated tumor cells., Cancer Res. 66 (2006) 517–26.

[67] E. Mariani, L. Pulsatelli, S. Neri, P. Dolzani, A. Meneghetti, T. Silvestri, et al., RANTES and MIP-1alpha production by T lymphocytes, monocytes and NK cells from nonagenarian subjects., Exp. Gerontol. 37 (2002) 219–26.

[68] G. Bernardini, A. Gismondi, A. Santoni, Chemokines and NK cells: regulators of development, trafficking and functions., Immunol. Lett. 145 (2012) 39–46.

[69] A. Moretta, E. Marcenaro, S. Sivori, M. Della Chiesa, M. Vitale, L. Moretta, Early liaisons between cells of the innate immune system in inflamed peripheral tissues., Trends Immunol. 26 (2005) 668–75.

[70] P. Krebs, M.J. Barnes, K. Lampe, K. Whitley, K.S. Bahjat, B. Beutler, et al., NK-cell-mediated killing of target cells triggers robust antigen-specific T-cell-mediated and humoral responses., Blood. 113 (2009) 6593–602.

[71] T. Michel, F. Hentges, J. Zimmer, Consequences of the crosstalk between monocytes/macrophages and natural killer cells., Front. Immunol. 3 (2012) 403.

[72] N. Anfossi, P. André, S. Guia, C.S. Falk, S. Roetynck, C.A. Stewart, et al., Human NK cell education by inhibitory receptors for MHC class I., Immunity. 25 (2006) 331–42.

[73] S. Kim, J. Poursine-Laurent, S.M. Truscott, L. Lybarger, Y.-J. Song, L. Yang, et al., Licensing of natural killer cells by host major histocompatibility complex class I molecules., Nature. 436 (2005) 709–13.

[74] N.S. Liao, M. Bix, M. Zijlstra, R. Jaenisch, D. Raulet, MHC class I deficiency: susceptibility to natural killer (NK) cells and impaired NK activity., Science. 253 (1991) 199–202.

[75] H. Furukawa, T. Yabe, K. Watanabe, R. Miyamoto, A. Miki, T. Akaza, et al., Tolerance of NK and LAK activity for HLA class I-deficient targets in a TAP1-deficient patient (bare lymphocyte syndrome type I)., Hum. Immunol. 60 (1999) 32–40.

[76] N.C. Fernandez, E. Treiner, R.E. Vance, A.M. Jamieson, S. Lemieux, D.H. Raulet, A subset of natural killer cells achieves self-tolerance without expressing inhibitory receptors specific for self-MHC molecules., Blood. 105 (2005) 4416–23.

[77] P. Brodin, T. Lakshmikanth, S. Johansson, K. Kärre, P. Höglund, The strength of inhibitory input during education quantitatively tunes the functional responsiveness of individual natural killer cells., Blood. 113 (2009) 2434–41.

[78] P. Brodin, K. Kärre, P. Höglund, NK cell education: not an on-off switch but a tunable rheostat., Trends Immunol. 30 (2009) 143–9.

[79] A. Chalifour, L. Scarpellino, J. Back, P. Brodin, E. Devèvre, F. Gros, et al., A Role for cis Interaction between the Inhibitory Ly49A receptor and MHC class I for natural killer cell education., Immunity. 30 (2009) 337–47.

[80] J.G. O'Leary, M. Goodarzi, D.L. Drayton, U.H. von Andrian, T cell- and B cell-independent adaptive immunity mediated by natural killer cells., Nat. Immunol. 7 (2006) 507–16.

[81] J.C. Sun, J.N. Beilke, L.L. Lanier, Adaptive immune features of natural killer cells., Nature. 457 (2009) 557–61.

[82] M.A. Cooper, J.M. Elliott, P.A. Keyel, L. Yang, J.A. Carrero, W.M. Yokoyama, Cytokine-induced memory-like natural killer cells., Proc. Natl. Acad. Sci. U. S. A. 106 (2009) 1915–9.

[83] R. Romee, S.E. Schneider, J.W. Leong, J.M. Chase, C.R. Keppel, R.P. Sullivan, et al., Cytokine activation induces human memory-like NK cells, Blood. 120 (2012) 4751–4760.

[84] S. Paust, H.S. Gill, B.-Z. Wang, M.P. Flynn, E.A. Moseman, B. Senman, et al., Critical role for the chemokine receptor CXCR6 in NK cell-mediated antigen-specific memory of haptens and viruses., Nat. Immunol. 11 (2010) 1127–35.

[85] O. Haller, R. Kiessling, A. Orn, H. Wigzell, Generation of natural killer cells: an autonomous function of the bone marrow., J. Exp. Med. 145 (1977) 1411–6.

[86] M. Kondo, I.L. Weissman, K. Akashi, Identification of clonogenic common lymphoid progenitors in mouse bone marrow., Cell. 91 (1997) 661–72.

[87] W.E. Seaman, T.D. Gindhart, J.S. Greenspan, M.A. Blackman, N. Talal, Natural killer cells, bone, and the bone marrow: studies in estrogen-treated mice and in congenitally osteopetrotic (mi/mi) mice., J. Immunol. 122 (1979) 2541–7.

[88] E.E. Rosmaraki, I. Douagi, C. Roth, F. Colucci, A. Cumano, J.P. Di Santo, Identification of committed NK cell progenitors in adult murine bone marrow., Eur. J. Immunol. 31 (2001) 1900–9.

[89] S. Kim, K. Iizuka, H.-S.P. Kang, A. Dokun, A.R. French, S. Greco, et al., In vivo developmental stages in murine natural killer cell maturation., Nat. Immunol. 3 (2002) 523–8.

[90] J.R. Dorfman, D.H. Raulet, Acquisition of Ly49 receptor expression by developing natural killer cells., J. Exp. Med. 187 (1998) 609–18.

[91] L. Chiossone, J. Chaix, N. Fuseri, C. Roth, E. Vivier, T. Walzer, Maturation of mouse NK cells is a 4-stage developmental program., Blood. 113 (2009) 5488–96.

[92] A.G. Freud, B. Becknell, S. Roychowdhury, H.C. Mao, A.K. Ferketich, G.J. Nuovo, et al., A human CD34(+) subset resides in lymph nodes and differentiates into CD56bright natural killer cells., Immunity. 22 (2005) 295–304.

[93] C.A.J. Vosshenrich, M.E. García-Ojeda, S.I. Samson-Villéger, V. Pasqualetto, L. Enault, O. Richard-Le Goff, et al., A thymic pathway of mouse natural killer cell development characterized by expression of GATA-3 and CD127., Nat. Immunol. 7 (2006) 1217–24.

[94] N.D. Huntington, H. Tabarias, K. Fairfax, J. Brady, Y. Hayakawa, M.A. Degli-Esposti, et al., NK cell maturation and peripheral homeostasis is associated with KLRG1 up-regulation., J. Immunol. 178 (2007) 4764–70.

[95] N.D. Huntington, C. a J. Vosshenrich, J.P. Di Santo, Developmental pathways that generate natural-killer-cell diversity in mice and humans., Nat. Rev. Immunol. 7 (2007) 703–14.

[96] J.H. Phillips, T. Hori, A. Nagler, N. Bhat, H. Spits, L.L. Lanier, Ontogeny of human natural killer (NK) cells: fetal NK cells mediate cytolytic function and express cytoplasmic CD3 epsilon,delta proteins., J. Exp. Med. 175 (1992) 1055–66.

[97] K. Takeda, E. Cretney, Y. Hayakawa, T. Ota, H. Akiba, K. Ogasawara, et al., TRAIL identifies immature natural killer cells in newborn mice and adult mouse liver., Blood. 105 (2005) 2082–9.

[98] D.M. Andrews, M.J. Smyth, A potential role for RAG-1 in NK cell development revealed by analysis of NK cells during ontogeny., Immunol. Cell Biol. 88 (2010) 107–16.

[99] J. Brady, S. Carotta, R.P.L. Thong, C.J. Chan, Y. Hayakawa, M.J. Smyth, et al., The interactions of multiple cytokines control NK cell maturation., J. Immunol. 185 (2010) 6679–88.

[100] J.C. Sun, L.L. Lanier, NK cell development, homeostasis and function: parallels with $CD8^+$ T cells., Nat. Rev. Immunol. 11 (2011) 645–57.

[101] M.K. Kennedy, M. Glaccum, S.N. Brown, E. a Butz, J.L. Viney, M. Embers, et al., Reversible defects in natural killer and memory CD8 T cell lineages in interleukin 15-deficient mice., J. Exp. Med. 191 (2000) 771–80.

[102] C.A.J. Vosshenrich, T. Ranson, S.I. Samson, E. Corcuff, F. Colucci, E.E. Rosmaraki, et al., Roles for common cytokine receptor gamma-chain-dependent cytokines in the generation, differentiation, and maturation of NK cell precursors and peripheral NK cells in vivo., J. Immunol. 174 (2005) 1213–21.

[103] J.P. Di Santo, Natural killer cell developmental pathways: a question of balance., Annu. Rev. Immunol. 24 (2006) 257–86.

[104] Y. Hayakawa, N.D. Huntington, S.L. Nutt, M.J. Smyth, Functional subsets of mouse natural killer cells., Immunol. Rev. 214 (2006) 47–55.

[105] J.W. Fathman, D. Bhattacharya, M.A. Inlay, J. Seita, H. Karsunky, I.L. Weissman, Identification of the earliest natural killer cell-committed progenitor in murine bone marrow., Blood. 118 (2011) 5439–47.

[106] S. Carotta, S.H.M. Pang, S.L. Nutt, G.T. Belz, Identification of the earliest NK-cell precursor in the mouse BM., Blood. 117 (2011) 5449–52.

[107] N.D. Huntington, S.L. Nutt, S. Carotta, Regulation of murine natural killer cell commitment., Front. Immunol. 4 (2013) 14.

[108] C.A. Vosshenrich, J.P. Di Santo, Developmental programming of natural killer and innate lymphoid cells., Curr. Opin. Immunol. 25 (2013) 130–8.

[109] M. Nieto, J.L. Rodríguez-Fernández, F. Navarro, D. Sancho, J.M. Frade, M. Mellado, et al., Signaling through CD43 induces natural killer cell activation, chemokine release, and PYK-2 activation., Blood. 94 (1999) 2767–77.

[110] Y. Hayakawa, M.J. Smyth, CD27 dissects mature NK cells into two subsets with distinct responsiveness and migratory capacity., J. Immunol. 176 (2006) 1517–24.

[111] A. Silva, D.M. Andrews, A.G. Brooks, M.J. Smyth, Y. Hayakawa, Application of CD27 as a marker for distinguishing human NK cell subsets., Int. Immunol. 20 (2008) 625–30.

[112] S. Chiesa, E. Tomasello, E. Vivier, F. Vély, Coordination of activating and inhibitory signals in natural killer cells., Mol. Immunol. 42 (2005) 477–84.

[113] D.H. Raulet, R.E. Vance, Self-tolerance of natural killer cells., Nat. Rev. Immunol. 6 (2006) 520–31.

[114] K.S. Campbell, J. Hasegawa, Natural killer cell biology: an update and future directions., J. Allergy Clin. Immunol. 132 (2013) 536–44.

[115] J.S. Orange, K.E. Harris, M.M. Andzelm, M.M. Valter, R.S. Geha, J.L. Strominger, The mature activating natural killer cell immunologic synapse is formed in distinct stages., Proc. Natl. Acad. Sci. U. S. A. 100 (2003) 14151–6.

[116] J.S. Orange, Formation and function of the lytic NK-cell immunological synapse., Nat. Rev. Immunol. 8 (2008) 713–25.

[117] K. Krzewski, J.E. Coligan, Human NK cell lytic granules and regulation of their exocytosis., Front. Immunol. 3 (2012) 335.

[118] Y.M. Vyas, K.M. Mehta, M. Morgan, H. Maniar, L. Butros, S. Jung, et al., Spatial organization of signal transduction molecules in the NK cell immune synapses during MHC class I-regulated noncytolytic and cytolytic interactions., J. Immunol. 167 (2001) 4358–67.

[119] Y.M. Vyas, H. Maniar, B. Dupont, Cutting edge: differential segregation of the SRC homology 2-containing protein tyrosine phosphatase-1 within the early NK cell immune synapse distinguishes noncytolytic from cytolytic interactions., J. Immunol. 168 (2002) 3150–4.

[120] E.O. Long, Negative signaling by inhibitory receptors: the NK cell paradigm., Immunol. Rev. 224 (2008) 70–84.

[121] C. Banh, S.M.S. Miah, W.G. Kerr, L. Brossay, Mouse natural killer cell development and maturation are differentially regulated by SHIP-1., Blood. 120 (2012) 4583–90.

[122] L.L. Lanier, Up on the tightrope: natural killer cell activation and inhibition., Nat. Immunol. 9 (2008) 495–502.

[123] K. Jiang, B. Zhong, D.L. Gilvary, B.C. Corliss, E. Vivier, E. Hong-Geller, et al., Syk regulation of phosphoinositide 3-kinase-dependent NK cell function., J. Immunol. 168 (2002) 3155–64.

[124] B. Riteau, D.F. Barber, E.O. Long, Vav1 phosphorylation is induced by beta2 integrin engagement on natural killer cells upstream of actin cytoskeleton and lipid raft reorganization., J. Exp. Med. 198 (2003) 469–74.

[125] J.L. Upshaw, L.N. Arneson, R.A. Schoon, C.J. Dick, D.D. Billadeau, P.J. Leibson, NKG2D-mediated signaling requires a DAP10-bound Grb2-Vav1 intermediate and phosphatidylinositol-3-kinase in human natural killer cells., Nat. Immunol. 7 (2006) 524–32.

[126] X. Chen, D.S.J. Allan, K. Krzewski, B. Ge, H. Kopcow, J.L. Strominger, CD28-stimulated ERK2 phosphorylation is required for polarization of the microtubule organizing center and granules in YTS NK cells., Proc. Natl. Acad. Sci. U. S. A. 103 (2006) 10346–51.

[127] X. Chen, P.P. Trivedi, B. Ge, K. Krzewski, J.L. Strominger, Many NK cell receptors activate ERK2 and JNK1 to trigger microtubule organizing center and granule polarization and cytotoxicity., Proc. Natl. Acad. Sci. U. S. A. 104 (2007) 6329–34.

[128] C. Li, B. Ge, M. Nicotra, J.N.H. Stern, H.D. Kopcow, X. Chen, et al., JNK MAP kinase activation is required for MTOC and granule polarization in NKG2D-mediated NK cell cytotoxicity., Proc. Natl. Acad. Sci. U. S. A. 105 (2008) 3017–22.

[129] K. Jiang, B. Zhong, D.L. Gilvary, B.C. Corliss, E. Hong-Geller, S. Wei, et al., Pivotal role of phosphoinositide-3 kinase in regulation of cytotoxicity in natural killer cells., Nat. Immunol. 1 (2000) 419–25.

[130] Y.T. Bryceson, M.E. March, D.F. Barber, H.-G. Ljunggren, E.O. Long, Cytolytic granule polarization and degranulation controlled by different receptors in resting NK cells., J. Exp. Med. 202 (2005) 1001–12.

[131] H.R.C. Smith, J.W. Heusel, I.K. Mehta, S. Kim, B.G. Dorner, O. V Naidenko, et al., Recognition of a virus-encoded ligand by a natural killer cell activation receptor., Proc. Natl. Acad. Sci. U. S. A. 99 (2002) 8826–31.

[132] O. Mandelboim, N. Lieberman, M. Lev, L. Paul, T.I. Arnon, Y. Bushkin, et al., Recognition of haemagglutinins on virus-infected cells by NKp46 activates lysis by human NK cells., Nature. 409 (2001) 1055–60.

[133] S. Bauer, Activation of NK Cells and T Cells by NKG2D, a Receptor for Stress-Inducible MICA, Science (80-.). 285 (1999) 727–729.

[134] A. Diefenbach, E.R. Jensen, A.M. Jamieson, D.H. Raulet, Rae1 and H60 ligands of the NKG2D receptor stimulate tumour immunity., Nature. 413 (2001) 165–71.

[135] J. Michaelsson, C. Teixeira de Matos, A. Achour, L.L. Lanier, K. Karre, K. Soderstrom, A Signal Peptide Derived from hsp60 Binds HLA-E and Interferes with CD94/NKG2A Recognition, J. Exp. Med. 196 (2002) 1403–1414.

[136] C. Watzl, D. Urlaub, Molecular mechanisms of natural killer cell regulation., Front. Biosci. (Landmark Ed. 17 (2012) 1418–32.

[137] D. Kägi, B. Ledermann, K. Bürki, P. Seiler, B. Odermatt, K.J. Olsen, et al., Cytotoxicity mediated by T cells and natural killer cells is greatly impaired in perforin-deficient mice., Nature. 369 (1994) 31–7.

[138] S. Shresta, J.W. Heusel, D.M. Macivor, R.L. Wesselschmidt, J.H. Russell, T.J. Ley, Granzyme B plays a critical role in cytotoxic lymphocyte-induced apoptosis., Immunol. Rev. 146 (1995) 211–21.

[139] S. Shresta, D.M. MacIvor, J.W. Heusel, J.H. Russell, T.J. Ley, Natural killer and lymphokine-activated killer cells require granzyme B for the rapid induction of apoptosis in susceptible target cells., Proc. Natl. Acad. Sci. U. S. A. 92 (1995) 5679–83.

[140] K. Ebnet, M. Hausmann, F. Lehmann-Grube, A. Müllbacher, M. Kopf, M. Lamers, et al., Granzyme A-deficient mice retain potent cell-mediated cytotoxicity., EMBO J. 14 (1995) 4230–9.

[141] D. Martinvalet, D.M. Dykxhoorn, R. Ferrini, J. Lieberman, Granzyme A cleaves a mitochondrial complex I protein to initiate caspase-independent cell death., Cell. 133 (2008) 681–92.

[142] D. Chowdhury, J. Lieberman, Death by a thousand cuts: granzyme pathways of programmed cell death., Annu. Rev. Immunol. 26 (2008) 389–420.

[143] A.W. Chung, M. Navis, G. Isitman, R. Centre, R. Finlayson, M. Bloch, et al., Activation of NK cells by ADCC responses during early HIV infection., Viral Immunol. 24 (2011) 171–5.

[144] U.J.E. Seidel, P. Schlegel, P. Lang, Natural killer cell mediated antibody-dependent cellular cytotoxicity in tumor immunotherapy with therapeutic antibodies., Front. Immunol. 4 (2013) 76.

[145] L. Zamai, M. Ahmad, I.M. Bennett, L. Azzoni, E.S. Alnemri, B. Perussia, Natural Killer (NK) Cell-mediated Cytotoxicity: Differential Use of TRAIL and Fas Ligand by Immature and Mature Primary Human NK Cells, J. Exp. Med. 188 (1998) 2375–2380.

[146] G. Bossi, G.M. Griffiths, Degranulation plays an essential part in regulating cell surface expression of Fas ligand in T cells and natural killer cells., Nat. Med. 5 (1999) 90–6.

[147] H. Schmidt, C. Gelhaus, R. Lucius, M. Nebendahl, M. Leippe, O. Janssen, Enrichment and analysis of secretory lysosomes from lymphocyte populations., BMC Immunol. 10 (2009) 41.

[148] D.M. Davis, I. Chiu, M. Fassett, G.B. Cohen, O. Mandelboim, J.L. Strominger, The human natural killer cell immune synapse., Proc. Natl. Acad. Sci. U. S. A. 96 (1999) 15062–7.

[149] D.M. Davis, Assembly of the immunological synapse for T cells and NK cells., Trends Immunol. 23 (2002) 356–63.

[150] D. Liu, Y.T. Bryceson, T. Meckel, G. Vasiliver-Shamis, M.L. Dustin, E.O. Long, Integrin-dependent organization and bidirectional vesicular traffic at cytotoxic immune synapses., Immunity. 31 (2009) 99–109.

[151] D.F. Barber, M. Faure, E.O. Long, LFA-1 contributes an early signal for NK cell cytotoxicity., J. Immunol. 173 (2004) 3653–9.

[152] M. Faure, D.F. Barber, S.M. Takahashi, T. Jin, E.O. Long, Spontaneous clustering and tyrosine phosphorylation of NK cell inhibitory receptor induced by ligand binding., J. Immunol. 170 (2003) 6107–14.

[153] B. Treanor, P.M.P. Lanigan, S. Kumar, C. Dunsby, I. Munro, E. Auksorius, et al., Microclusters of inhibitory killer immunoglobulin-like receptor signaling at natural killer cell immunological synapses., J. Cell Biol. 174 (2006) 153–61.

[154] T.P. Abeyweera, E. Merino, M. Huse, Inhibitory signaling blocks activating receptor clustering and induces cytoskeletal retraction in natural killer cells., J. Cell Biol. 192 (2011) 675–90.

[155] A.N. Mentlik, K.B. Sanborn, E.L. Holzbaur, J.S. Orange, Rapid lytic granule convergence to the MTOC in natural killer cells is dependent on dynein but not cytolytic commitment., Mol. Biol. Cell. 21 (2010) 2241–56.

[156] J.C. Stinchcombe, M. Salio, V. Cerundolo, D. Pende, M. Arico, G.M. Griffiths, Centriole polarisation to the immunological synapse directs secretion from cytolytic cells of both the innate and adaptive immune systems., BMC Biol. 9 (2011) 45.

[157] J.C. Stinchcombe, E. Majorovits, G. Bossi, S. Fuller, G.M. Griffiths, Centrosome polarization delivers secretory granules to the immunological synapse., Nature. 443 (2006) 462–5.

[158] A.C.N. Brown, S. Oddos, I.M. Dobbie, J.-M. Alakoskela, R.M. Parton, P. Eissmann, et al., Remodelling of cortical actin where lytic granules dock at natural killer cell immune synapses revealed by super-resolution microscopy., PLoS Biol. 9 (2011) e1001152.

[159] G.D. Rak, E.M. Mace, P.P. Banerjee, T. Svitkina, J.S. Orange, Natural killer cell lytic granule secretion occurs through a pervasive actin network at the immune synapse., PLoS Biol. 9 (2011) e1001151.

[160] E.M. Mace, J.S. Orange, Dual channel STED nanoscopy of lytic granules on actin filaments in natural killer cells., Commun. Integr. Biol. 5 (2012) 184–6.

[161] M.M. Andzelm, X. Chen, K. Krzewski, J.S. Orange, J.L. Strominger, Myosin IIA is required for cytolytic granule exocytosis in human NK cells., J. Exp. Med. 204 (2007) 2285–91.

[162] K.B. Sanborn, G.D. Rak, S.Y. Maru, K. Demers, A. Difeo, J.A. Martignetti, et al., Myosin IIA associates with NK cell lytic granules to enable their interaction with F-actin and function at the immunological synapse., J. Immunol. 182 (2009) 6969–84.

[163] S.M. Wood, M. Meeths, S.C.C. Chiang, A.G. Bechensteen, J.J. Boelens, C. Heilmann, et al., Different NK cell-activating receptors preferentially recruit Rab27a or Munc13-4 to perforin-containing granules for cytotoxicity., Blood. 114 (2009) 4117–27.

[164] S.D. Catz, Regulation of vesicular trafficking and leukocyte function by Rab27 GTPases and their effectors., J. Leukoc. Biol. (2013).

[165] J.S. Orange, N. Ramesh, E. Remold-O'Donnell, Y. Sasahara, L. Koopman, M. Byrne, et al., Wiskott-Aldrich syndrome protein is required for NK cell cytotoxicity and colocalizes with actin to NK cell-activating immunologic synapses., Proc. Natl. Acad. Sci. U. S. A. 99 (2002) 11351–6.

[166] J.S. Orange, K.D. Stone, S.E. Turvey, K. Krzewski, The Wiskott-Aldrich syndrome., Cell. Mol. Life Sci. 61 (2004) 2361–85.

[167] K. Krzewski, X. Chen, J.S. Orange, J.L. Strominger, Formation of a WIP-, WASp-, actin-, and myosin IIA-containing multiprotein complex in activated NK cells and its alteration by KIR inhibitory signaling., J. Cell Biol. 173 (2006) 121–32.

[168] H. Stabile, C. Carlino, C. Mazza, S. Giliani, S. Morrone, L.D. Notarangelo, et al., Impaired NK-cell migration in WAS/XLT patients: role of Cdc42/WASp pathway in the control of chemokine-induced beta2 integrin high-affinity state., Blood. 115 (2010) 2818–26.

[169] E. Serrano-Pertierra, E. Cernuda-Morollón, C. López-Larrea, Wiskott-Aldrich syndrome protein (WASp) and N-WASp are involved in the regulation of NK-cell migration upon NKG2D activation., Eur. J. Immunol. 42 (2012) 2142–51.

[170] B. Butler, D.H. Kastendieck, J. a Cooper, Differently phosphorylated forms of the cortactin homolog HS1 mediate distinct functions in natural killer cells., Nat. Immunol. 9 (2008) 887–97.

[171] B. Butler, J.A. Cooper, Distinct roles for the actin nucleators Arp2/3 and hDia1 during NK-mediated cytotoxicity., Curr. Biol. 19 (2009) 1886–96.

[172] T.D. Pollard, J.A. Cooper, Actin, a central player in cell shape and movement., Science. 326 (2009) 1208–12.

[173] R.D. Goldman, M.M. Cleland, S.N.P. Murthy, S. Mahammad, E.R. Kuczmarski, Inroads into the structure and function of intermediate filament networks., J. Struct. Biol. 177 (2012) 14–23.

[174] T. Vignaud, L. Blanchoin, M. Théry, Directed cytoskeleton self-organization., Trends Cell Biol. 22 (2012) 671–82.

[175] F. Cvrcková, F. Rivero, B. Bavlnka, Evolutionarily conserved modules in actin nucleation: lessons from Dictyostelium discoideum and plants. Review article., Protoplasma. 224 (2004) 15–31.

[176] E.D. Korn, M.F. Carlier, D. Pantaloni, Actin polymerization and ATP hydrolysis., Science. 238 (1987) 638–44.

[177] K. Murakami, T. Yasunaga, T.Q.P. Noguchi, Y. Gomibuchi, K.X. Ngo, T.Q.P. Uyeda, et al., Structural basis for actin assembly, activation of ATP hydrolysis, and delayed phosphate release., Cell. 143 (2010) 275–87.

[178] T.D. Pollard, Regulation of actin filament assembly by Arp2/3 complex and formins., Annu. Rev. Biophys. Biomol. Struct. 36 (2007) 451–77.

[179] F. Li, H.N. Higgs, The mouse Formin mDia1 is a potent actin nucleation factor regulated by autoinhibition., Curr. Biol. 13 (2003) 1335–40.

[180] I. Rouiller, X.-P. Xu, K.J. Amann, C. Egile, S. Nickell, D. Nicastro, et al., The structural basis of actin filament branching by the Arp2/3 complex., J. Cell Biol. 180 (2008) 887–95.

[181] M. Cella, K. Fujikawa, I. Tassi, S. Kim, K. Latinis, S. Nishi, et al., Differential requirements for Vav proteins in DAP10- and ITAM-mediated NK cell cytotoxicity., J. Exp. Med. 200 (2004) 817–23.

[182] D.B. Graham, M. Cella, E. Giurisato, K. Fujikawa, A. V Miletic, T. Kloeppel, et al., Vav1 controls DAP10-mediated natural cytotoxicity by regulating actin and microtubule dynamics., J. Immunol. 177 (2006) 2349–55.

[183] K. Krzewski, X. Chen, J.L. Strominger, WIP is essential for lytic granule polarization and NK cell cytotoxicity., Proc. Natl. Acad. Sci. U. S. A. 105 (2008) 2568–73.

[184] L.M. Machesky, E. Reeves, F. Wientjes, F.J. Mattheyse, A. Grogan, N.F. Totty, et al., Mammalian actin-related protein 2/3 complex localizes to regions of lamellipodial protrusion and is composed of evolutionarily conserved proteins., Biochem. J. 328 (Pt 1 (1997) 105–12.

[185] C.L. Humphries, H.I. Balcer, J.L. D'Agostino, B. Winsor, D.G. Drubin, G. Barnes, et al., Direct regulation of Arp2/3 complex activity and function by the actin binding protein coronin., J. Cell Biol. 159 (2002) 993–1004.

[186] L. Cai, T.W. Marshall, A.C. Uetrecht, D.A. Schafer, J.E. Bear, Coronin 1B coordinates Arp2/3 complex and cofilin activities at the leading edge., Cell. 128 (2007) 915–29.

[187] M. Yan, C. Di Ciano-Oliveira, S. Grinstein, W.S. Trimble, Coronin function is required for chemotaxis and phagocytosis in human neutrophils., J. Immunol. 178 (2007) 5769–78.

[188] E.L. de Hostos, The coronin family of actin-associated proteins., Trends Cell Biol. 9 (1999) 345–50.

[189] A.C. Uetrecht, J.E. Bear, Coronins: the return of the crown., Trends Cell Biol. 16 (2006) 421–6.

[190] K.T. Chan, S.J. Creed, J.E. Bear, Unraveling the enigma: progress towards understanding the coronin family of actin regulators., Trends Cell Biol. 21 (2011) 481–8.

[191] C.S. Clemen, V. Rybakin, L. Eichinger, The coronin family of proteins., Subcell. Biochem. 48 (2008) 1–5.

[192] M. Gandhi, B.L. Goode, Coronin: the double-edged sword of actin dynamics., Subcell. Biochem. 48 (2008) 72–87.

[193] E.L. de Hostos, B. Bradtke, F. Lottspeich, R. Guggenheim, G. Gerisch, Coronin, an actin binding protein of Dictyostelium discoideum localized to cell surface projections, has sequence similarities to G protein beta subunits., EMBO J. 10 (1991) 4097–104.

[194] E.L. de Hostos, C. Rehfuess, B. Bradtke, D.R. Waddell, R. Albrecht, J. Murphy, et al., Dictyostelium mutants lacking the cytoskeletal protein coronin are defective in cytokinesis and cell motility., J. Cell Biol. 120 (1993) 163–73.

[195] G. Gerisch, R. Albrecht, C. Heizer, S. Hodgkinson, M. Maniak, Chemoattractant-controlled accumulation of coronin at the leading edge of Dictyostelium cells monitored using a green fluorescent protein-coronin fusion protein., Curr. Biol. 5 (1995) 1280–5.

[196] M. Maniak, R. Rauchenberger, R. Albrecht, J. Murphy, G. Gerisch, Coronin involved in phagocytosis: dynamics of particle-induced relocalization visualized by a green fluorescent protein Tag., Cell. 83 (1995) 915–24.

[197] R. Rauchenberger, U. Hacker, J. Murphy, J. Niewöhner, M. Maniak, Coronin and vacuolin identify consecutive stages of a late, actin-coated endocytic compartment in Dictyostelium., Curr. Biol. 7 (1997) 215–8.

[198] R.A. Heil-Chapdelaine, N.K. Tran, J.A. Cooper, The role of Saccharomyces cerevisiae coronin in the actin and microtubule cytoskeletons., Curr. Biol. 8 (1998) 1281–4.

[199] M. Mishima, E. Nishida, Coronin localizes to leading edges and is involved in cell spreading and lamellipodium extension in vertebrate cells., J. Cell Sci. 112 (Pt 17 (1999) 2833–42.

[200] B.L. Goode, J.J. Wong, A.C. Butty, M. Peter, A.L. McCormack, J.R. Yates, et al., Coronin promotes the rapid assembly and cross-linking of actin filaments and may link the actin and microtubule cytoskeletons in yeast., J. Cell Biol. 144 (1999) 83–98.

[201] C.A. Rappleye, A.R. Paredez, C.W. Smith, K.L. McDonald, R. V Aroian, The coronin-like protein POD-1 is required for anterior-posterior axis formation and cellular architecture in the nematode caenorhabditis elegans., Genes Dev. 13 (1999) 2838–51.

[202] V. Bharathi, S.K. Pallavi, R. Bajpai, B.S. Emerald, L.S. Shashidhara, Genetic characterization of the Drosophila homologue of coronin., J. Cell Sci. 117 (2004) 1911–22.

[203] B. Nal, Coronin-1 expression in T lymphocytes: insights into protein function during T cell development and activation, Int. Immunol. 16 (2004) 231–240.

[204] N. Föger, L. Rangell, D.M. Danilenko, A.C. Chan, Requirement for coronin 1 in T lymphocyte trafficking and cellular homeostasis., Science. 313 (2006) 839–42.

[205] M.C. Shina, A.A. Noegel, Invertebrate coronins., Subcell. Biochem. 48 (2008) 88–97.

[206] C.-P. Xavier, L. Eichinger, M.P. Fernandez, R.O. Morgan, C.S. Clemen, Evolutionary and functional diversity of coronin proteins., Subcell. Biochem. 48 (2008) 98–109.

[207] C. Eckert, B. Hammesfahr, M. Kollmar, A holistic phylogeny of the coronin gene family reveals an ancient origin of the tandem-coronin, defines a new subfamily, and predicts protein function., BMC Evol. Biol. 11 (2011) 268.

[208] V. Rybakin, C.S. Clemen, Coronin proteins as multifunctional regulators of the cytoskeleton and membrane trafficking., Bioessays. 27 (2005) 625–32.

[209] B.A. Appleton, P. Wu, C. Wiesmann, The crystal structure of murine coronin-1: a regulator of actin cytoskeletal dynamics in lymphocytes., Structure. 14 (2006) 87–96.

[210] C.U. Stirnimann, E. Petsalaki, R.B. Russell, C.W. Müller, WD40 proteins propel cellular networks., Trends Biochem. Sci. 35 (2010) 565–74.

[211] C. Xu, J. Min, Structure and function of WD40 domain proteins., Protein Cell. 2 (2011) 202–14.

[212] L. Cai, N. Holoweckyj, M.D. Schaller, J.E. Bear, Phosphorylation of coronin 1B by protein kinase C regulates interaction with Arp2/3 and cell motility., J. Biol. Chem. 280 (2005) 31913–23.

[213] Z. Spoerl, M. Stumpf, A.A. Noegel, A. Hasse, Oligomerization, F-actin interaction, and membrane association of the ubiquitous mammalian coronin 3 are mediated by its carboxyl terminus., J. Biol. Chem. 277 (2002) 48858–67.

[214] T. Oku, S. Itoh, R. Ishii, K. Suzuki, W.M. Nauseef, S. Toyoshima, et al., Homotypic dimerization of the actin-binding protein p57/coronin-1 mediated by a leucine zipper motif in the C-terminal region., Biochem. J. 387 (2005) 325–31.

[215] J. Gatfield, I. Albrecht, B. Zanolari, M.O. Steinmetz, J. Pieters, Association of the leukocyte plasma membrane with the actin cytoskeleton through coiled coil-mediated trimeric coronin 1 molecules., Mol. Biol. Cell. 16 (2005) 2786–98.

[216] R.A. Kammerer, D. Kostrewa, P. Progias, S. Honnappa, D. Avila, A. Lustig, et al., A conserved trimerization motif controls the topology of short coiled coils., Proc. Natl. Acad. Sci. U. S. A. 102 (2005) 13891–6.

[217] V. Rybakin, M. Stumpf, A. Schulze, I. V Majoul, A.A. Noegel, A. Hasse, Coronin 7, the mammalian POD-1 homologue, localizes to the Golgi apparatus., FEBS Lett. 573 (2004) 161–7.

[218] A. Gloss, F. Rivero, N. Khaire, R. Müller, W.F. Loomis, M. Schleicher, et al., Villidin, a novel WD-repeat and villin-related protein from Dictyostelium, is associated with membranes and the cytoskeleton., Mol. Biol. Cell. 14 (2003) 2716–27.

[219] T. Nakamura, K. Takeuchi, S. Muraoka, H. Takezoe, N. Takahashi, N. Mori, A neurally enriched coronin-like protein, ClipinC, is a novel candidate for an actin cytoskeleton-cortical membrane-linking protein., J. Biol. Chem. 274 (1999) 13322–7.

[220] K. Suzuki, J. Nishihata, Y. Arai, N. Honma, K. Yamamoto, T. Irimura, et al., Molecular cloning of a novel actin-binding protein, p57, with a WD repeat and a leucine zipper motif., FEBS Lett. 364 (1995) 283–8.

[221] M. Okumura, C. Kung, S. Wong, M. Rodgers, M.L. Thomas, Definition of family of coronin-related proteins conserved between humans and mice: close genetic linkage between coronin-2 and CD45-associated protein., DNA Cell Biol. 17 (1998) 779–87.

[222] N. Föger, A. Jenckel, Z. Orinska, K.-H. Lee, A.C. Chan, S. Bulfone-Paus, Differential regulation of mast cell degranulation versus cytokine secretion by the actin regulatory proteins Coronin1a and Coronin1b., J. Exp. Med. 208 (2011) 1777–87.

[223] J.A. Parente, X. Chen, C. Zhou, A.C. Petropoulos, C.S. Chew, Isolation, cloning, and characterization of a new mammalian coronin family member, coroninse, which is regulated within the protein kinase C signaling pathway., J. Biol. Chem. 274 (1999) 3017–25.

[224] S. Di Giovanni, A. De Biase, A. Yakovlev, T. Finn, J. Beers, E.P. Hoffman, et al., In vivo and in vitro characterization of novel neuronal plasticity factors identified following spinal cord injury., J. Biol. Chem. 280 (2005) 2084–91.

[225] H.C. Williams, A. San Martín, C.M. Adamo, B. Seidel-Rogol, L. Pounkova, S.R. Datla, et al., Role of coronin 1B in PDGF-induced migration of vascular smooth muscle cells., Circ. Res. 111 (2012) 56–65.

[226] A. Hasse, A. Rosentreter, Z. Spoerl, M. Stumpf, A.A. Noegel, C.S. Clemen, Coronin 3 and its role in murine brain morphogenesis., Eur. J. Neurosci. 21 (2005) 1155–68.

[227] M. Iizaka, H. HJ, H. Akashi, Y. Furukawa, Y. Nakajima, S. Sugano, et al., Isolation and chromosomal assignment of a novel human gene, CORO1C, homologous to coronin-like actin-binding proteins., Cytogenet Cell Genet. 88 (2000) 221–224.

[228] R.O. Morgan, M.P. Fernandez, Molecular phylogeny and evolution of the coronin gene family., Subcell. Biochem. 48 (2008) 41–55.

[229] L. Cai, A.M. Makhov, J.E. Bear, F-actin binding is essential for coronin 1B function in vivo., J. Cell Sci. 120 (2007) 1779–90.

[230] L. Cai, A.M. Makhov, D.A. Schafer, J.E. Bear, Coronin 1B antagonizes cortactin and remodels Arp2/3-containing actin branches in lamellipodia., Cell. 134 (2008) 828–42.

[231] V.E. Galkin, A. Orlova, W. Brieher, H.Y. Kueh, T.J. Mitchison, E.H. Egelman, Coronin-1A stabilizes F-actin by bridging adjacent actin protomers and stapling opposite strands of the actin filament., J. Mol. Biol. 376 (2008) 607–13.

[232] H.Y. Kueh, G.T. Charras, T.J. Mitchison, W.M. Brieher, Actin disassembly by cofilin, coronin, and Aip1 occurs in bursts and is inhibited by barbed-end cappers., J. Cell Biol. 182 (2008) 341–53.

[233] M. Gandhi, V. Achard, L. Blanchoin, B.L. Goode, Coronin switches roles in actin disassembly depending on the nucleotide state of actin., Mol. Cell. 34 (2009) 364–74.

[234] M. Gandhi, M. Jangi, B.L. Goode, Functional surfaces on the actin-binding protein coronin revealed by systematic mutagenesis., J. Biol. Chem. 285 (2010) 34899–908.

[235] W. Huang, S. Ghisletti, K. Saijo, M. Gandhi, M. Aouadi, G.J. Tesz, et al., Coronin 2A mediates actin-dependent de-repression of inflammatory response genes., Nature. 470 (2011) 414–8.

[236] C.Z. Liu, Y. Chen, S.F. Sui, The identification of a new actin-binding region in p57., Cell Res. 16 (2006) 106–12.

[237] T. Oku, S. Itoh, M. Okano, A. Suzuki, K. Suzuki, S. Nakajin, et al., Two regions responsible for the actin binding of p57, a mammalian coronin family actin-binding protein., Biol. Pharm. Bull. 26 (2003) 409–16.

[238] K. Tsujita, T. Itoh, A. Kondo, M. Oyama, H. Kozuka-Hata, Y. Irino, et al., Proteome of acidic phospholipid-binding proteins: spatial and temporal regulation of Coronin 1A by phosphoinositides., J. Biol. Chem. 285 (2010) 6781–9.

[239] T. Kimura, S. Taniguchi, I. Niki, Actin assembly controlled by GDP-Rab27a is essential for endocytosis of the insulin secretory membrane., Arch. Biochem. Biophys. 496 (2010) 33–7.

[240] K.T. Chan, D.W. Roadcap, N. Holoweckyj, J.E. Bear, Coronin 1C harbours a second actin-binding site that confers co-operative binding to F-actin., Biochem. J. 444 (2012) 89–96.

[241] A. Rosentreter, A. Hofmann, C.-P. Xavier, M. Stumpf, A.A. Noegel, C.S. Clemen, Coronin 3 involvement in F-actin-dependent processes at the cell cortex., Exp. Cell Res. 313 (2007) 878–95.

[242] S.-L. Liu, K.M. Needham, J.R. May, B.J. Nolen, Mechanism of a concentration-dependent switch between activation and inhibition of Arp2/3 complex by coronin., J. Biol. Chem. 286 (2011) 17039–46.

[243] A.M. Weaver, A. V Karginov, A.W. Kinley, S.A. Weed, Y. Li, J.T. Parsons, et al., Cortactin promotes and stabilizes Arp2/3-induced actin filament network formation., Curr. Biol. 11 (2001) 370–4.

[244] M.-C. Lin, B.J. Galletta, D. Sept, J.A. Cooper, Overlapping and distinct functions for cofilin, coronin and Aip1 in actin dynamics in vivo., J. Cell Sci. 123 (2010) 1329–42.

[245] S. Ono, Mechanism of depolymerization and severing of actin filaments and its significance in cytoskeletal dynamics., Int. Rev. Cytol. 258 (2007) 1–82.

[246] W.M. Brieher, H.Y. Kueh, B.A. Ballif, T.J. Mitchison, Rapid actin monomer-insensitive depolymerization of Listeria actin comet tails by cofilin, coronin, and Aip1., J. Cell Biol. 175 (2006) 315–24.

[247] M. Yamamoto, K. Nagata-Ohashi, Y. Ohta, K. Ohashi, K. Mizuno, Identification of multiple actin-binding sites in cofilin-phosphatase Slingshot-1L., FEBS Lett. 580 (2006) 1789–94.

[248] S. Itoh, K. Suzuki, J. Nishihata, M. Iwasa, T. Oku, S. Nakajin, et al., The role of protein kinase C in the transient association of p57, a coronin family actin-binding protein, with phagosomes., Biol. Pharm. Bull. 25 (2002) 837–44.

[249] T.K. Pareek, E. Lam, X. Zheng, D. Askew, A.B. Kulkarni, M.R. Chance, et al., Cyclin-dependent kinase 5 activity is required for T cell activation and induction of experimental autoimmune encephalomyelitis., J. Exp. Med. 207 (2010) 2507–19.

[250] T. Oku, Y. Kaneko, K. Murofushi, Y. Seyama, S. Toyoshima, T. Tsuji, Phorbol ester-dependent phosphorylation regulates the association of p57/coronin-1 with the actin cytoskeleton., J. Biol. Chem. 283 (2008) 28918–25.

[251] T. Oku, M. Nakano, Y. Kaneko, Y. Ando, H. Kenmotsu, S. Itoh, et al., Constitutive turnover of phosphorylation at Thr-412 of human p57/coronin-1 regulates the interaction with actin., J. Biol. Chem. 287 (2012) 42910–20.

[252] G. Ferrari, H. Langen, M. Naito, J. Pieters, A coat protein on phagosomes involved in the intracellular survival of mycobacteria., Cell. 97 (1999) 435–47.

[253] R. Jayachandran, V. Sundaramurthy, B. Combaluzier, P. Mueller, H. Korf, K. Huygen, et al., Survival of mycobacteria in macrophages is mediated by coronin 1-dependent activation of calcineurin., Cell. 130 (2007) 37–50.

[254] T.W. Marshall, H.L. Aloor, J.E. Bear, Coronin 2A regulates a subset of focal-adhesion-turnover events through the cofilin pathway., J. Cell Sci. 122 (2009) 3061–9.

[255] a Grogan, E. Reeves, N. Keep, F. Wientjes, N.F. Totty, a L. Burlingame, et al., Cytosolic phox proteins interact with and regulate the assembly of coronin in neutrophils., J. Cell Sci. 110 (Pt 2 (1997) 3071–81.

[256] B. Combaluzier, P. Mueller, J. Massner, D. Finke, J. Pieters, Coronin 1 is essential for IgM-mediated Ca2+ mobilization in B cells but dispensable for the generation of immune responses in vivo., J. Immunol. 182 (2009) 1954–61.

[257] B. Combaluzier, J. Pieters, Chemotaxis and phagocytosis in neutrophils is independent of coronin 1., J. Immunol. 182 (2009) 2745–52.

[258] K. Westritschnig, S. BoseDasgupta, V. Tchang, K. Siegmund, J. Pieters, Antigen processing and presentation by dendritic cells is independent of coronin 1., Mol. Immunol. 53 (2013) 379–86.

[259] B. Mugnier, B. Nal, C. Verthuy, C. Boyer, D. Lam, L. Chasson, et al., Coronin-1A links cytoskeleton dynamics to TCR alpha beta-induced cell signaling., PLoS One. 3 (2008) e3467.

[260] L.R. Shiow, D.W. Roadcap, K. Paris, S.R. Watson, I.L. Grigorova, T. Lebet, et al., The actin regulator coronin 1A is mutant in a thymic egress-deficient mouse strain and in a patient with severe combined immunodeficiency., Nat. Immunol. 9 (2008) 1307–15.

[261] L.R. Shiow, K. Paris, M.C. Akana, J.G. Cyster, R.U. Sorensen, J.M. Puck, Severe combined immunodeficiency (SCID) and attention deficit hyperactivity disorder (ADHD) associated with a Coronin-1A mutation and a chromosome 16p11.2 deletion., Clin. Immunol. 131 (2009) 24–30.

[262] D. Moshous, E. Martin, W. Carpentier, A. Lim, I. Callebaut, D. Canioni, et al., Whole-exome sequencing identifies Coronin-1A deficiency in 3 siblings with immunodeficiency and EBV-associated B-cell lymphoproliferation., J. Allergy Clin. Immunol. 131 (2013) 1594–1603.e9.

[263] P. Mueller, X. Liu, J. Pieters, Migration and homeostasis of naive T cells depends on coronin 1-mediated prosurvival signals and not on coronin 1-dependent filamentous actin modulation., J. Immunol. 186 (2011) 4039–50.

[264] R. Jayachandran, J. Gatfield, J. Massner, I. Albrecht, B. Zanolari, J. Pieters, RNA interference in J774 macrophages reveals a role for coronin 1 in mycobacterial trafficking but not in actin-dependent processes., Mol. Biol. Cell. 19 (2008) 1241–51.

[265] S. Seto, K. Tsujimura, Y. Koide, Coronin-1a inhibits autophagosome formation around Mycobacterium tuberculosis-containing phagosomes and assists mycobacterial survival in macrophages., Cell. Microbiol. 14 (2012) 710–27.

[266] S. Arandjelovic, D. Wickramarachchi, S. Hemmers, S.S. Leming, D.H. Kono, K.A. Mowen, Mast cell function is not altered by Coronin-1A deficiency., J. Leukoc. Biol. 88 (2010) 737–45.

[267] P. V Usatyuk, M. Burns, V. Mohan, S. Pendyala, D. He, D.L. Ebenezer, et al., Coronin 1B Regulates S1P-Induced Human Lung Endothelial Cell Chemotaxis: Role of PLD2, Protein Kinase C and Rac1 Signal Transduction., PLoS One. 8 (2013) e63007.

[268] J. Pieters, P. Müller, R. Jayachandran, On guard: coronin proteins in innate and adaptive immunity., Nat. Rev. Immunol. (2013).

[269] Z. Orinska, E. Bulanova, V. Budagian, M. Metz, M. Maurer, S. Bulfone-Paus, TLR3-induced activation of mast cells modulates CD8+ T-cell recruitment., Blood. 106 (2005) 978–87.

[270] R. Rückert, K. Brandt, M. Ernst, K. Marienfeld, E. Csernok, C. Metzler, et al., Interleukin-15 stimulates macrophages to activate CD4+ T cells: a role in the pathogenesis of rheumatoid arthritis?, Immunology. 126 (2009) 63–73.

[271] M.B. Lutz, N. Kukutsch, A.L. Ogilvie, S. Rössner, F. Koch, N. Romani, et al., An advanced culture method for generating large quantities of highly pure dendritic cells from mouse bone marrow., J. Immunol. Methods. 223 (1999) 77–92.

[272] D.N. Burshtyn, J. Shin, C. Stebbins, E.O. Long, Adhesion to target cells is disrupted by the killer cell inhibitory receptor., Curr. Biol. 10 (2000) 777–80.

[273] G. Alter, J.M. Malenfant, M. Altfeld, CD107a as a functional marker for the identification of natural killer cell activity., J. Immunol. Methods. 294 (2004) 15–22.

[274] R.H. Buckley, Molecular defects in human severe combined immunodeficiency and approaches to immune reconstitution., Annu. Rev. Immunol. 22 (2004) 625–55.

[275] A. Fischer, Human primary immunodeficiency diseases., Immunity. 27 (2007) 835–45.

[276] T.D. Pollard, G.G. Borisy, Cellular motility driven by assembly and disassembly of actin filaments., Cell. 112 (2003) 453–65.

[277] T. Ikawa, S. Fujimoto, H. Kawamoto, Y. Katsura, Y. Yokota, Commitment to natural killer cells requires the helix-loop-helix inhibitor Id2., Proc. Natl. Acad. Sci. U. S. A. 98 (2001) 5164–9.

[278] T.M. Kündig, H. Schorle, M.F. Bachmann, H. Hengartner, R.M. Zinkernagel, I. Horak, Immune responses in interleukin-2-deficient mice., Science. 262 (1993) 1059–61.

[279] J.P. Lodolce, D.L. Boone, S. Chai, R.E. Swain, T. Dassopoulos, S. Trettin, et al., IL-15 receptor maintains lymphoid homeostasis by supporting lymphocyte homing and proliferation., Immunity. 9 (1998) 669–76.

[280] T. Ohteki, S. Ho, H. Suzuki, T.W. Mak, P.S. Ohashi, Role for IL-15/IL-15 receptor beta-chain in natural killer 1.1+ T cell receptor-alpha beta+ cell development., J. Immunol. 159 (1997) 5931–5.

[281] W.E. Carson, J.G. Giri, M.J. Lindemann, M.L. Linett, M. Ahdieh, R. Paxton, et al., Interleukin (IL) 15 is a novel cytokine that activates human natural killer cells via components of the IL-2 receptor., J. Exp. Med. 180 (1994) 1395–403.

[282] M. Prlic, B.R. Blazar, M. a Farrar, S.C. Jameson, In vivo survival and homeostatic proliferation of natural killer cells., J. Exp. Med. 197 (2003) 967–76.

[283] A.M. Gamero, D. Ussery, D.S. Reintgen, C.A. Puleo, J.Y. Djeu, Interleukin 15 induction of lymphokine-activated killer cell function against autologous tumor cells in melanoma patient lymphocytes by a CD18-dependent, perforin-related mechanism., Cancer Res. 55 (1995) 4988–94.

[284] J.E. Boudreau, K.B. Stephenson, F. Wang, A. a Ashkar, K.L. Mossman, L.L. Lenz, et al., IL-15 and type I interferon are required for activation of tumoricidal NK cells by virus-infected dendritic cells., Cancer Res. 71 (2011) 2497–506.

[285] O. Ozdemir, S. Savaşan, Combinational IL-2/IL-15 induction does not further enhance IL-15-induced lymphokine-activated killer cell cytotoxicity against human leukemia/lymphoma cells., Clin. Immunol. 115 (2005) 240–9.

[286] M. Salagianni, E. Lekka, A. Moustaki, E.G. Iliopoulou, C.N. Baxevanis, M. Papamichail, et al., NK cell adoptive transfer combined with Ontak-mediated regulatory T cell elimination induces effective adaptive antitumor immune responses., J. Immunol. 186 (2011) 3327–35.

[287] G. Matsumoto, M.P. Nghiem, N. Nozaki, R. Schmits, J.M. Penninger, Cooperation between CD44 and LFA-1/CD11a adhesion receptors in lymphokine-activated killer cell cytotoxicity., J. Immunol. 160 (1998) 5781–9.

[288] O. Carpén, I. Virtanen, V.P. Lehto, E. Saksela, Polarization of NK cell cytoskeleton upon conjugation with sensitive target cells., J. Immunol. 131 (1983) 2695–8.

[289] R. Trotta, K. a Puorro, M. Paroli, L. Azzoni, B. Abebe, L.C. Eisenlohr, et al., Dependence of both spontaneous and antibody-dependent, granule exocytosis-mediated NK cell cytotoxicity on extracellular signal-regulated kinases., J. Immunol. 161 (1998) 6648–56.

[290] S. Wei, A.M. Gamero, J.H. Liu, A.A. Daulton, N.I. Valkov, J.A. Trapani, et al., Control of lytic function by mitogen-activated protein kinase/extracellular regulatory kinase 2 (ERK2) in a human natural killer cell line: identification of perforin and granzyme B mobilization by functional ERK2., J. Exp. Med. 187 (1998) 1753–65.

[291] J.D. Bonnema, L.M. Karnitz, R. a Schoon, R.T. Abraham, P.J. Leibson, Fc receptor stimulation of phosphatidylinositol 3-kinase in natural killer cells is associated with protein kinase C-independent granule release and cell-mediated cytotoxicity., J. Exp. Med. 180 (1994) 1427–35.

[292] K. Jiang, B. Zhong, C. Ritchey, D.L. Gilvary, E. Hong-Geller, S. Wei, et al., Regulation of Akt-dependent cell survival by Syk and Rac., Blood. 101 (2003) 236–44.

[293] A. Kupfer, G. Dennert, S.J. Singer, Polarization of the Golgi apparatus and the microtubule-organizing center within cloned natural killer cells bound to their targets., Proc. Natl. Acad. Sci. U. S. A. 80 (1983) 7224–8.

[294] J.C. Stinchcombe, G. Bossi, S. Booth, G.M. Griffiths, The immunological synapse of CTL contains a secretory domain and membrane bridges., Immunity. 15 (2001) 751–61.

[295] J.P. O'Keefe, T.F. Gajewski, Cutting edge: cytotoxic granule polarization and cytolysis can occur without central supramolecular activation cluster formation in CD8+ effector T cells., J. Immunol. 175 (2005) 5581–5.

[296] S. Nedvetzki, S. Sowinski, R.A. Eagle, J. Harris, F. Vély, D. Pende, et al., Reciprocal regulation of human natural killer cells and macrophages associated with distinct immune synapses., Blood. 109 (2007) 3776–85.

[297] M.J. Smyth, C.O. Zachariae, Y. Norihisa, J.R. Ortaldo, A. Hishinuma, K. Matsushima, IL-8 gene expression and production in human peripheral blood lymphocyte subsets., J. Immunol. 146 (1991) 3815–23.

[298] H.S. Warren, B.F. Kinnear, J.H. Phillips, L.L. Lanier, Production of IL-5 by human NK cells and regulation of IL-5 secretion by IL-4, IL-10, and IL-12., J. Immunol. 154 (1995) 5144–52.

[299] E.M. Bluman, K.J. Bartynski, B.R. Avalos, M. a Caligiuri, Human natural killer cells produce abundant macrophage inflammatory protein-1 alpha in response to monocyte-derived cytokines., J. Clin. Invest. 97 (1996) 2722–7.

[300] a Oliva, a L. Kinter, M. Vaccarezza, A. Rubbert, A. Catanzaro, S. Moir, et al., Natural killer cells from human immunodeficiency virus (HIV)-infected individuals are an important source of CC-chemokines and suppress HIV-1 entry and replication in vitro., J. Clin. Invest. 102 (1998) 223–31.

[301] C. Fauriat, E.O. Long, H.-G. Ljunggren, Y.T. Bryceson, Regulation of human NK-cell cytokine and chemokine production by target cell recognition., Blood. 115 (2010) 2167–76.

[302] E. Vivier, E. Tomasello, M. Baratin, T. Walzer, S. Ugolini, Functions of natural killer cells., Nat. Immunol. 9 (2008) 503–10.

[303] J.-B. Manneville, S. Etienne-Manneville, P. Skehel, T. Carter, D. Ogden, M. Ferenczi, Interaction of the actin cytoskeleton with microtubules regulates secretory organelle movement near the plasma membrane in human endothelial cells., J. Cell Sci. 116 (2003) 3927–38.

[304] N.R. Jog, M.J. Rane, G. Lominadze, G.C. Luerman, R.A. Ward, K.R. McLeish, The actin cytoskeleton regulates exocytosis of all neutrophil granule subsets., Am. J. Physiol. Cell Physiol. 292 (2007) C1690–700.

[305] G. de Saint Basile, G. Ménasché, A. Fischer, Molecular mechanisms of biogenesis and exocytosis of cytotoxic granules., Nat. Rev. Immunol. 10 (2010) 568–79.

[306] Y. Arinobu, H. Iwasaki, K. Akashi, Origin of basophils and mast cells., Allergol. Int. 58 (2009) 21–8.

[307] P. Mueller, J. Massner, R. Jayachandran, B. Combaluzier, I. Albrecht, J. Gatfield, et al., Regulation of T cell survival through coronin-1-mediated generation of inositol-1,4,5-trisphosphate and calcium mobilization after T cell receptor triggering., Nat. Immunol. 9 (2008) 424–31.

[308] F. Vauti, B.R. Prochnow, E. Freese, S.K. Ramasamy, P. Ruiz, H.-H. Arnold, Arp3 is required during preimplantation development of the mouse embryo., FEBS Lett. 581 (2007) 5691–7.

[309] C. Yan, N. Martinez-Quiles, S. Eden, T. Shibata, F. Takeshima, R. Shinkura, et al., WAVE2 deficiency reveals distinct roles in embryogenesis and Rac-mediated actin-based motility., EMBO J. 22 (2003) 3602–12.

[310] C.B. Gurniak, E. Perlas, W. Witke, The actin depolymerizing factor n-cofilin is essential for neural tube morphogenesis and neural crest cell migration., Dev. Biol. 278 (2005) 231–41.

[311] D.C. Wickramarachchi, A.N. Theofilopoulos, D.H. Kono, Immune pathology associated with altered actin cytoskeleton regulation., Autoimmunity. 43 (2010) 64–75.

[312] N.D. Huntington, H. Puthalakath, P. Gunn, E. Naik, E.M. Michalak, M.J. Smyth, et al., Interleukin 15-mediated survival of natural killer cells is determined by interactions among Bim, Noxa and Mcl-1., Nat. Immunol. 8 (2007) 856–63.

[313] G.S. Duncan, H.W. Mittrücker, D. Kägi, T. Matsuyama, T.W. Mak, The transcription factor interferon regulatory factor-1 is essential for natural killer cell function in vivo., J. Exp. Med. 184 (1996) 2043–8.

[314] S.M. Gordon, J. Chaix, L.J. Rupp, J. Wu, S. Madera, J.C. Sun, et al., The transcription factors T-bet and Eomes control key checkpoints of natural killer cell maturation., Immunity. 36 (2012) 55–67.

[315] S.I. Samson, O. Richard, M. Tavian, T. Ranson, C.A.J. Vosshenrich, F. Colucci, et al., GATA-3 promotes maturation, IFN-gamma production, and liver-specific homing of NK cells., Immunity. 19 (2003) 701–11.

[316] D.M. Gascoyne, E. Long, H. Veiga-Fernandes, J. de Boer, O. Williams, B. Seddon, et al., The basic leucine zipper transcription factor E4BP4 is essential for natural killer cell development., Nat. Immunol. 10 (2009) 1118–24.

[317] N.S. Williams, J. Klem, I.J. Puzanov, P. V Sivakumar, M. Bennett, V. Kumar, Differentiation of NK1.1+, Ly49+ NK cells from flt3+ multipotent marrow progenitor cells., J. Immunol. 163 (1999) 2648–56.

[318] S.M. Lehar, J. Dooley, A.G. Farr, M.J. Bevan, Notch ligands Delta 1 and Jagged1 transmit distinct signals to T-cell precursors., Blood. 105 (2005) 1440–7.

[319] D.M. Andrews, H.E. Farrell, E.H. Densley, A.A. Scalzo, G.R. Shellam, M.A. Degli-Esposti, NK1.1+ cells and murine cytomegalovirus infection: what happens in situ?, J. Immunol. 166 (2001) 1796–802.

[320] A.O. Dokun, D.T. Chu, L. Yang, A.S. Bendelac, W.M. Yokoyama, Analysis of in situ NK cell responses during viral infection., J. Immunol. 167 (2001) 5286–93.

[321] J.T. Parsons, A.R. Horwitz, M.A. Schwartz, Cell adhesion: integrating cytoskeletal dynamics and cellular tension., Nat. Rev. Mol. Cell Biol. 11 (2010) 633–43.

[322] K. Krzewski, J.L. Strominger, The killer's kiss: the many functions of NK cell immunological synapses., Curr. Opin. Cell Biol. 20 (2008) 597–605.

[323] S.N. Samarin, S. Koch, A.I. Ivanov, C.A. Parkos, A. Nusrat, Coronin 1C negatively regulates cell-matrix adhesion and motility of intestinal epithelial cells., Biochem. Biophys. Res. Commun. 391 (2010) 394–400.

[324] F.E. McCann, B. Vanherberghen, K. Eleme, L.M. Carlin, R.J. Newsam, D. Goulding, et al., The size of the synaptic cleft and distinct distributions of filamentous actin, ezrin, CD43, and CD45 at activating and inhibitory human NK cell immune synapses., J. Immunol. 170 (2003) 2862–70.

[325] M.S. Fassett, D.M. Davis, M.M. Valter, G.B. Cohen, J.L. Strominger, Signaling at the inhibitory natural killer cell immune synapse regulates lipid raft polarization but not class I MHC clustering., Proc. Natl. Acad. Sci. U. S. A. 98 (2001) 14547–52.

[326] K.F. Meiri, Lipid rafts and regulation of the cytoskeleton during T cell activation., Philos. Trans. R. Soc. Lond. B. Biol. Sci. 360 (2005) 1663–72.

[327] P.P. Banerjee, R. Pandey, R. Zheng, M.M. Suhoski, L. Monaco-Shawver, J.S. Orange, Cdc42-interacting protein-4 functionally links actin and microtubule networks at the cytolytic NK cell immunological synapse., J. Exp. Med. 204 (2007) 2305–20.

[328] N. Kanwar, J.A. Wilkins, IQGAP1 involvement in MTOC and granule polarization in NK-cell cytotoxicity., Eur. J. Immunol. 41 (2011) 2763–73.

[329] J.-M. Trifaró, S. Gasman, L.M. Gutiérrez, Cytoskeletal control of vesicle transport and exocytosis in chromaffin cells., Acta Physiol. (Oxf). 192 (2008) 165–72.

[330] M. Malacombe, M.-F. Bader, S. Gasman, Exocytosis in neuroendocrine cells: new tasks for actin., Biochim. Biophys. Acta. 1763 (2006) 1175–83.

[331] C. Dillon, Y. Goda, The actin cytoskeleton: integrating form and function at the synapse., Annu. Rev. Neurosci. 28 (2005) 25–55.

[332] R. Flaumenhaft, J.R. Dilks, N. Rozenvayn, R.A. Monahan-Earley, D. Feng, A.M. Dvorak, The actin cytoskeleton differentially regulates platelet alpha-granule and dense-granule secretion., Blood. 105 (2005) 3879–87.

[333] C. Ehre, A.H. Rossi, L.H. Abdullah, K. De Pestel, S. Hill, J.C. Olsen, et al., Barrier role of actin filaments in regulated mucin secretion from airway goblet cells., Am. J. Physiol. Cell Physiol. 288 (2005) C46–56.

[334] K. Woronowicz, J.R. Dilks, N. Rozenvayn, L. Dowal, P.S. Blair, C.G. Peters, et al., The platelet actin cytoskeleton associates with SNAREs and participates in alpha-granule secretion., Biochemistry. 49 (2010) 4533–42.

[335] K.B. Sanborn, E.M. Mace, G.D. Rak, A. Difeo, J. a Martignetti, A. Pecci, et al., Phosphorylation of the myosin IIA tailpiece regulates single myosin IIA molecule association with lytic granules to promote NK-cell cytotoxicity., Blood. 118 (2011) 5862–71.

[336] T.T. Chiu, N. Patel, A.E. Shaw, J.R. Bamburg, A. Klip, Arp2/3- and cofilin-coordinated actin dynamics is required for insulin-mediated GLUT4 translocation to the surface of muscle cells., Mol. Biol. Cell. 21 (2010) 3529–39.

[337] K. Yokoyama, H. Kaji, J. He, C. Tanaka, R. Hazama, T. Kamigaki, et al., Rab27a negatively regulates phagocytosis by prolongation of the actin-coating stage around phagosomes., J. Biol. Chem. 286 (2011) 5375–82.

[338] A.C. Stanley, P. Lacy, Pathways for cytokine secretion., Physiology (Bethesda). 25 (2010) 218–29.

[339] E. Reefman, J.G. Kay, S.M. Wood, C. Offenhäuser, D.L. Brown, S. Roy, et al., Cytokine secretion is distinct from secretion of cytotoxic granules in NK cells., J. Immunol. 184 (2010) 4852–62.

[340] K. Chemin, A. Bohineust, S. Dogniaux, M. Tourret, S. Guégan, F. Miro, et al., Cytokine secretion by CD4+ T cells at the immunological synapse requires Cdc42-dependent local actin remodeling but not microtubule organizing center polarity., J. Immunol. 189 (2012) 2159–68.

[341] A.R. French, W.M. Yokoyama, Natural killer cells and autoimmunity., Arthritis Res. Ther. 6 (2004) 8–14.

[342] Z. Tian, M.E. Gershwin, C. Zhang, Regulatory NK cells in autoimmune disease., J. Autoimmun. 39 (2012) 206–15.

[343] S. Zompi, J.A. Hamerman, K. Ogasawara, E. Schweighoffer, V.L.J. Tybulewicz, J.P. Di Santo, et al., NKG2D triggers cytotoxicity in mouse NK cells lacking DAP12 or Syk family kinases., Nat. Immunol. 4 (2003) 565–72.

[344] S.E. Johansson, Broadly impaired NK cell function in non-obese diabetic mice is partially restored by NK cell activation in vivo and by IL-12/IL-18 in vitro, Int. Immunol. 16 (2004) 1–11.

[345] A. Saudemont, S. Burke, F. Colucci, A simple method to measure NK cell cytotoxicity in vivo., Methods Mol. Biol. 612 (2010) 325–34.

[346] Z.K. Ballas, C.M. Buchta, T.R. Rosean, J.W. Heusel, M.R. Shey, Role of NK cell subsets in organ-specific murine melanoma metastasis., PLoS One. 8 (2013) e65599.

8 Summary

NK cells play an important role in the clearance of viral and intracellular bacterial infections as well as in the elimination of tumor cells and have also been implicated in the regulation of other immune cells. Recent work demonstrates a crucial role of actin cytoskeletal-activities in controlling NK cell function. In eukaryotic cells, the maintenance of the actin cytoskeleton and its quick remodeling in response to various stimuli is orchestrated by a cohort of actin-associated proteins. Coronin proteins are part of this complex network of actin-regulatory proteins and, as such, have been implicated in various actin-mediated cellular activities in different cellular systems. However, the role of coronins in the control of NK cell functions is yet unknown.

In this thesis, I provide genetic evidence for an important role of two mammalian coronins, coronin 1a (Coro1a) and coronin 1b (Coro1b), in the regulation of NK cell development and function. By utilizing gene-deficient mice I could demonstrate that the loss of Coro1a-function was directly linked to dysregulated F-actin organization in NK cells. While *Coro1a*$^{-/-}$ mice had normal numbers of peripheral NK cells, *Coro1a*$^{-/-}$ NK cells generally were of a more immature phenotype compared to *wild type* counterparts. The impaired NK cell maturation in *Coro1a*$^{-/-}$ mice was additionally associated with developmental alterations in the bone marrow. Although the single loss of Coro1b-function did not affect NK cell development and maturation, the immature phenotype of *Coro1a*$^{-/-}$ NK cells was further augmented by the additional loss of *Coro1b*. *In vitro*, IL-15-expanded *Coro1a*$^{-/-}$ and *Coro1a*$^{-/-}$*Coro1b*$^{-/-}$ NK cells exhibited a comparable maturation status as *wild type* NK cells, but showed clear defects in central NK cell functions like killing of tumor cells, chemokine-induced migration and cytokine secretion. The decreased cytotoxicity of *Coro1a*$^{-/-}$ and *Coro1a*$^{-/-}$*Coro1b*$^{-/-}$ NK cells was associated with an impaired polarization of cytolytic granules and a reduced NK cell degranulation, whereas no major defects were found in early steps of the cytolytic response, including the formation of the cytolytic synapse and the consequent activation of NK cells. Thus, distinct actin-associated processes involved in NK cell activities have different requirements on coronin proteins and the actin cytoskeleton.

In conclusion, this study expands our knowledge on the function of actin-regulatory coronin proteins, by demonstrating that they do not only regulate known actin-dependent processes in NK cells, such as cell migration and cytotoxic granule release, but also control NK cell development. As coronin proteins and actin regulation are highly conserved between mice and man, the results obtained from this study are relevant for the human system. Thus, defective NK cell responses may contribute to the clinical symptoms observed in SCID patients with an inborn defect of *Coro1a*.

9 Zusammenfassung

NK Zellen übernehmen wichtige Aufgaben in der Abwehr viraler und intrazellulärer bakterieller Infektionen sowie bei der Eliminierung von Tumorzellen. Des Weiteren tragen sie zur Regulation anderer Immunzellen bei. In aktuellen Publikationen konnte gezeigt werden, dass das Aktin-Zytoskelett eine entscheidende Funktion bei der Kontrolle von NK Zell-Aktivitäten übernimmt. In eukaryotischen Zellen werden die Aufrechterhaltung und der Umbau des Aktin-Zytoskeletts durch eine Vielzahl von Aktin-assoziierten Proteinen gesteuert. Einen wichtigen Bestandteil dieses komplexen Netzwerkes Aktin-regulierender Proteine bilden die Coronine. Diese werden mit der Regulation einer Vielzahl Aktin-vermittelter Prozesse in unterschiedlichen Zellsystemen in Verbindung gebracht. Eine Beteiligung von Coroninen an der Steuerung von NK Zell-Funktionen ist bisher jedoch unbekannt.

In dieser Arbeit konnte ich durch die Verwendung von Gen-defizienten Mausstämmen eine wichtige regulative Rolle zweier Säugetier Coronine, genauer Coronin 1a (Coro1a) und Coronin 1b (Coro1b), für die Entwicklung und Funktion von NK Zellen nachweisen. Des Weiteren konnte ich zeigen, dass der Verlust der Funktion von Coro1a in direkter Verbindung mit einer fehlgesteuerten Aktin-Zytoskelett-Organisation in NK Zellen steht.

Coro1a-defiziente Mäuse wiesen eine normale Anzahl peripherer NK Zellen auf, diese waren jedoch im Vergleich zu den Wildtyp Kontrollen durch einen generell unreiferen Phänotyp gekennzeichnet. Ein vergleichbarer Effekt bezüglich des Reifegrades von *Coro1a*$^{-/-}$ NK Zellen wurde auch im Knochenmark beobachtet. Dieser war jedoch zusätzlich mit einer Steigerung der Anzahl der *Coro1a*-defizienten NK Zellen und somit einer veränderten NK Zell-Entwicklung im Knochenmark assoziiert. Der alleinige Verlust von *Coro1b* hatte hingegen keine Auswirkung auf die Entwicklung und Reifung der NK Zellen, jedoch wurde der unreife Phänotyp *Coro1a*-defizienter NK Zellen durch den zusätzlichen Verlust von *Coro1b* weiter verstärkt.

IL-15-expandierte *Coro1a*$^{-/-}$ und *Coro1a*$^{-/-}$*Coro1b*$^{-/-}$ NK Zellen zeigten im Vergleich zu Wildtyp-Zellen einen ähnlichen Reifegrad, wiesen allerdings in *in vitro* Studien klare Defizite bezüglich zentraler NK Zell-Funktionen wie der Abtötung von Tumorzellen, der Chemokin-induzierten Migration und der Zytokinfreisetzung auf. Die geminderte Zytotoxizität der *Coro1a*$^{-/-}$ und *Coro1a*$^{-/-}$*Coro1b*$^{-/-}$ NK Zellen war assoziiert mit einer verringerten Polarisierung zytolytischer Granula sowie einer reduzierten NK Zell-Degranulation. Hingegen konnten keine nennenswerten Defekte im Bereich der frühen zytolytischen Antwort bezüglich einer gestörten Ausbildung der zytolytischen Synapse und einer daraus resultierenden verminderten Aktivierung der NK Zellen nachgewiesen werden. Daraus lässt sich schließen, dass Coronine und das Aktin-Zytoskelett differentiell bei unterschiedlichen Aktin-vermittelten Prozessen beansprucht werden.

Zusammenfassend lässt sich sagen, dass die Untersuchungen im Rahmen dieser Arbeit das Wissen um Aktin-regulierende Coronine erweitern, indem gezeigt wird, dass nicht nur nachweislich Aktin-abhängige Prozesse wie die Zellmigration und die Freisetzung zytotoxischer Granula durch diese Proteine in NK Zellen reguliert werden sondern zusätzlich auch die Entwicklung von NK Zellen durch Coronine gesteuert wird. Da die untersuchten Coronin-Proteine sowie generelle Aktin-regulierende Prozesse zwischen Maus und Mensch stark konserviert sind, sind die Ergebnisse dieser Arbeit ebenfalls für das humane System relevant. Fehlerhafte NK Zell-Antworten könnten somit als weitere Ursache für die klinischen Symptome in SCID Patienten, die einen angeborenen *Coro1a*-Defekt aufweisen, verantwortlich sein.

10 Appendix

10.1 Protein alignments of mouse and human Coro1a and Coro1b

The amino acid sequences of mouse Coro1a (accession no.: NP_034028, version: NP_034028.1) and Coro1b (accession no.: NP_035908, version: NP_035908.1) as well as human Coro1a (accession no.: NP_009005, version: NP_009005.1) and Coro1b (accession no.: NP_001018080, version NP_001018080.1) were aligned with ClustalW2 (EMBL-EBI; version: 2.1; http://www.ebi.ac.uk/Tools/msa/clustalw2/) using default settings. The calculated amino acid sequence homologies are shown in Table 10-1, the underlying protein-alignments are depicted in Figure 10-1 to 10-3.

Table 10-1. Amino acid sequence homologies of murine and human coronins

Proteins	Identities	Similarity	Gaps
mCoro1a vs. hCoro1a	94%	97%	0%
mCoro1b vs. hCoro1b	94%	95%	1%
mCoro1a vs. mCoro1b	63%	79%	5%

```
mCoro1a      MS-RQVVRSSKFRHVFGQPAKADQCYEDVRVSQTTWDSGFCAVNPKFMAL 49
mCoro1b      MSFRKVVRQSKFRHVFGQPVKNDQCYEDIRVSRVTWDSTFCAVNPKFLAV 50
             ** *:***.**********.* ******:***:.**** ********:*:

mCoro1a      ICEASGGGAFLVLPLGKTGRVDKNVPLVCGHTAPVLDIAWCPHNDNVIAS 99
mCoro1b      IVEASGGGAFMVLPLNKTGRIDKAYPTVCGHTGPVLDIDWCPHNDEVIAS 100
             * ********:****.****:**  * *****.***** ******:****

mCoro1a      GSEDCTVMVWEIPDGGLVLPLREPVITLEGHTKRVGIVAWHPTAQNVLLS 149
mCoro1b      GSEDCTVMVWQIPENGLTSPLTEPVVVLEGHTKRVGIITWHPTARNVLLS 150
             **********:**:.**. ** ***:.**********::*****:*****

mCoro1a      AGCDNVILVWDVGTGAAVLTLGPDVHPDTIYSVDWSRDGALICTSCRDKR 199
mCoro1b      AGCDNVVLIWNVGTAEELYRLD-SLHPDLIYNVSWNHNGSLFCSACKDKS 199
             ******:*:*:***.  :  *. .:*** **.*.*.::*:*:*::*:**

mCoro1a      VRVIEPRKGTVVAEKDRPHEGTRPVHAVFVSEGKILTTGFSRMSERQVAL 249
mCoro1b      VRIIDPRRGTLVAEREKAHEGARPMRAIFLADGKVFTTGFSRMSERQLAL 249
             **:*:**:**:***:::.***:**::*:*:::**::***********:**

mCoro1a      WDTKHLEEPLSLQELDTSSGVLLPFFDPDTNIVYLCGKGDSSIRYFEITS 299
mCoro1b      WDPENLEEPMALQELDSSNGALLPFYDPDTSVVYVCGKGDSSIRYFEITD 299
             **.::****::*****:*.*.****:****.:**:**************.

mCoro1a      EAPFLHYLSMFSSKESQRGMGYMPKRGLEVNKCEIARFYKLHERKCEPIA 349
mCoro1b      EPPYIHFLNTFTSKEPQRGMGSMPKRGLEVSKCEIARFYKLHERKCEPIV 349
             *.*::*:*. *:***.***** ********.******************.

mCoro1a      MTVPRKSDLFQEDLYPPTAGPDPALTAEEWLGGRDAGPLLISLKDGYVPP 399
mCoro1b      MTVPRKSDLFQDDLYPDTAGPEAALEAEDWVSGQDANPILISLREAYVPS 399
             ***********:**** ****:.** **:*:.*:**.*:****::.***.

mCoro1a      KSRELRVN-RGLDSARRRATPEPSGTPSSDTVS----------------- 431
mCoro1b      KQRDLKVSRRNVLSDSRPASYSRSGASTATAVTDVPSGNLAGAGEAGKLE 449
             *.*:*:*. *.: *  * *: . **:.:: :*:

mCoro1a      RLEEDVRNLNAIVQKLQERLDRLEETVQAK----- 461
mCoro1b      EVMQELRALRMLVKEQGERISRLEEQLGRMENGDT 484
             .: :::* *. :*::  **:.**** :
```

Figure 10-1. Protein alignment of mouse Coro1a and Coro1b.
Mouse Coro1a and Coro1b amino acid sequences were aligned using ClustalW (version 2.1.) Identical residues are highlighted by an asterisk, conserved substitutions are indicated by an colon and semi-conserved by an point.

```
mCoro1a      MSRQVVRSSKFRHVFGQPAKADQCYEDVRVSQTTWDSGFCAVNPKFMALI 50
hCoro1a      MSRQVVRSSKFRHVFGQPAKADQCYEDVRVSQTTWDSGFCAVNPKFVALI 50
             ************************************************:***

mCoro1a      CEASGGGAFLVLPLGKTGRVDKNVPLVCGHTAPVLDIAWCPHNDNVIASG 100
hCoro1a      CEASGGGAFLVLPLGKTGRVDKNAPTVCGHTAPVLDIAWCPHNDNVIASG 100
             ***********************.* ************************

mCoro1a      SEDCTVMVWEIPDGGLVLPLREPVITLEGHTKRVGIVAWHPTAQNVLLSA 150
hCoro1a      SEDCTVMVWEIPDGGLMLPLREPVVTLEGHTKRVGIVAWHTTAQNVLLSA 150
             ****************:*******:***************.*********

mCoro1a      GCDNVILVWDVGTGAAVLTLGPDVHPDTIYSVDWSRDGALICTSCRDKRV 200
hCoro1a      GCDNVIMVWDVGTGAAMLTLGPEVHPDTIYSVDWSRDGGLICTSCRDKRV 200
             ******:*********:*****:***************.***********

mCoro1a      RVIEPRKGTVVAEKDRPHEGTRPVHAVFVSEGKILTTGFSRMSERQVALW 250
hCoro1a      RIIEPRKGTVVAEKDRPHEGTRPVRAVFVSEGKILTTGFSRMSERQVALW 250
             *:**********************:************************

mCoro1a      DTKHLEEPLSLQELDTSSGVLLPFFDPDTNIVYLCGKGDSSIRYFEITSE 300
hCoro1a      DTKHLEEPLSLQELDTSSGVLLPFFDPDTNIVYLCGKGDSSIRYFEITSE 300
             **************************************************

mCoro1a      APFLHYLSMFSSKESQRGMGYMPKRGLEVNKCEIARFYKLHERKCEPIAM 350
hCoro1a      APFLHYLSMFSSKESQRGMGYMPKRGLEVNKCEIARFYKLHERRCEPIAM 350
             ******************************************:*******

mCoro1a      TVPRKSDLFQEDLYPPTAGPDPALTAEEWLGGRDAGPLLISLKDGYVPPK 400
hCoro1a      TVPRKSDLFQEDLYPPTAGPDPALTAEEWLGGRDAGPLLISLKDGYVPPK 400
             **************************************************

mCoro1a      SRELRVNRGLDSARRRATPEPSGTPSSDTVSRLEEDVRNLNAIVQKLQER 450
hCoro1a      SRELRVNRGLDTGRRRAAPEASGTPSSDAVSRLEEEMRKLQATVQELQKR 450
             ***********:.****:**.*******:******::*:*:* **:**:*

mCoro1a      LDRLEETVQAK 461
hCoro1a      LDRLEETVQAK 461
             ***********
```

Figure 10-2. Protein alignment of mouse Coro1a and human Coro1a.
Mouse and human Coro1a amino acid sequences were aligned using ClustalW (version 2.1.) Identical residues are highlighted by an asterisk, conserved substitutions are indicated by an colon and semi-conserved by an point.

```
mCoro1b      MSFRKVVRQSKFRHVFGQPVKNDQCYEDIRVSRVTWDSTFCAVNPKFLAV 50
hCoro1b      MSFRKVVRQSKFRHVFGQPVKNDQCYEDIRVSRVTWDSTFCAVNPKFLAV 50
             **************************************************

mCoro1b      IVEASGGGAFMVLPLNKTGRIDKAYPTVCGHTGPVLDIDWCPHNDEVIAS 100
hCoro1b      IVEASGGGAFLVLPLSKTGRIDKAYPTVCGHTGPVLDIDWCPHNDEVIAS 100
             **********:****.********************************

mCoro1b      GSEDCTVMVWQIPENGLTSPLTEPVVVLEGHTKRVGIITWHPTARNVLLS 150
hCoro1b      GSEDCTVMVWQIPENGLTSPLTEPVVVLEGHTKRVGIIAWHPTARNVLLS 150
             ************************************:***********

mCoro1b      AGCDNVVLIWNVGTAEELYRLDSLHPDLIYNVSWNHNGSLFCSACKDKSV 200
hCoro1b      AGCDNVVLIWNVGTAEELYRLDSLHPDLIYNVSWNHNGSLFCSACKDKSV 200
             **************************************************

mCoro1b      RIIDPRRGTLVAEREKAHEGARPMRAIFLADGKVFTTGFSRMSERQLALW 250
hCoro1b      RIIDPRRGTLVAEREKAHEGARPMRAIFLADGKVFTTGFSRMSERQLALW 250
             **************************************************

mCoro1b      DPENLEEPMALQELDSSNGALLPFYDPDTSVVYVCGKGDSSIRYFEITDE 300
hCoro1b      DPENLEEPMALQELDSSNGALLPFYDPDTSVVYVCGKGDSSIRYFEITEE 300
             **************************************************:*

mCoro1b      PPYIHFLNTFTSKEPQRGMGSMPKRGLEVSKCEIARFYKLHERKCEPIVM 350
hCoro1b      PPYIHFLNTFTSKEPQRGMGSMPKRGLEVSKCEIARFYKLHERKCEPIVM 350
             **************************************************

mCoro1b      TVPRKSDLFQDDLYPDTAGPEAALEAEDWVSGQDANPILISLREAYVPSK 400
hCoro1b      TVPRKSDLFQDDLYPDTAGPEAALEAEEWVSGRDADPILISLREAYVPSK 400
             **************************:****:**:**************

mCoro1b      QRDLKVSRRNVLSDSRPASYSRS-----GASTATAVTDVPSGNLAGAGEA 445
hCoro1b      QRDLKISRRNVLSDSRPAMAPGSSHLGAPASTTTAADATPSGSLARAGEA 450
             *****:************  . *      ***:**.  .***.** ****

mCoro1b      GKLEEVMQELRALRMLVKEQGERISRLEEQLGRMENGDT 484
hCoro1b      GKLEEVMQELRALRALVKEQGDRICRLEEQLGRMENGDA 489
             ************** ******:**.*************:
```

Figure 10-3. Protein alignment of mouse Coro1b and human Coro1b.
Mouse and human Coro1b amino acid sequences were aligned using ClustalW (version 2.1.) Identical residues are highlighted by an asterisk, conserved substitutions are indicated by an colon and semi-conserved by an point.

10.2 Gating strategies used for flow cytometry

The following representative gating strategies were used for the phenotyping and the analysis of naïve NK cells isolated from the spleen, the bone marrow and the liver (Figure 10-4) as well as for the analysis of IL-15-expanded NK cells (Figure 10-5).

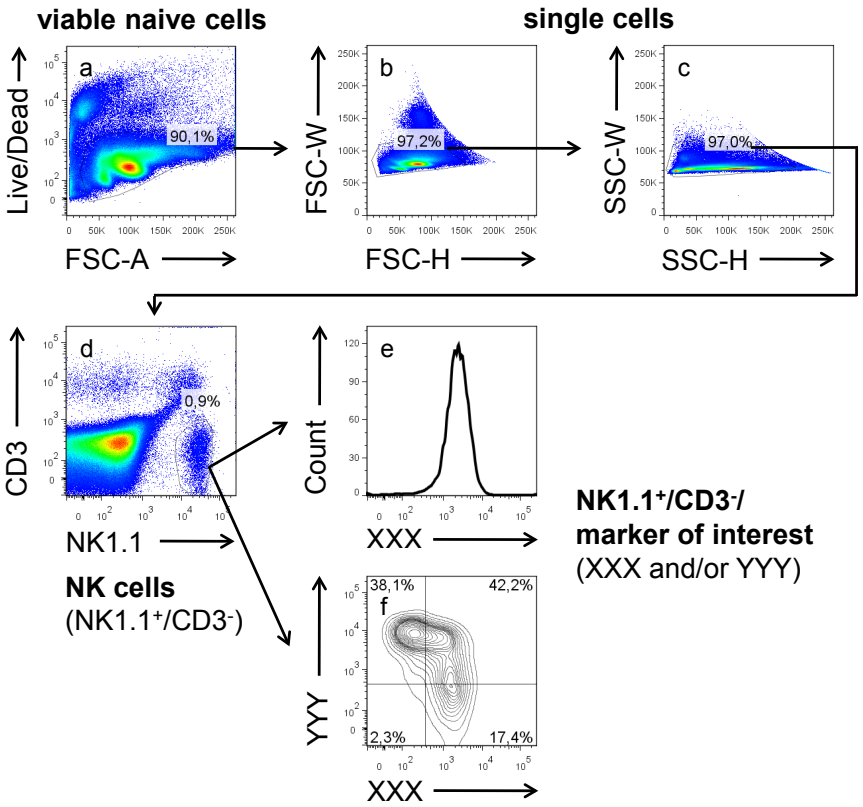

Figure 10-4. General gating strategy used for the analysis of freshly isolated naïve NK cells. Shown representative dot plots, histograms and contour plots demonstrate the general gating strategy used for the analysis of naïve NK cells isolated from bone marrow, spleen and liver. For dead cell exclusion, isolated naïve cells were stained with Fixable blue fluorescent reactive dye® (Live/Dead) and analyzed versus forward scatter (FSC) as shown in Figure 10-4 (a). Doublets were excluded using FSC and side scatter (SSC) height versus width (b and c). NK cells were identified by the expression of NK1.1 and the absence of CD3 expression (d) and used for further analysis (e and f). For data analysis, NK cells stained with isotype controls were used as reference.

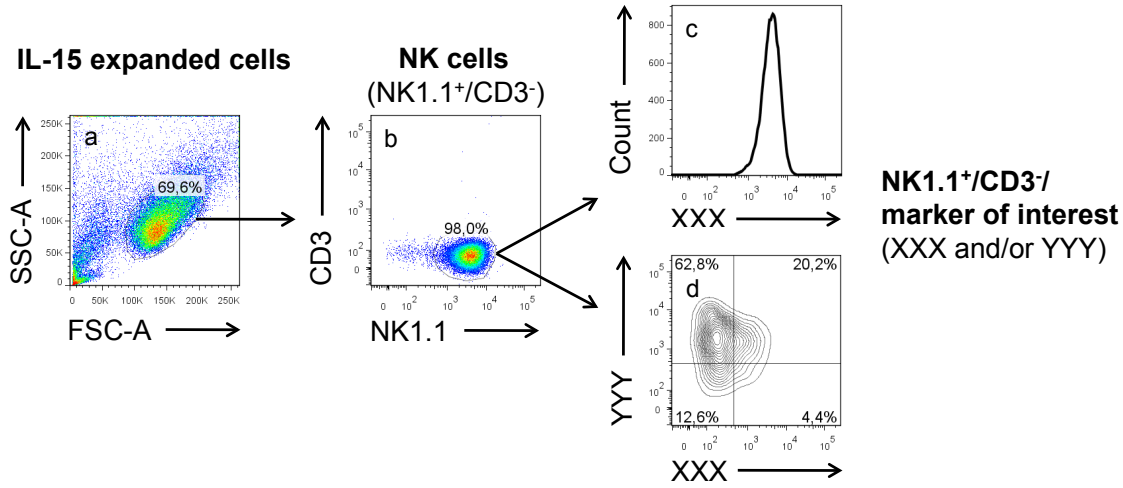

Figure 10-5. General gating strategy used for the analysis of IL-15-expanded NK cells Shown representative dot plots, histograms and contour plots demonstrate the general gating strategy to characterize IL-15-expanded NK cells based on FSC- versus SSC area to exclude cell debris (a) and NK1.1 and CD3 staining to identify NK cells (b). NK1.1^{+}/CD3^{-} NK cells were used for further analysis (c and d). For data analysis, either NK cells stained with isotype controls or sec. Abs or corresponding knockout NK cells were used as reference.

Danksagung

Meiner Doktormutter Frau Prof. Dr. Silvia Bulfone-Paus danke ich für die Möglichkeit der Anfertigung dieser Arbeit sowie für ihre Betreuung.

Besonderer Dank gilt auch Frau Dr. Kyeong-Hee Lee die mir freundlicherweise als Mentorin innerhalb der BBRS als kompetente Ansprechpartnerin zur Verfügung stand.

Im großen Maße bin ich auch Herrn Dr. Niko Föger für die intensive Betreuung und Anleitung sowie die vielen konstruktiven und wissenschaftlichen Diskussionen zum Dank verpflichtet.

Des Weiteren möchte ich mich bei Manuel Hein für seine Hilfsbereitschaft und technische Unterstützung im Labor bedanken.

Danke auch dir, Holger, für die Mühe und Unterstützung. Es war nicht umsonst!

Ein ganz besonders herzlicher Dank gilt meinen Eltern, die mir diesen Weg ermöglicht haben und auf deren Unterstützung ich immer bauen konnte.

Nicht zuletzt gilt ein besonderer Dank auch meiner Familie für deren Geduld, Rückhalt und Motivation.

Lebenslauf

PERSÖNLICHE DATEN

André Jenckel
Diplom-Biologe

*20. Juni 1979 in Hagenow

Theodor-Storm-Str. 30
23795 Bad Segeberg

PROMOTION

Seit 10/2008	Promotionsarbeit am Forschungszentrum Borstel, Leibniz-Zentrum für Medizin und Biowissenschaften, Borstel Titel: „The role of the actin-regulatory proteins coronin 1a and coronin 1b in the regulation of natural killer cell development and function “

STUDIUM

10/2003 – 10/2008	Studium der Biologie an der Christian-Albrechts-Universität zu Kiel Diplomarbeit am Institut für Infektionsmedizin des Universitätsklinikum Schleswig-Holstein, Kiel Titel: „Etablierung von *in vitro*-Systemen zur Quantifizierung der Genomreplikation des humanen Coronavirus NL63“ *Abschluss: Diplom-Biologe*

BERUFSAUSBILDUNG/ BERUFSTÄTIGKEIT

02/2003 – 10/2003	Biologielaborant am Forschungszentrum Borstel, Borstel
09/1999 – 01/2003	Ausbildung zum Biologielaboranten am Forschungszentrum Borstel, Borstel *Abschluss: Biologielaborant*

WEHRDIENST

09/1998 – 06/1999	Grundwehrdienst bei der Bundeswehr

SCHULBILDUNG

08/1992 – 07/1998	Robert-Stock-Gymnasium in Hagenow *Abschluss: Allgemeine Hochschulreife*
08/1990 – 07/1992	Orientierungsstufe der Theodor-Körner-Schule in Picher
09/1986 – 07/1990	Grundschule in Redefin

Liste eigener Publikationen

Originalpublikationen

[1] K. Brandt, S. Bulfone-Paus, **A. Jenckel**, D.C. Foster, R. Paus, R. Rückert, Interleukin-21 inhibits dendritic cell-mediated T cell activation and induction of contact hypersensitivity in vivo., The Journal of Investigative Dermatology. 121 (2003) 1379–82.

[2] N. Föger, **A. Jenckel**, Z. Orinska, K.-H. Lee, A.C. Chan, S. Bulfone-Paus, Differential regulation of mast cell degranulation versus cytokine secretion by the actin regulatory proteins Coronin1a and Coronin1b., The Journal of Experimental Medicine. 208 (2011) 1777–87.

[3] **A. Jenckel**, M. Hein, K.-H. Lee, S. Bulfone-Paus, N. Föger, Altered NK cell maturation and function in mice deficient for the actin-regulatory proteins coronin 1a and coronin 1b., (Manuscript in preparation).

Ausgewählte Abstracts

[1] **A. Jenckel**, S. Bulfone-Paus, N. Föger, Fc-epsilon-receptor stimulation induces the phosphorylation and subcellular redistribution of the actin regulatory protein coronin 1a., in: 2nd European Congress of Immunology, Berlin, Germany, 2009.

[2] **A. Jenckel**, S. Bulfone-Paus, N. Föger, Fc-epsilon-receptor stimulation induces the phosphorylation and subcellular redistribution of the actin regulatory protein coronin 1a and coronin 1b, in: 32. Arbeitstagung der Norddeutschen Immunologen, Borstel, Germany, 2009.

[3] **A. Jenckel**, S. Bulfone-Paus, N. Föger, Regulation of NK cell development and function by the actin-regulatory proteins coronin 1a and coronin 1b., in: 33. Arbeitstagung der Norddeutschen Immunologen, Borstel, Germany, 2010.

[4] **A. Jenckel**, S. Bulfone-Paus, N. Föger, Altered NK cell maturation and function in mice deficient for the actin-regulatory proteins coronin 1a and coronin 1b., in: Joint Meeting of the Italian Society for Immunology, Clinical Immunology and Allergology (SIICA) and the German Society for Immunology (DGfI), Riccione, Italy, 2011.

[5] **A. Jenckel**, N. Föger, Regulation of NK cell maturation and function by the actin-regulatory proteins coronin 1a and coronin 1b, in: European Congress of Immunology, Immunology, Volume 137, Issue Supplement s1 Pages 1–809, September 2012, Glasgow, Scotland, 2012.

Ausgewählte Vorträge

[1] **A. Jenckel**, S. Bulfone-Paus, N. Föger, The actin-regulatory proteins coronin 1a and coronin 1b regulate NK cell development and function., in: 34. Arbeitstagung der Norddeutschen Immunologen, Borstel, Germany, 2011.

Preise

[1] Posterpreis 33. Arbeitstagung der Nordeutschen Immunologen.

A. Jenckel, S. Bulfone-Paus, N. Föger, Regulation of NK cell development and function by the actin-regulatory proteins coronin 1a and coronin 1b., in: 33. Arbeitstagung der Norddeutschen Immunologen, Borstel, Germany, 2010.

Erklärung

Hiermit erkläre ich an Eides statt, die vorliegende Arbeit mit dem Titel: „The role of the actin-regulatory proteins coronin 1a and coronin 1b in the regulation of natural killer cell development and function“ nach den Regeln guter wissenschaftlicher Praxis selbstständig und unter ausschließlicher Verwendung der angegebenen Quellen und Hilfsmittel erstellt zu haben. Bei der Erstellung der Arbeit habe ich keine Hilfe außer der wissenschaftlichen Beratung durch meine Doktormutter Frau Prof. Silvia Bulfone-Paus in Anspruch genommen. Die Arbeit hat weder in gleicher noch in ähnlicher Form an anderer Stelle im Rahmen eines Prüfungsverfahrens vorgelegen und wurde bisher nicht veröffentlicht beziehungsweise zur Veröffentlichung eingereicht.

Bad Segeberg, 14.11.2013 

André Jenckel